FFI-RAPPORT

20/02219

Increasing robustness of HF communications at high latitudes

– utilizing ionospheric data and space diversity

Vivianne Jodalen
Terje Mikal Mjelde

Increasing robustness of HF communications at high latitudes

– utilizing ionospheric data and space diversity

Vivianne Jodalen
Terje Mikal Mjelde

Norwegian Defence Research Establishment (FFI) 6 November 2020

Keywords
HF (High Frequency)
Kommunikasjon
Romvær
Ionosfæren
Målinger

FFI-rapport
20/02219

Prosjektnummer
1523

Elektronisk ISBN
978-82-464-3300-4

Approvers
Åshild Grønstad Solheim, *Research Manager*
Jan Erik Voldhaug, *Research Director*

Summary

HF-radio provides long range, infrastructure-independent communications to the Norwegian Armed Forces in the Arctic. This is important in an area with increasing activity and where satellite communications is less available. The high latitude HF-channel experiences large variations in time and space depending on the space weather, and HF communications must therefore make use of robust waveform- and network designs, adaptivity and real-time channel assessments in order to achieve optimum communications. In 2017–2018, measurements of HF communications were conducted in a network of stations at high latitudes.

The primary aim of the study was to investigate how much the availability of HF communications at high latitudes can be improved by exploiting space diversity. If various geographical paths exhibit very different channel characteristics, modern HF-networking radios are able to exploit this, and robustness of the HF communications can be gained. The idea was first explored in previous work conducted at FFI [4].

A secondary aim of this study was to investigate the correlation between the performance of modern HF communications and certain ionospheric parameters measured by ionospheric instruments. Real-time space situational awareness will enable the HF-operators to make optimum choices for their communications. A final aim of this report was to summarize the factors of importance to HF communications at high latitudes for educational purposes.

The study has confirmed that HF-networks that utilize space diversity, increase robustness and improve availability of HF communications. In a network of 20 W radios, space diversity gains of 10–30 % were achieved by including a node positioned further south at a distance of ~400 km from the transmitter. In a network of 400 W radios, space diversity gains of 10–50 % were achieved by a southern node at a distance of ~1300 km. The gains were largest during ionospherically disturbed periods.

Our comparison of the HF-measurements with ionospheric data has shown that using the latter may give useful insight in the prevailing propagation conditions, and give guidance for making favourable choices for the communication networks. Real-time ionograms in combination with riometer measurements were found particularly useful. In particular, for the short measurement paths in northern Norway with close proximity to riometer measurements in Abisko in Sweden, absorption levels above 0.2 dB (measured at 30 MHz) gave generally decreasing linking probability with hardly no linking at an absorption level of 1 dB. The long paths towards the south were also affected by the absorption measured in Abisko, but to a lesser extent. The absorption can be counteracted by the HF-operator by avoiding the area of increased absorption (utilizing space diversity) or increasing the transmit power, if that is an option.

Further work should include examination of space weather data sources available on the Internet, including radio amateur tools, for relevance to high latitudes and HF communications. Real-time data from relevant sources could be included in a software application tool, tailor-made for the HF-operator. The application, together with modern networking radios and smart ways of exploiting the high latitude ionosphere, would improve HF communications and thereby information exchange for the Norwegian Armed Forces. The results of this report can provide a basis for such further work.

Sammendrag

HF-radio gir kommunikasjon over lange avstander uten bruk av fast infrastruktur for norske militære styrker i nordområdene. Dette er viktig i et område med økt aktivitet, og hvor satellitt-kommunikasjon er mindre tilgjengelig. Ionosfærekanalen for HF på høye breddegrader opplever store variasjoner i tid og rom avhengig av romværet, og HF-kommunikasjon bør derfor benytte robuste bølgeformer, adaptivitet og sanntidsinformasjon om ionosfærekanalen for å gi optimal kommunikasjon. I 2017-2018 ble det gjort målinger av HF-kommunikasjon i et nettverk av stasjoner på høye breddegrader.

Hovedmålet med studien var å finne ut hvor mye tilgjengeligheten av HF-kommunikasjon kan økes ved å utnytte romlig diversitet. Dersom forskjellige geografiske radiostrekk har svært forskjellig kanalkarakteristikk, kan moderne HF-radioer med nettverksfunksjonalitet utnytte dette til å øke robustheten av kommunikasjonen. Konseptet ble først lansert i et tidligere arbeid ved FFI [4].

Et annet mål med studien var å undersøke graden av korrelasjon mellom ytelsen av moderne HF-radioer og visse ionosfæreparametere som måles av ionosfæriske måleinstrumenter. Situasjonsbevissthet om kanalforholdene vil være nyttig for HF-operatørene og gir dem mulighet til å gjøre optimale valg for kommunikasjonen. Et siste mål med denne rapporten var å oppsummere kjent kunnskap om faktorer som påvirker HF-kommunikasjon på høye breddegrader.

Denne studien har bekreftet at HF-nettverk som utnytter romlig diversitet, kan gi økt robusthet og bedre tilgjengelighet av HF-kommunikasjon. I et nettverk av 20 W radioer ble det oppnådd 10–30 % økt sannsynlighet for å oppnå linking ved å inkludere et punkt i en avstand ~400 km lengre sør. I et nettverk av 400 W radioer ble det oppnådd 10–50 % økt linkesannsynlighet ved å inkludere et punkt ~1300 km lengere sør. Den største gevinsten ble oppnådd under ionosfærisk forstyrrede perioder.

Våre sammenligninger av HF-målingene med andre ionosfæremålinger har vist at de siste gir god innsikt i de rådende kanalforholdene, og kan gi grunnlag for gode valg for kommunikasjons-nettverket. Sanntids ionogrammer kombinert med riometer-målinger ble funnet spesielt nyttig. Mer konkret, for korte radiostrekk i Nord-Norge med nærhet til absorpsjonsmålingene i Abisko, ga målte absorpsjonsnivåer over 0,2 dB (målt på 30 MHz) minkende linkesannsynlighet, med svært liten linkesannsynlighet når absorpsjonen ble målt til 1 dB. De lange radiostrekkene mot sør ble også berørt av økt absorpsjon målt i Abisko, men i mindre grad. Absorpsjon av radio-signalet kan omgås ved å unngå den delen av ionosfæren som har høy absorpsjon (utnytte romlig diversitet), eller øke sende-effekten, hvis det er en mulighet.

I videre arbeid bør romværsinformasjon på Internett, inkludert radioamatørkilder, vurderes for relevans for HF-kommunikasjon. Sanntidsdata fra relevante datakilder som ionogrammer og riometer absorpsjon bør inkluderes i en programvareapplikasjon som skreddersys for HF-operatøren. En slik applikasjon, sammen med moderne HF-radioer og smarte måter å utnytte ionosfæren på høy breddegrad, vil gi Forsvaret bedre HF-kommunikasjon og vil derfor kunne understøtte informasjonsutveksling bedre. Resultatene i denne rapporten kan utgjøre et grunnlag for et slikt videre arbeid.

Contents

1 Introduction and background

HF-radio provides long range communications without dependency on fixed infrastructure. This is a main reason for HF communications still being important for military forces. For Norway, HF is particularly valuable for providing communications in the maritime environment in the Arctic. Land forces may also benefit from the long range, infrastructure independent capabilities of HF communications. In the maritime domain, HF communications has traditionally been used for point-to-point connections or for broadcast at fixed frequencies. The Norwegian Navy and Norwegian HF fixed infrastructure are now in a transition phase to be equipped with modern HF communications, comprising functionalities such as networking, automatic link establishment (ALE), data rate adaptivity and wider bandwidths (WBHF). The Norwegian Army is already equipped with modern HF-radios, although they are still lacking wideband capabilities.

The radio signals in the HF-requency band are reflected by the ionosphere and provide beyond-line-of-sight communications with low- to medium data rates. However, the high latitude ionosphere is a highly dynamic medium influenced by the solar zenith angle as well as by irregular solar events such as flares causing particle precipitation, the aurora borealis, ionospheric irregularities and magnetospheric disturbances. Thus, the high latitude HF-channel is also highly variable in time and space with excess absorption, non-predictable reflections, Doppler- and delay spreads, all caused by auroral ionization. Some of the effects mentioned may be handled by radio waveform design using adaptive communications protocols and signal processing. Different kinds of diversity are additional means to overcome the problems of the high latitude channel. References [4] and [5] both address frequency diversity at high latitudes. Antenna polarization diversity and time diversity may be other options [6], [7]. Reference [7] describes how resilient HF-networks can be formed based on modern HF-technology.

The measurements and analysis in this report address *geographical diversity* in particular. In a previous study at FFI [4], measurements showed that at times when a transmission path inside a disturbed high latitude region experiences heavy absorption, another transmission may be more successful on a different, longer path towards the south, out of the disturbed region to an intermediate node located in the south. The recipient of the transmission may be reached with a return HF transmission or a return by some other wired or wireless medium back into the disturbed region. The exploitation of different paths with different channel characteristics (geographical diversity) will in the following be called *space diversity*. The study in the present report is a follow-up of the work reported in [4] with more data collection and additional considerations.

Today, the Internet offers completely new opportunities for exploiting measurements of the ionosphere, compared to the 50’s and 60’s when HF was the primary means of long range communications. Solar events and the state of the ionosphere and magnetosphere are continuously monitored by instruments at the ground and in space, and data are made available on the Internet in real time. Such “big data” form the basis for space situational awareness, and

deep learning algorithms may combine the data from various instruments to improve the operational use of HF communications and other technologies. Ionospheric propagation may be better predicted and optimized choices for HF communications may be made. In particular, the electron density measured by ionosondes, the ionospheric absorption measured by riometers and the magnetic activity measured by magnetometers are relevant for the wave propagation in the HF-frequency band. By using such data, either as input to prediction programs for communications planning, or for increasing own space situational awareness during communications, better performance and operational utilization of HF are expected. This report also addresses the relationship between HF communications and data from other measuring instruments. As expressed in [14]: *Familiarity with the pattern of events which accompanies the numerous disturbances of the polar ionosphere will enable the operator of HF to derive more benefit from warnings of disturbances.*

The activity reported here was in 2016 funded by the Concept Development and Experimentation (CD&E) project in the Norwegian Armed Forces "HF i nettverk" to conduct long-term measurements of HF communications in a network of stations at high latitudes. The measurements and analysis were also partly funded by two FFI-projects "*Kommunikasjon i nordområdene*" and "*Forsvarets fremtidige kommunikasjonsinfrastruktur*". This report was finally published by the FFI-project "*Robust trådløs kommunikasjonsteknologi*", and it documents the analysis results from those measurements. Previously, a final report of the CD&E project has been produced [1], and more detailed documentation of the measurement setup can be found in [2]. Parts of the results described in this report were presented at the Nordic Shortwave Conference in 2019 [3].

2 Aims of the study and possible implications for military forces

The primary aim of the study was to investigate how much the availability of HF communications at high latitudes can be improved by exploiting space diversity. The hypothesis was that if parts of the transmission path are outside the disturbed ionospheric region, instead of the path being entirely within the disturbed region, there will be less auroral absorption, and the probability of linking and transfer success will be higher. An intermediate node in the south may be able to receive the signal and relay the signal back to the recipient also located within the disturbed region. Space diversity has been measured and quantified in this study, and the work builds on previous work described in [14], further investigated in [4]. An illustration of the high latitude D-region[1] of the ionosphere where auroral absorption takes place, relative to two

[1] Described in Section 3.1.

different HF-skywave paths, is shown in Figure 2.1. The figure seeks to illustrate the hypothesis.

If space diversity in our study is found to be valuable for communications in the Arctic, modern HF-radio technology will be needed to exploit it. With modern HF-radios supporting Automatic Link Establishment (ALE), 2G[2], 3G[3] and 4G[4] data link protocols, networking is possible and frequencies can be shared between units and applications. If mobile users, as well as fixed HF-radio stations, are equipped with this technology, networks that involve a diversity of channels and sites can be set up in order to avoid the channel problems at high latitudes, to some degree. Reference [7] describes this as one way of building resilient networks at HF. An important factor in our measurements was to use operational radios as measurement instruments instead of a scientifically designed instrument, in order to get results in close agreement with the operational experience.

A secondary aim of this study was to investigate the correlation between the performance of modern HF communications and certain ionospheric parameters measured by ionospheric instruments. The main focus was on auroral absorption measured by riometers, but other measurements have also been considered. Auroral absorption is one of the most important factors that influences HF communications at high latitudes [14].

The correlation between the performance of HF communications and the measured riometer absorption is investigated and described, and this information can presumeably be used by the HF-operator to better plan communications, including avoiding unnecessary exposure on air if the absorption is too high to give any communications at all. However, forecasting absorption levels several hours into the future is difficult, and the current study does not comprise a model for HF communication forecasting based on real-time riometer data. The results can nevertheless be used in the definition of such a model.

A final aim of this report was for educational purposes to summarize from older literature the factors of importance to HF communications at high latitudes.

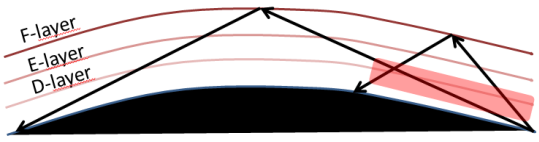

Figure 2.1 Path geometries relative to the region of excess D-region absorption at high latitudes.

The report is structured as follows: Chapter 3 gives some theoretical background for HF communications at high latitudes for educational purposes. Chapter 4 gives a brief introduction to the measurements with more details found in Appendix A. Chapter 5 contains the analysis

[2] 2G: STANAG 4539, STANAG 5066.
[3] 3G: STANAG 4538.
[4] 4G: STANAG 5069, STANAG 4539 Annex H, draft STANAG 5070.

results, addressing space diversity in Section 5.1 and the relationship between HF communications and ionospheric measurements in Section 5.2. Without reading about the analysis in detail, a summary of the observations concerning space diversity is found in Section 5.1.11. In Chapter 6 we discuss the relevance of the results to the HF-community before we draw the conclusions in Chapter 7.

3 Some aspects of high latitude ionospheric radio communication

Ionospheric radio wave propagation at high latitudes has been studied extensively in the past, and there exists a large number of references.

Reference [14] describes ionospheric communications in general, but has a particular emphasis on HF communication problems in polar regions, their causes and how they can be circumnavigated. Another reference, [10], gives a more in-depth and scientific description of each of the phenomena that may occur. In this chapter we use these references in particular to give some background knowledge for the current work and also to give the reader a basic understanding of the high latitude ionospheric channel.

3.1 Basic principles

Communication at the frequencies between 3 and 30 MHz (the HF-band) is possible either with ground wave propagation along the surface of the earth with limited range, or with skywave propagation where the electromagnetic signals are refracted and reflected in the ionosphere providing very long range of communications. The ionosphere is a very complex medium, but the main source of its creation is the electromagnetic radiation from the sun ionizing various gases in the atmosphere giving a certain density of free electrons in different heights of the atmosphere. The D-layer[5] in the range 60–90 km above the surface of the earth is characterized by low electron density and a high collision frequency between electrons and neutral molecules giving rise to absorption of the electromagnetic wave travelling through it. Hardly no refraction of the wave takes place in the D-layer. The E-layer in the range 90–150 km has a higher electron density that may cause refraction and reflection of a signal back to earth. The E-layer is not as strong a reflector as the F-layer in the range 150–500 km where the electron density is the highest. This is the layer that most frequently reflects the signals back to earth. The F-layer is most of the time present in the upper atmosphere, but with varying electron density. The electron density in all layers is somehow dependent on the angle of incidence of the sun, and

[5] In this report the terms “layer” and “region” will both be used. Although there exist no strict definitions of the two, the term “layer” reflects a more regular horizontal structure of ionization whereas the term “region” merely refers to the height range above the surface of the earth, where also irregular ionization is present.

therefore the time of day, time of year and the geographical position on the earth. The intensity of radiation from the sun depends upon the 11-year sunspot cycle, so the conditions for communications via the skywave are also dependent on this cycle. In general, the propagation of an electromagnetic wave through the ionosphere is a very complex interaction between the wave energy, the gaseous ionized media and the geomagnetic field.

The frequency band that is allowed skywave transmission is determined in the following way, according to Eriksen et al [14] : "Radio wave propagation is possible between a higher limit, called the Maximum Useable Frequency and a lower limit called the Lowest Useful High Frequency. The upper limit is principally given by the properties of the ionosphere, chiefly the electron density, and does not depend upon transmitted power or any other factor under our influence. The lower limit is determined by the absorption in the ionosphere, but also on the radiated power, the efficiency of the aerials involved and the noise level at and in the receiver. The lower limit is, therefore, a much more complicated limit to calculate and does not, in the same way as the upper limit, represent a physical boundary given by nature."

Overlaid the "normal" ionosphere created by the electromagnetic radiation from the sun, there may be additional ionization. The sun is also a secondary source of ionization in the earth's atmosphere, namely by emitting ionized particles through irregularly occurring solar flares. These particles are trapped within the earths magnetosphere[6], where they follow the magnetic dipole field lines to the geomagnetic poles and are precipitated there over the geomagnetic poles. The magnetosphere is thus governing the ionization caused by particle precipitation. The effects of this ionization is the visible aurora and disturbed conditions for navigation and communication signals. The conditions for signal propagation may at times be improved because the ionization is strengthened, for example by the creation of auroral/sporadic E-layers that may reflect high and very high frequencies. At other times the conditions may be worse because increased ionization in the D-layer causes excess absorption. The velocity of the ionization may also cause increased Doppler spreads which may be a problem for communications.

3.2 Monitoring the ionosphere – ionospheric measurements

3.2.1 Ionosondes and the measurement of ionospheric reflection

An ionospheric sounder (ionosonde) is an instrument that transmits short pulses of radio waves vertically and measures the delay of the signal that is returned to the receiver which is located at the same position as the transmitter (radar at HF).[7] A series of delays are measured as the transmission frequency is continously increased. The delays are translated into a virtual height of reflection of the signal, and these virtual heights versus frequencies transmitted are displayed in an ionogram. Typical characteristics of an ionosonde could be: Frequency range 0.5–30 MHz,

[6] The magnetosphere is the space around the earth (or another planet) where a magnetic field is present.
[7] Oblique incidence sounders also exist. The receiver is then located at a different position from the transmitter.

bandwidth 34 kHz, ionogram scan time 2–200 s, peak pulse power 150 W, sensitivity -130 dBm [16].

An ionosonde has been operated from Tromsø in Norway for several decades, and data are available since the 1980's [9]. The current instrument [16] has been running since 2003 providing a real-time ionogram every 15 minutes. These data have been used in the current study. Another high latitude ionosonde can be found in Kiruna in Sweden, and a mid-latitude ionosonde in Lycksele [17], also in Sweden. The latter has been used in this study.

The ionogram shows the presence and strength of ionospheric layers at the time of the measurement. It also shows extraordinary ionization caused by particle precipitation. If no layer is present in an ionogram, the cause may be either that there is simply no ionization in the atmosphere to reflect the signal at that particular moment (rather seldom), or, there may be a disturbance with greatly enhanced electron densities in the D-layer which causes absorption and therefore no registered echoes by the ionosonde. Thus the ionosonde does not distinguish between these two situations. An example of an absorption event in the D-layer lasting approximately an hour, "hiding" the ionization above it, is shown in Figure 3.1. The solar F-layer is visible at 12 Universal Time (UT), disappears, and then is visible again at 13:15 UT.

To distinguish between a situation where absorption is the cause of a blank ionogram and a situation where there is a lack of ionization, additional data from a riometer could be of help (see the next section). However, if the ionogram is not completely blanked out by absorption, there is a possibility of identifying the presence of smaller absorption levels from the ionogram itself by inspecting the lowest frequency where a signal is registered. If absorption is present, the lowest observed frequency will be higher compared to a situation where there is no absorption. This is further explained in Section 3.5.

The ionograms may also show the dynamic nature of high latitude ionization due to particle precipitation. During geomagnetic disturbances, dense auroral ionization at E-layer heights may suddenly occur, "hiding" the regular solar ionosphere above it. This is illustrated in Figure 3.2 by two ionograms from Tromsø measured 15 minutes apart. From 13:30 UT to 13:45 UT an auroral E-layer is created that reflects the signal, preventing the signal from being reflected at the solar F-layer above it.

12:00 UT **12:15 UT**

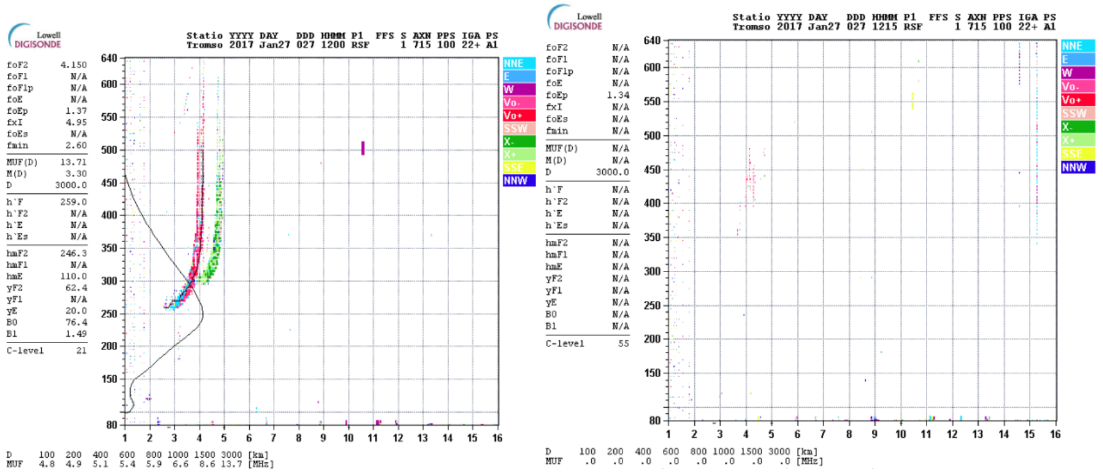

13:00 UT **13:15 UT**

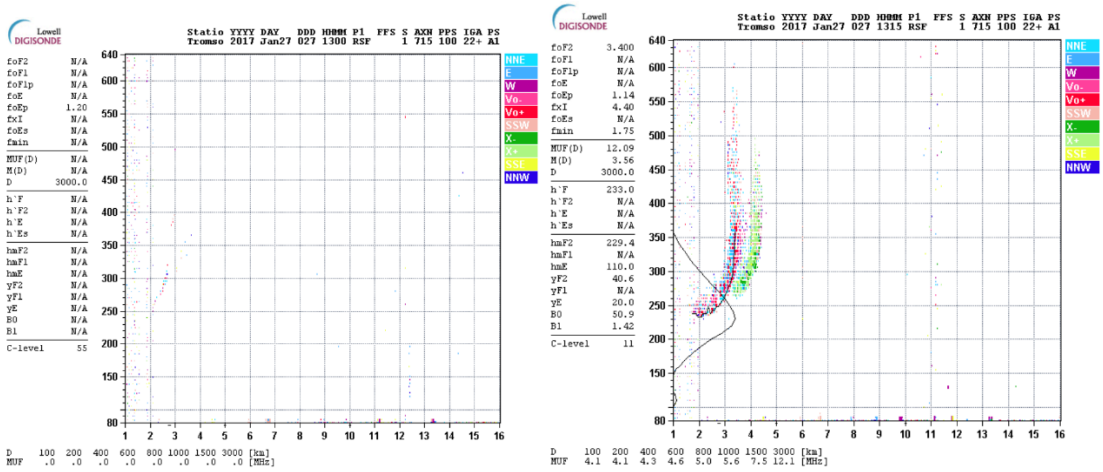

Figure 3.1 Absorption in the D-layer is hiding the ionization in the F-layer above it for a period of time [9]. Transmitted frequency on the x-axis and virtual height of reflection on the y-axis. The two traces shown correspond to different ray paths with different polarization of the signal as it traverses the ionosphere (ordinary and extraordinary wave). Ionospheric parameters and electron density profile are extracted from the measurements and displayed in the plot.

13:30 UT **13:45 UT**

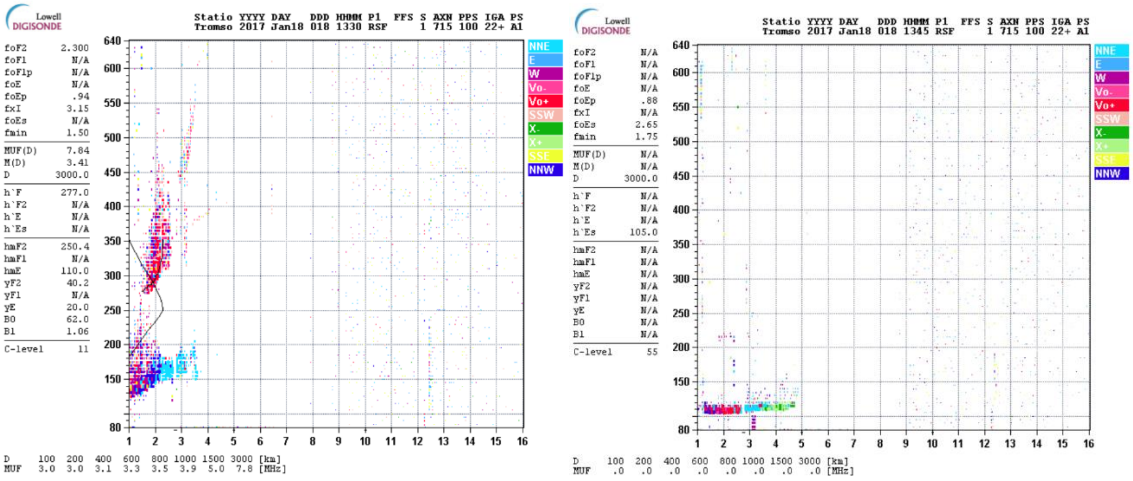

Figure 3.2 Particle precipitation causes rapid changes of the ionization at high latitudes [9].

The ionograms from polar regions are much more "complex" than ionograms from lower latitudes, meaning that the curves shown are spread out, not showing a simple trace. As an example, ionograms from Tromsø and Lycksele, taken at approximately the same time, are shown in Figure 3.3, showing the larger complexity of the high latitude ionogram.

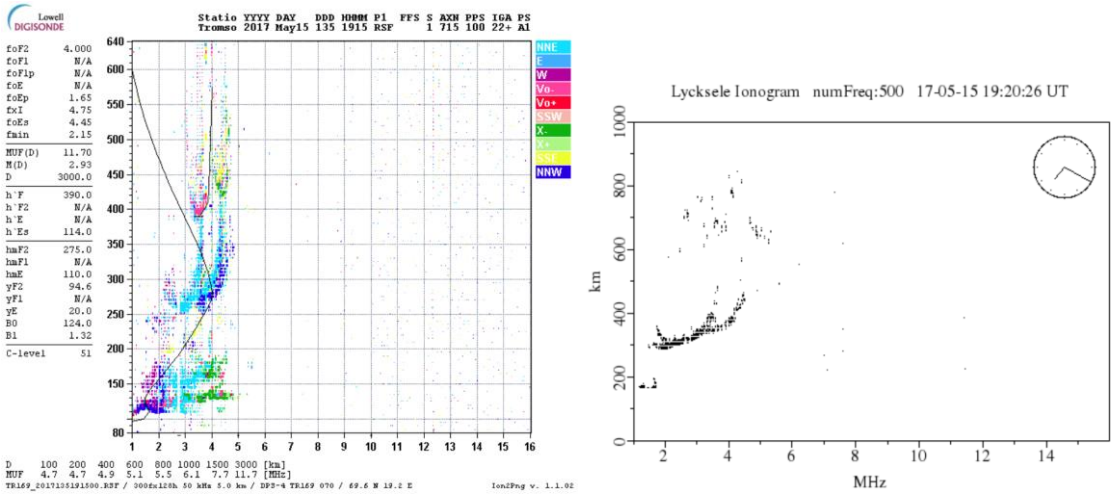

Figure 3.3 Ionograms at high latitudes are more complex than at lower latitudes. Ionograms taken five minutes apart in Tromsø (left) and Lycksele (right).

3.2.2 Riometers and the measurement of ionospheric absorption

A riometer is a particularly valuable instrument to measure the ionospheric absorption. Eriksen et al. [14] says: "A riometer (Relative Ionospheric Opacity meter) measures the cosmic radio noise which mainly comes from the area near the center of the galaxy. The riometer method

assumes that the intensity of this radio noise is constant in time. Therefore, as the earth rotates relative to the noise sources, the intensity of radio noise falling on the earth's atmosphere at a fixed geographical position will vary in a regular manner and be a function of sidereal time[8] only. The radio noise reaching the ground will have suffered absorption in the ionosphere, and variations in this absorption can be found by comparing measurements made at corresponding sidereal times. A typical riometer operates on a frequency of about 30 MHz. A radio wave on 30 MHz travelling from space through the undisturbed ionosphere will suffer an absorption between 0.1 and 0.5 dB depending on the solar zenith angle. During disturbed conditions at high latitudes the absorption may be up to 15 dB."

The riometer in its basic form is simple and not expensive, but there also exist more advanced imaging riometers that provide high resolution, two-dimensional images of the cosmic radio noise in an area of several hundred km around the riometer. Riometers can be set up in a net of stations to map the geographical extent of ionospheric phenomena.

There are several riometer stations located at high latitudes, for instance in Ny Ålesund, Longyearbyen and Skibotn in Norway [9] and Kiruna [17] and Abisko [8] in Sweden. There is also a "chain" of riometers at different latitudes in Finland [8]. Data from Abisko have been used in this study. An example of measured absorption from [8] is shown in Figure 3.4.

The measured absorption at a frequency of 30 MHz corresponds to a much larger absorption at frequencies in the lower HF-band, which we will come back to in Section 3.5. The elevation angle of an oblique incidence skywave path and the distance through the absorbing D-region must also be taken into account when "translating" a measured riometer absorption to an expected absorption loss of a particular skywave path.

[8] Sidereal time is a time scale that is based on the earths rate of rotation measured relative to the fixed stars.

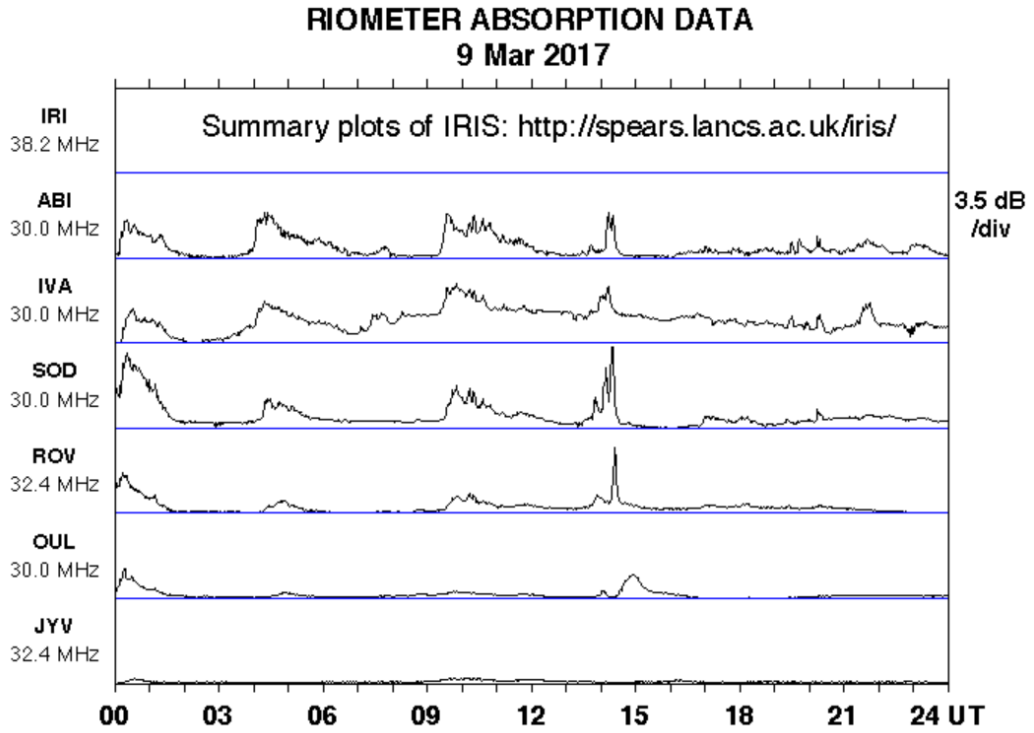

Figure 3.4 Example measurements of riometer absorption at frequencies around 30 MHz at six stations in Finland/Sweden [8].

3.3 Ionospheric F2-layer characteristics

The time variations of solar origin of the D- and E-layers are regular over the day and over the year, and they can be attributed to the time variations in the solar elevation and the solar radiation [14].

The F-layer that most often reflects the radio signals, hereafter called the F2-layer, is not as regular as the D- and E-layers. The variations of the solar elevation alone cannot account for the behaviour of this layer.

The critical frequency[9], f_oF2, of the F2-layer measured at a mid-latitude station is displayed in Figure 3.5 [14]. It shows that during the winter, f_oF2 of the F2-layer has a diurnal variation similar to the diurnal variation of the solar elevation, whereas in summer the critical frequency is almost constant over the day. The winter curve is explained by the fact that the largest ionization occurs during the highest solar elevation angles which occur around noon. The summer curve with approximately the same f_oF2 throughout the day is explained in [14] as being due to a seasonal variation in the upper atmosphere temperature and an expansion of the atmosphere (and ionosphere) in the summer time, lowering the electron density around noon

[9] The critical frequency of a layer is the maximum frequency at which a signal can be transmitted vertically and be reflected back to a receiver at the same position as the transmitter.

and therefore “flattening” the curve showing the diurnal variation. It is surprising that in spite of the fact that the sun is much higher above the horizon during the summer time than in winter, the noon value of f_oF2 in the winter is about 5 MHz higher than the summer noon value.

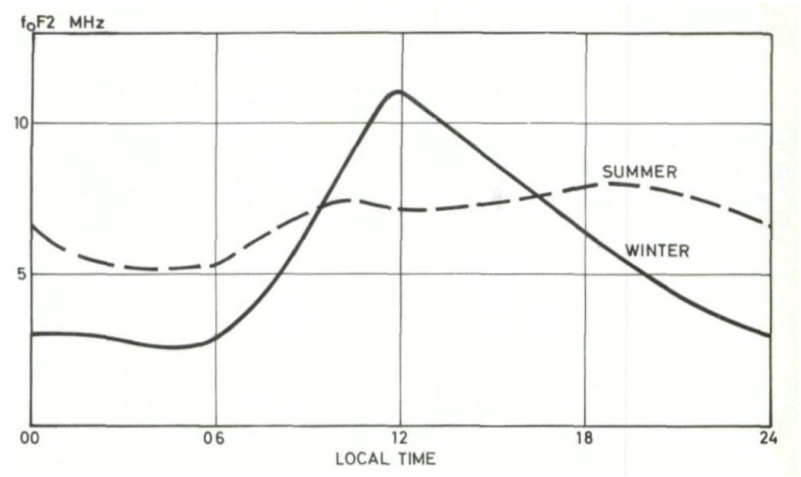

Figure 3.5 Critical frequency for F2-layer measured at a mid-latitude station [14]. Average diurnal variation shown. Unknown measurement period.

At higher latitudes, the F2-layer ionization is significantly lower than the numbers for lower latitudes indicated in Figure 3.5. The f_oF_2 decreases about 1 MHz per 10º of latitude between 20º and 70º. During a geomagnetic disturbance, the F-layer may become thicker, and the f_oF_2 may decrease significantly.

For the longer term variation of the f_oF2, the dependence on the sunspot cycle seems to be much stronger than for the E- and D-layers, see Figure 3.6. In the figure, *noon* values of f_oF2 over one month have been averaged and plotted, therefore the maximum values occur during winter. The critical frequency of the E-layer, f_0E, has its maximum value in summer time.

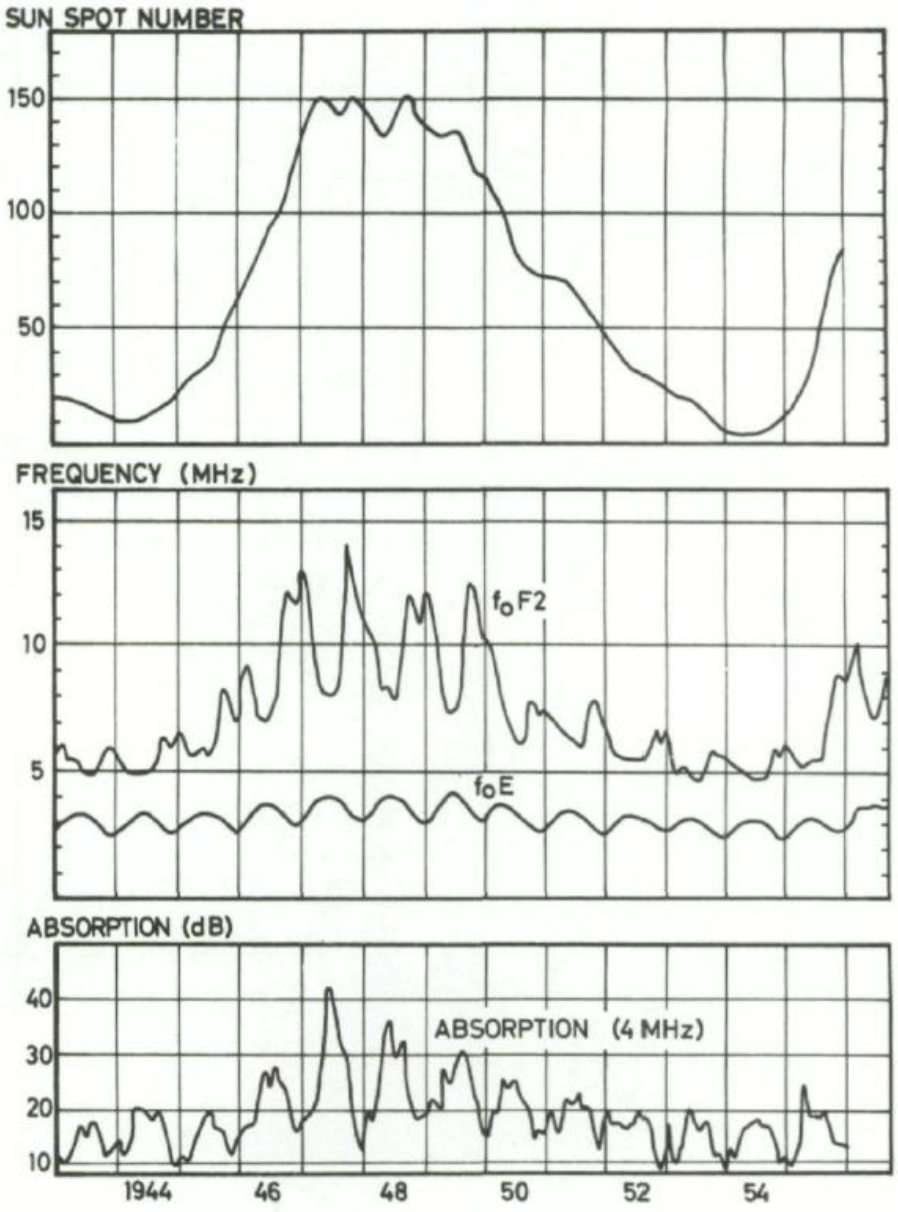

Figure 3.6 Long term variations of critical frequencies in the F2- and E-layers at a mid-latitude station. Absorption at 4 MHz for the same period is also shown [14].

3.4 Auroral E-layer characteristics

At high latitudes, irregular ionization in the D- and E-layers often occurs as a result of variations in the radiation and particle precipitation from the sun. Hence, the electron density and the conditions for radio wave propagation are dependent on these events rather than the regular time variation of the solar elevation.

Irregular ionization takes place in the height range 100–150 km above the surface of the earth, and this ionization is refered to in different literature as the sporadic E-layer (E_s), the night E-layer or the auroral E-layer. This auroral ionization may sometimes provide help in arctic communication. The sporadic E-layer at high latitudes is restricted to a certain latitude interval, about 10° wide, which is centered at a latitude close to the maximum of visual auroral activity, that is at a geographical latitude of about 70° over northern Europe and about 60° over North America.

The mean annual occurrence of a critical frequency, f_oE_s, greater than 5 MHz is given in Figure 3.7 [14]. The f_oE_s exceeds 5 MHz in 10–30 % of all hours at high latitudes, except very close to the North Pole where sporadic-E rarely occurs. It may also be seen that the sporadic-E is dependent on geographic longitude. The phenomenon occurs about three times as frequently over North America as over Siberia. The difference is believed to be attributed to the geomagnetic field, but it is not fully understood. At Scandinavian longitudes the occurrence rate is closer to 10 %. At times the f_oE_s may even exceed 15 MHz, which for oblique incidence ray paths would mean the reflection of frequencies way into the VHF-band [10].

According to [14]: "Ionosonde records show two types of E_s-ionization, and these two types are referred to as the *retardation* and the *non-retardation* types of E_s-ionization, respectively. The layer that gives rise to the retardation type of E_s-ionization on the ionogram is fairly thick, whereas the non-retardation type of E_s-ionization may be referred to as a thin, blobby, ionospheric layer. The retardation type of E_s-ionization is fairly uniform in a horizontal direction, and ionosonde recordings at points separated by 100 km are almost identical. The ionization shows slow variations during the night, and it behaves more like a regular ionopheric layer. The retardation types of sporadic-E are quite common phenomena and are therefore of considerable interest for radio communications in the polar regions. This layer occurs during conditions when no distinct disturbances are present. The non-retardation E_s-ionization, on the other hand, shows a very irregular structure and high variability also in time. For that reason this layer is not very reliable for radio communications."

The high latitude sporadic-E is a night time phenomenon. During 70–100 % of all nights the f_oE_s exceeds 5 MHz in the auroral zone, whereas such high critical frequencies are seldom observed during day-time. At stations situated at the northern border of the auroral zone, the strongest E_s-ionization is found at about 21 hours local time. Further south this maximum of the E_s-ionization occurs later in the night, and at the lower latitudes where sporadic-E occurs, the maximum ionization is found in the early morning hours.

The sporadic-E also undergoes a typical "storm-time variation". During geomagnetic storms, the sporadic-E near the auroral zone is particularly well developed. It is also observed south of the visual auroral zone rather than in the middle of the zone. It may be shifted 3º–6º south of its normal geographical latitude during heavily disturbed periods.

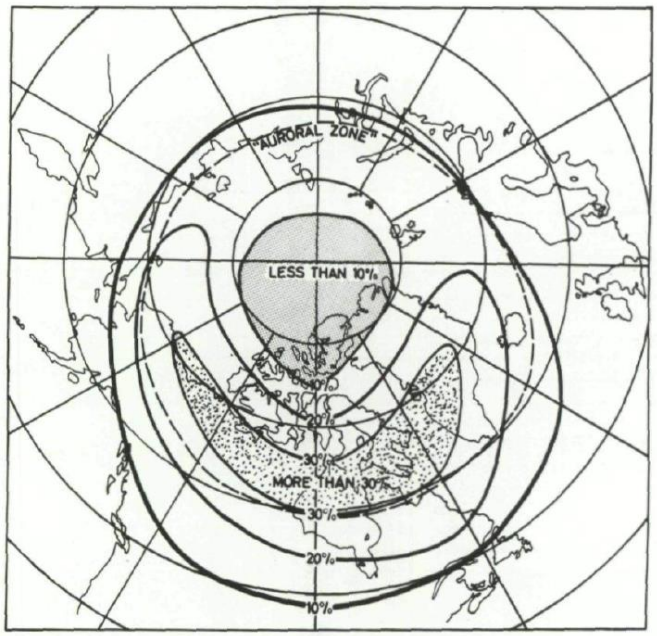

Figure 3.7 Percentage number of hours when f_oE_s is greater than 5 MHz at various geographical locations [14, but originally in E.K. Smith, National Bureau of Standards Circular 582, 1957]. The zone of visual aurora is shown by the broken line.

3.5 D-layer ionospheric absorption

The greatest loss of an electromagnetic radio wave travelling through air or vacuum is the free space loss. However, for skywave paths at high latitudes, the ionospheric absorption can sometimes be severe and of equal magnitude to the free space loss. The physical process of this so-called non-deviative[10] ionospheric loss is explained in Eriksen et al. [14]: "A free electron oscillating in the electric field of the radio wave will pick up energy from the wave. If the electron is allowed to oscillate freely in the wave field, this energy will be reradiated. If, however, the electron collides with heavy particles like ions or neutral air molecules, then the electron may lose its oscillatory energy. This latter energy will not be reradiated and will therefore be removed from the wave. We will appreciate that the loss the wave suffers in this manner must depend on the electron density N, the collision frequency v of electrons with heavy particles and on the time the wave remains in the layer. The absorption will decrease when the wave frequency increases. This is to be expected since, at a high frequency, an electron in the wave field may oscillate many times between collisions which will therefore, play a minor role."

[10] There is also an additional deviative ionospheric loss associated with the refraction process of the radio wave in the upper ionospheric layers. The deviative loss is in most circumstances much smaller than the non-deviative loss.

3.5.1 Simplified calculations of the non-deviative ionospheric absorption

In the following, some details are given about the calculation of the ionospheric absorption, in order to understand the factors influencing it. We have further calculated the absorption values of the actual measurement paths in this study using the simplified formulas.

The non-deviative loss L at a frequency f can be expressed in a simpified form by the formula [14]:

$$L = \text{constant} \cdot \frac{1}{f^2} \int_{s1}^{s2} N \cdot v \, ds$$

where N is electron density, v is collision frequency and s_1 and s_2 are end points of the ray path within the region where the product $N \cdot v$ is sufficiently high. This turns out to be the D-layer. The formula indicates that the loss has a strong dependence on the frequency, where the lower frequencies are subject to the largest losses.

If a riometer measures an absorption of L_{30} dB at a frequency of 30 MHz, the corresponding absorption L at another frequency f can then be calculated according to the formula:

$$L = L_{30}(\tfrac{30}{f})^2 \; [dB]$$

During normal, undistured ionospheric conditions the absorption measured by riometers at 30 MHz will be between 0.1 and 0.5 dB. If the measured riometer absorption is 0.2 dB at 30 MHz, the formula above tells us that the corresponding absorption at 5 MHz will be 7.2 dB. If the measured riometer absorption increases to 1 dB at 30 MHz, this corresponds to an absorption of 36 dB at 5 MHz, which is a fairly high loss for a radio signal.

If simplifications are made with an assumption of a constant N and v, and a specific height of reflection, the calculation using the formulas above reduces to a geometric consideration taking into account only the angle of elevation and the frequency. The following formula can be used for a simplified estimation of the non-deviative oblique incidence ionospheric loss L_{obl} where the signal is traversing the D-region two times:

$$L_{obl} = 2 \cdot L_v \cdot \left(\frac{30}{f + f_L}\right)^2 \cdot \frac{1}{\sin \alpha} \; [dB]$$

L_v is the vertical loss measured by the riometer, α is the angle of elevation of the ray path and f_L is the gyrofrequency[11] caused by the magnetic field (which is approximately 1.4 MHz at high latitudes).

Using this simplified formula, we have estimated the ionospheric loss at three of the paths in our measurements (Chapter 4) using their path lengths and an assumed height of reflection of 200

[11] The gyro frequency is the frequency of rotation of an electron or other charged particle in a magnetic field.

km. If we assume a measured riometer absorption of 0.5 dB, the corresponding ionospheric losses at a few different frequencies that are likely to propagate on the respective paths are shown in Table 3.1. The numbers are based on the assumption that the ionosphere is the same on both the upleg and the downleg, which may not be true, especially on the long-haul paths. For a riometer absorption of 1 dB the absorption values will be doubled.

	Harstad (75 km)	**Boden (370 km)**	**Växjö (1345 km)**
2.5 MHz	60 dB	80 dB	
5.0 MHz	22 dB	30 dB	77 dB
9.0 MHz			29 dB

Table 3.1 Ionospheric absorption at various frequencies and oblique incidence skywave paths from Setermoen when riometer absorption is measured to 0.5 dB. (Calculations based on certain assumptions and using the simplified formula.)

For a more accurate calculation of the absorption, the electron densities and collision frequencies along the ray path has to be known. Several authors have described the relationship between measured riometer absorption and D-layer ionization [18], [19]. A D-layer model [19] with measured riometer absorption as the driving input, was proposed for the calculation of absorption on HF-skywave paths in prediction programs [11]. The approach gave predictions in much better agreement with measurements at high latitudes than without this D-layer model.

3.5.2 Characteristic of various types of absorption

At high latitudes, the irregular ionization of the D-layer has its origin in solar flares emitting electromagnetic radiation and charged particles. The increased D-layer ionization associated with solar flares is the cause of increased ionospheric absorption of the radio signal. There are different processes with different time lags associated with a solar flare that cause the enhanced D-layer ionization, as shown in Figure 3.8. A thorough treatment of the different disturbances and the effects upon radio communications is given in [10] and [14]. The following paragraphs present short characteristics of the most important phenomenas, to be used as a foundation for the data analysis in the current work.

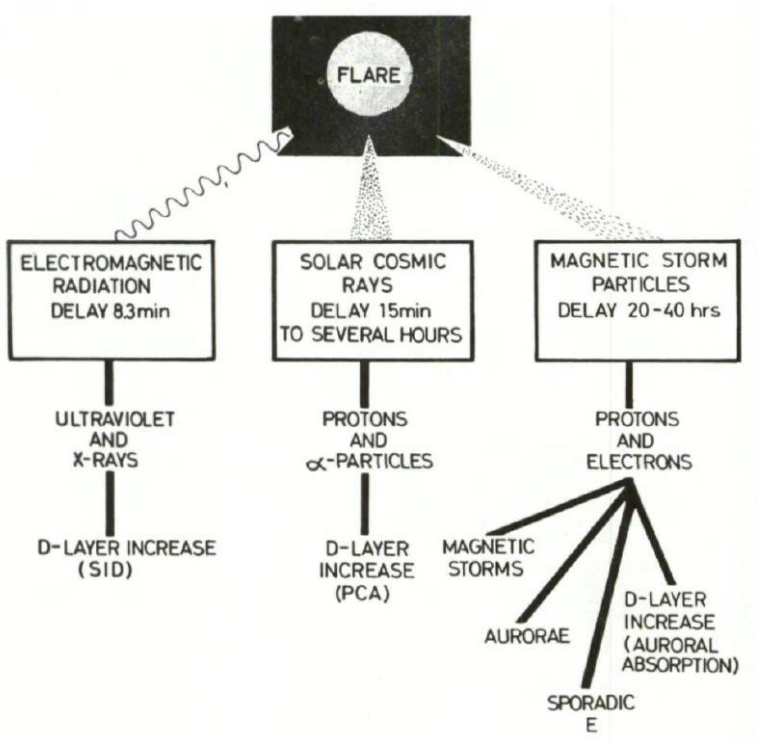

Figure 3.8 Consequences of a solar flare on the ionosphere [14].

Sudden ionospheric disturbances (SID) are caused by enhanced ultraviolet and x-ray radiation from the sun, and the increased absorption on earth is observed 8 minutes after the flare (determined by the speed of light).

Polar cap absorption (PCA) is the result of very energetic protons and alfa-particles associated with major storms arriving at the earth approximately 15 minutes after a solar flare. The particle influx is uniform over the entire polar region. The absorption decreases at nighttime, due to chemical processes triggered by the solar radiation [14].

The number of PCA events ranges from 0–1 per year at sunspot minimum to 10–15 at sunspot maximum. No seasonal dependence of the occurrence rate is known. The average duration of a PCA is about 1.5 days, but particular events may last for several days. A PCA has the most servere impact on HF communications with radio “blackouts” that may last for days.

Auroral absorption is caused by particle precipitation consisting of electrons and protons with energies below 100 keV[12]. The time of occurrence is not strictly connected with the time of the solar flare since the particles are trapped in the magnetosphere and may be precipitated days after the occurrence of the flare. These particles can be associated with minor as well as major solar disturbances. Minor solar disturbances occur quite frequently so they generally have a large impact on radio communication in the polar regions. The absorption associated with this

[12] Measure of energy, kilo electron Volt (keV)

type of particle precipitation is closely related to geomagnetic disturbances measured by magnetometers and auroral activity. In the following, we show some of the characteristics of measured absorption at high latitudes.

Figure 3.9 (from [14]) shows a curve giving the diurnal variation of the percentage time the absorption exceeds 1 dB at a typical high latitude station. We see that there is a maximum of absorption in the early morning hours local time (LMT). At 06 local time (which means 05 UT), the absorption exceeds 1 dB for 16 % of the total time. The time period and number of measurements analysed is unknown. We have done a similar analysis for all riometer data measured in Abisko for the year 2017, and the results are shown in Figure 3.10. We see the same trend with a maximum absorption in the early morning hours, although more hours are affected. The maximum percentage of time is 8 % occurring at 06 UT, which is somewhat lower than the maximum in Figure 3.9. When we examined the absorption measurements month-by-month, there was a small tendency of highest absorption around the equinoxes and lower absorption during the winter and summer months.

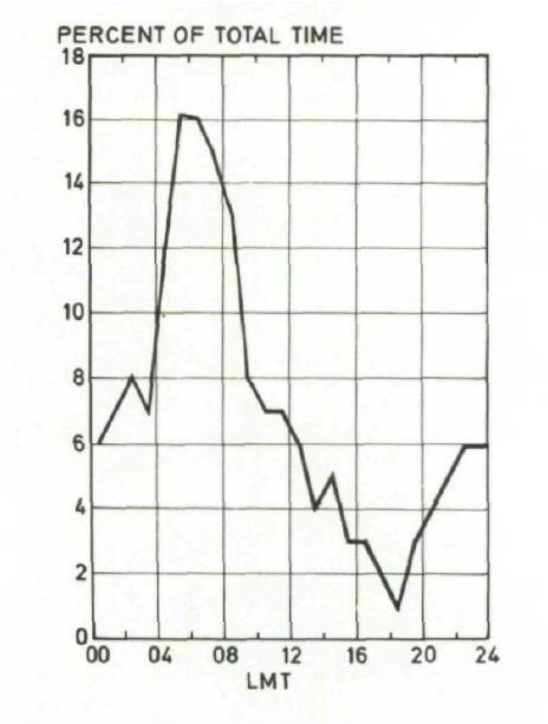

Figure 3.9 Percentage of time that riometer absorption at 27 MHz exceeds 1 dB. Measured in Skibotn, Norway [14].

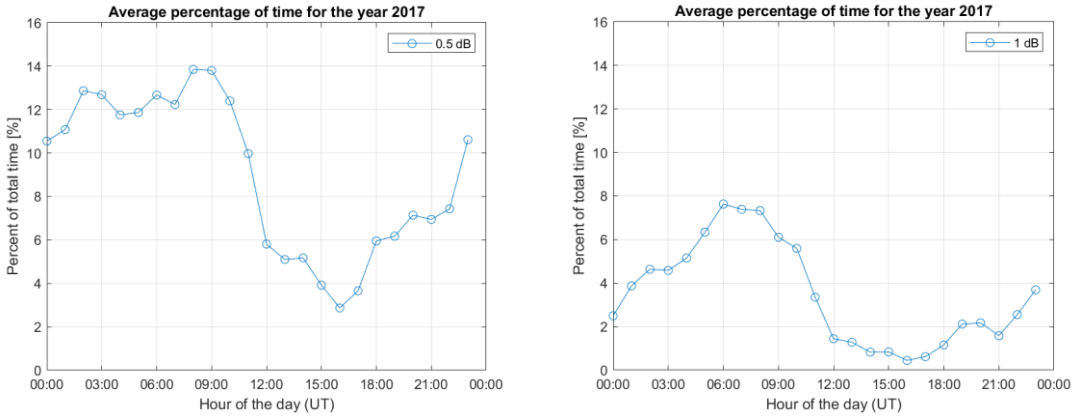

Figure 3.10 Percentage of time that riometer absorption measured at 27 MHz in Abisko exceeds 0.5 dB (left) and 1 dB (right). One year of data from 2017.

It has been found that the time of maximum probability of auroral absorption is governed by local geomagnetic time[13] rather than local solar time. The difference between the two varies throughout the day up to a few hours. Figure 3.11 (from [14]) plots contours showing the percentage of time with absorption greater than 1 dB on a map in geomagnetic coordinates, (geomagnetic latitude and time). We see that the absorption occurs most frequently in the morning hours. The geomagnetic latitude where the absorption is most frequent, corresponds roughly to the zone of maximum auroral activity.

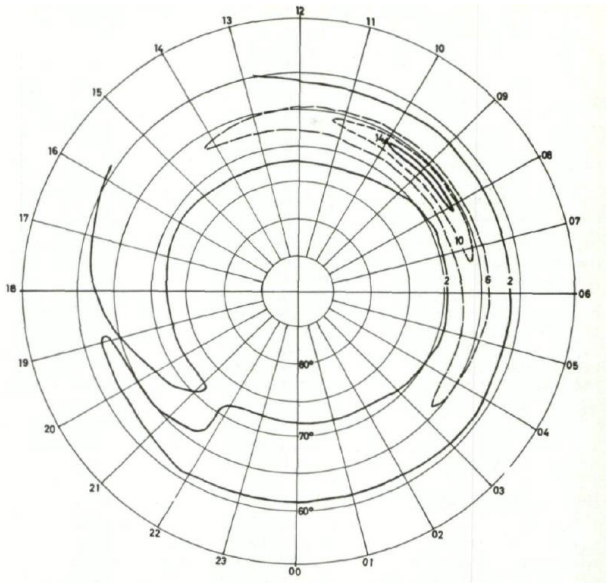

Figure 3.11 Contours showing percentage of time (2 %, 6 %, 10 %, 14 %) the absorption exceeds 1 dB plotted in geomagnetic latitude and time [14].

[13] Geomagnetic time gives solar orientation with respect to geomagnetic meridians in a centered dipole representation of the Earth's magnetic field. The angle between the geomagnetic north pole and the geographical north pole is less than 10º.

The auroral absorption varies rapidly in time and space. The average duration of the absorption events has been calculated in [14] by examining riometer measurements throughout a year (1958–1959, near sunspot maximum) at five stations in respectively Longyearbyen, Bear Island, Skibotn, Trondheim and Kjeller. The duration of all periods of continuous absorption greater than 0.5 dB was calculated. The distribution of the durations is shown in Figure 3.12. It is seen that for 83 % of the cases the duration of an event is shorter than 3 hours.

We have conducted a similar study using riometer data measured in Abisko in 2017. A complementary cumulative distribution function (CCDF) was calculated in order to show the duration of all absorption events. An absorption "event" was defined as the duration of continuous absorption above a certain threshold, but with allowance of short excursions below the threshold lasting less than 10 minutes. All events in the whole dataset were identified and plotted as a CCDF with the durations shown on the x-axis (abscissa) and the probability on the y-axis. Thresholds of 0.2 dB, 0.5 dB and 1 dB absorption were investigated. The results for the various thresholds are shown in Figure 3.13. 50 % of the 0.2 dB events have a duration longer than 50 minutes, whereas 50 % of the 0.5 and 1 dB events have a duration longer than 30 minutes. 10 % of the 0.2 dB events have a duration longer than 210 minutes (3.5 hours), whereas 10 % of the 0.5 dB events have a duration longer than 160 minutes (2.8 hours). When the data were examined month-by-month, no clear seasonal trend could be observed. The data are not directly comparable with the previous result in Figure 3.12, since the dataset included measurements from many different locations. Nevertheless, the results are similar.

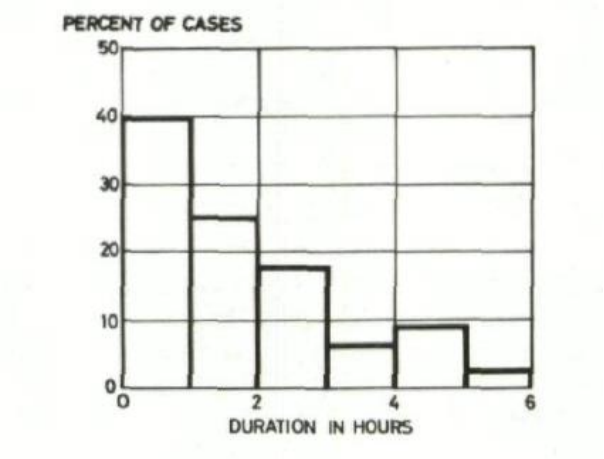

Figure 3.12 Probability that an interval with absorption greater than 0.5 dB is of a certain duration [14].

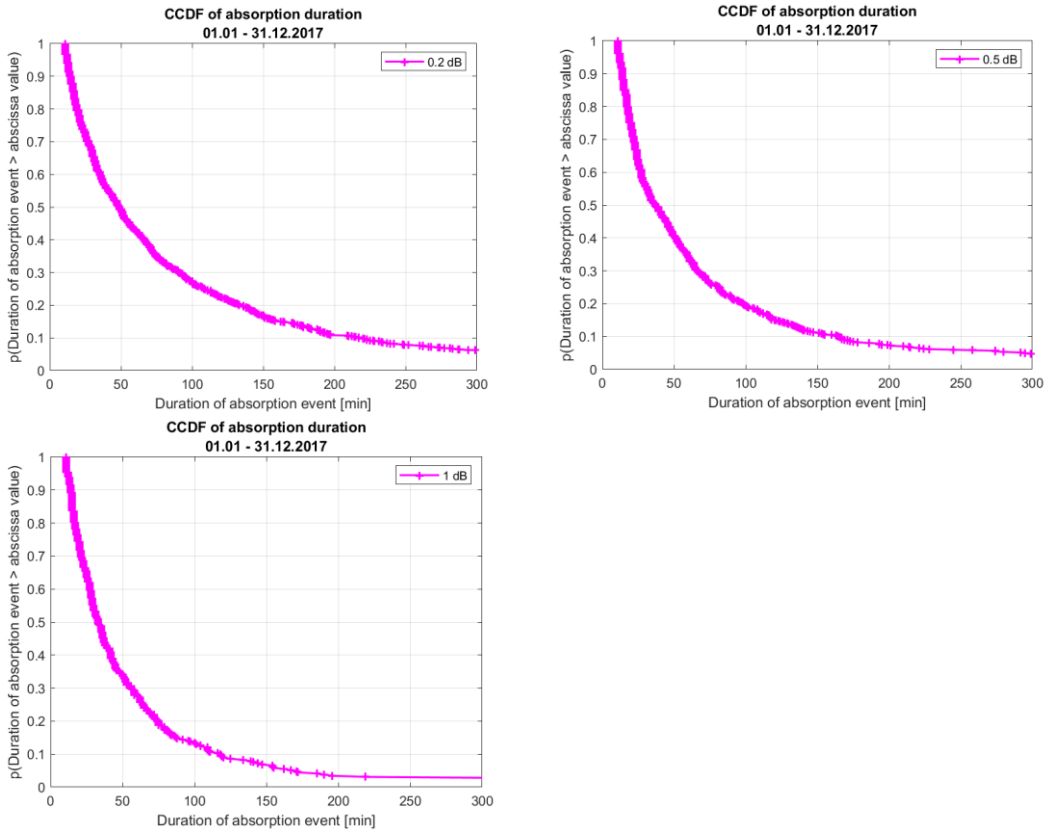

Figure 3.13 Complementary cumulative distribution functions for the duration of absorption events measured in Abisko for the year 2017. ≥0.2 dB events (upper left), ≥0.5 dB events (upper right) and ≥1 dB events (lower left).

The geographical extension of ionospheric absorption has also been studied in [14]. For a one-year period close to the sunspot maximum, data were collected from five riometer stations at, respectively, Hammerfest, Alta, Kautokeino, Skibotn and Harstad (that is, fairly closely spaced locations). The time variations of absorption measured at the five stations were found to be very similar, except for some details. The result indicates that the absorbing clouds are fairly large (of the order of some hundred kilometres) in horizontal extent. Similar data can be studied from the Finnish riometer chain provided in reference [8].

There is a close relationship between the increased absorption due to D-region ionization and geomagnetic and auroral activity. An analysis in [22] states that large absorption never occurs without large geomagnetic activity, whereas large geomagnetic activity can occur without simultaneous absorption measured by riometers. The relationship between measured geomagnetic activity and absorption was also analysed in [11].

Both the sporadic-E ionization described in Section 3.4 and the auroral type ionization in the D-region are considerably enhanced during geomagnetic storms. As a result, communications exploiting sporadic-E propagation will be of particular importance during periods when communication becomes difficult because of the auroral type absorption. The auroral absorption

is occurring over distances of ~100 km exention, but it varies rather rapidly with time. In the periods between the high absorption peaks, the sporadic E-layer often provides possibilities of communication. Sporadic-E propagation may also be possible at quite high frequencies. Also, if a relay station may be used for communications in addition to the direct path between two nodes, the presence of sporadic-E propagation on one of the paths, but not the other, may increase the total time with ionospheric propagation, and therefore communication.

As a conclusion of this chapter, Figure 3.14 shows an artist impression of the sun-earth interactions [9].

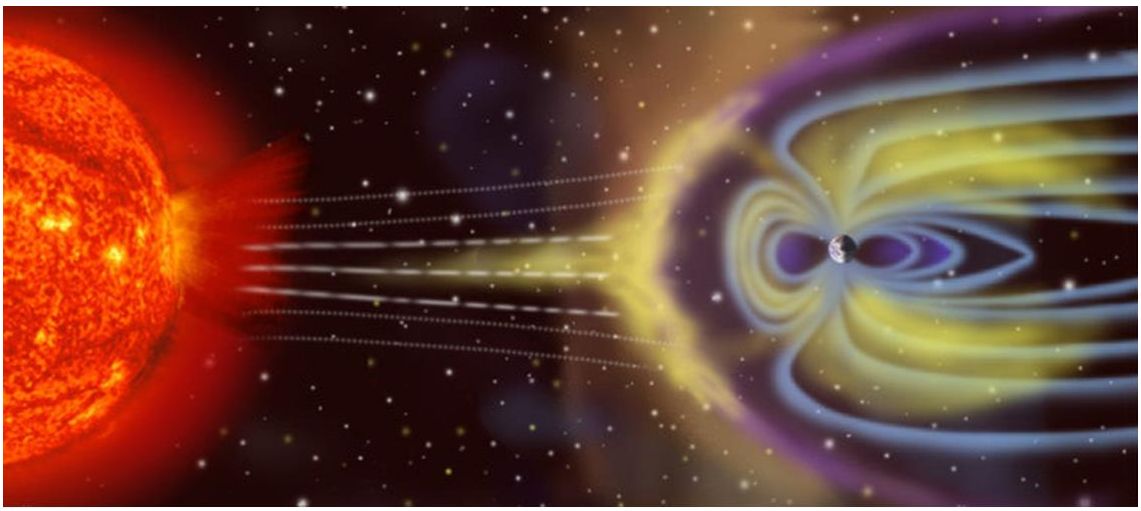

Figure 3.14 Artist impression of sun-earth interactions [9].

4 Measurements overview

We used Harris RF-5800H and RF-7800H radios in the measurement setup, running STANAG 4538 (3G) protocols with automatic link establishment and adaptive data rate within 3 kHz bandwidth. Two 3G networks were set up, comprising two different frequency plans (each of 6 frequencies): The short-haul network consisted of a 20 W transmitter at Setermoen with receivers in Harstad, Alta and Boden. The long-haul network consisted of a 400 W transmitter at Setermoen with receivers in Bergen and Växjö. A small test message was sent sequentially and repeatedly from the transmit site at Setermoen to each of the receivers, running 24 hours a day. The control- and data logging software was developed at FFI, and valuable assistance was received from Harris Corporation during the work. The test setup and software are thoroughly described in [2].

In collaboration with Försvarets Materielverk (FMV) and Combitech in Sweden, we ran measurements from January 2017 until June 2018. We received assistance and support by many people, both at the Norwegian Armed Forces test sites and at the Swedish test site in Boden, during the execution of the experiment.

A more thorough description of the equipment and measurement procedures are found in Appendix A, which is an extract of the conference paper [3]. A map of the measured paths is shown in Figure 4.1, and another map showing the sites of ionospheric measurements by riometers and ionosondes is shown in Figure 4.2.

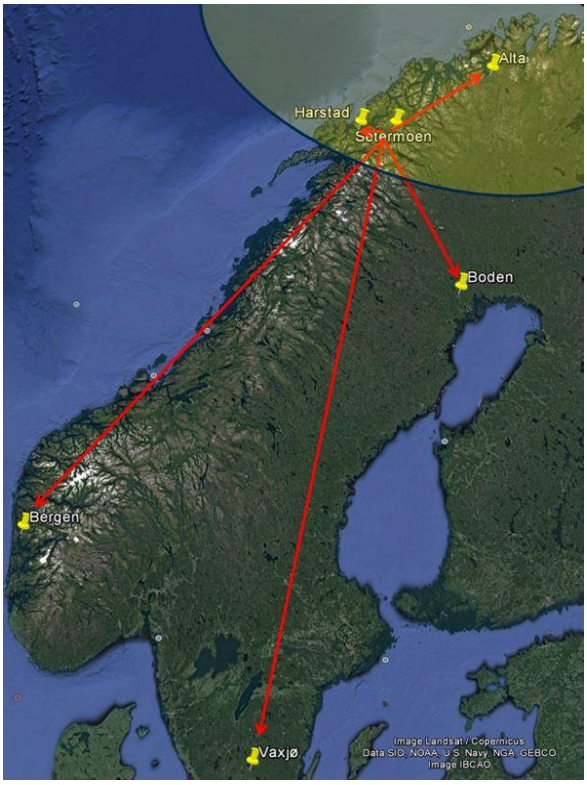

Figure 4.1 Measurement paths. Two transmitters at Setermoen. Receivers in the short-haul network are located in Harstad, Alta and Boden, and receivers in the long-haul network are located in Bergen and Vaxjø. A disturbed high latitude ionospere is illustrated by a highlighted area.

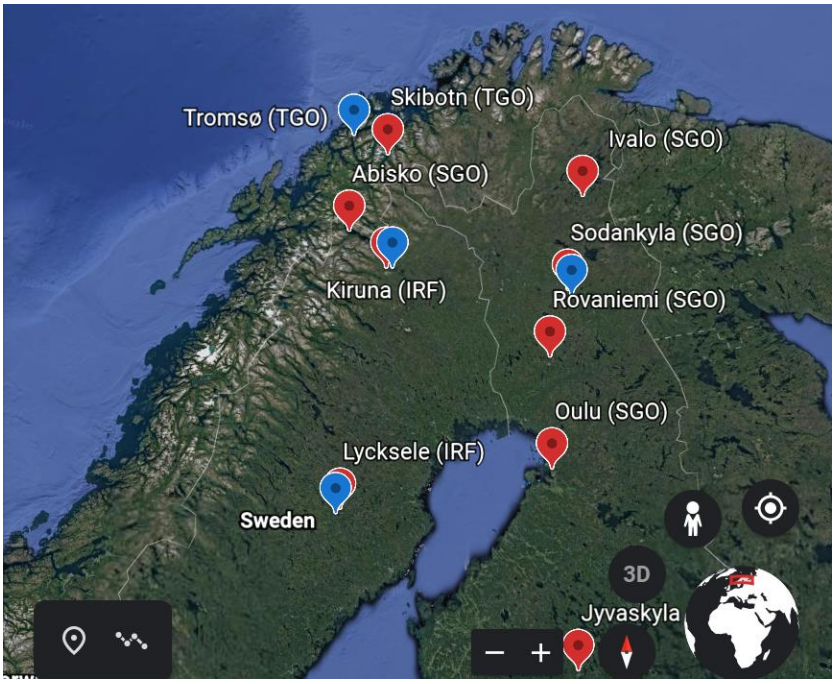

Figure 4.2 Sites of ionospheric measurements in the north. Red markers indicate riometers, and blue markers indicate ionosondes. The sites are run by Tromsø Geophysical Observatory (TGO), Swedish Institute of Space Physics (IRF) and Sodankylä Geophysical Observatory (SGO).

There were numerous technical problems that caused halts in the data collection on the different paths, and there were relatively few longer time periods where *all* the stations were running simultaneously, collecting valid data throughout the full day. This caused complications in the data analysis, since many individual days had different amounts of data on different paths, thus requiring individual treatment of each day. Nevertheless, on the long-haul network, data have been collected for more than a year, and all seasons are well represented in the database. The short-haul network experienced more problems, and particularly during the last half year, the transmitter operation halted regularly from midnight until morning so that night conditions are not well represented in the data from December 2017 until the end of the measurements.

On the long-haul network, we also chose to collect a few periods of wideband HF (WBHF) data. This was not possible on the short-haul network because WBHF was not implemented in the Harris RF-5800H radios used in this network. Towards the end of the data collection period, the power was also reduced to 50 W in certain periods on the long-haul paths to test the possibility of using less power.

5 Analysis and results

The data were collected from January 17th 2017 until June 19th 2018. This period is near the sunspot minimum and the data thus represent the conditions that can be expected around sunspot minimum. The results may be different in other parts of the 11-year sunspot cycle.

The data analysis method is stepwise described in Appendix A. While only some examples of the analysis results were presented in the conference paper [3], we present here the complete set of results from all periods of good data collection, and interpret the results in the light of other types of data such as riometer absorption and ionograms.

5.1 Probability of linking and space diversity over various months

First, the probability of linking measured nearly simultaneously on various paths are compared. For each hour, there were a number of transmission attempts from Setermoen to each of the receivers. From the number of transmission attempts, the number of link successes were counted. The probability of linking is calculated as the percentage of the transmission linking attempts that succeeded for a particular hour over all days within a given period. In this analysis the number of measurements on each path and hour may vary somewhat, but the number is for each case considered to be large enough to give a representative picture.

For the evaluation of space diversity, we have imagined an operational scenario where two military units want to communicate with each other at a relatively short distance within the disturbed region; in our analysis exemplified by the path from Setermoen to Harstad. Given that the units have the option of linking to another site as an intermediate node (one of the other paths in our experiment), we define two different measures that both represent space diversity: 1) The percentage number of hours where higher linking probability is achieved on the other path, and 2) the average increase in linking probability compared to the linking probability on the single path within the disturbed region. In the latter measure, for the hours where the difference in linking probability was negative (meaning that the Harstad path had the highest probability), the difference was set to zero, so that the average always will be positive. This measure thus represents an average “additional advantage” of having the second path on which to establish a link. For this analysis of space diversity, an unequal number of data points for the different datasets can have a large impact on the results, thus this analysis is not performed for all the data sets (where we otherwise have useful data).

In order to isolate different propagation characteristics, we defined periods of days that were analyzed together. All the days of one period were within approximately one month (to have the same solar conditions), and they also experienced approximately the same degree of disturbance as measured by the riometer in Abisko (Sweden) [8]. For the periods analyzed in this section, the selected days were picked only by roughly inspecting each day of riometer measurements. Days with (long or short) absorption events larger than 2 dB at 30 MHz were categorized as *disturbed*, whereas days with no peak of absorption larger than 2 dB were categorized as

undisturbed. The position of the riometer in Abisko is at a distance of 60 km from Setermoen, and the measured absorption events are thus expected to correlate well with channel degradation on the short-haul paths, albeit less so for data on the long-haul paths.

In a few cases where only few days had valid data that could be sorted in disturbed/undisturbed periods within a month, we plotted all days together, giving an average over all conditions. This average will thus hide the relatively large difference between disturbed and undisturbed days.

In the following, we present the different data sets for each month of the year. Undisturbed periods are shown in the following figures to the left, disturbed periods to the right, and if a mixture of undisturbed and disturbed days is shown, the plot is shown in the middle.

5.1.1 January

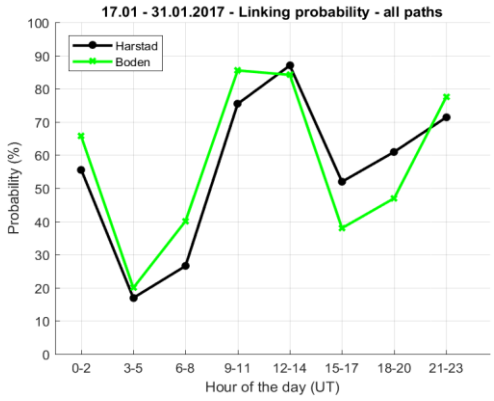

Figure 5.1 January 2017. 15 days analysed containing both undisturbed and disturbed days. Data available only from Harstad and Boden.

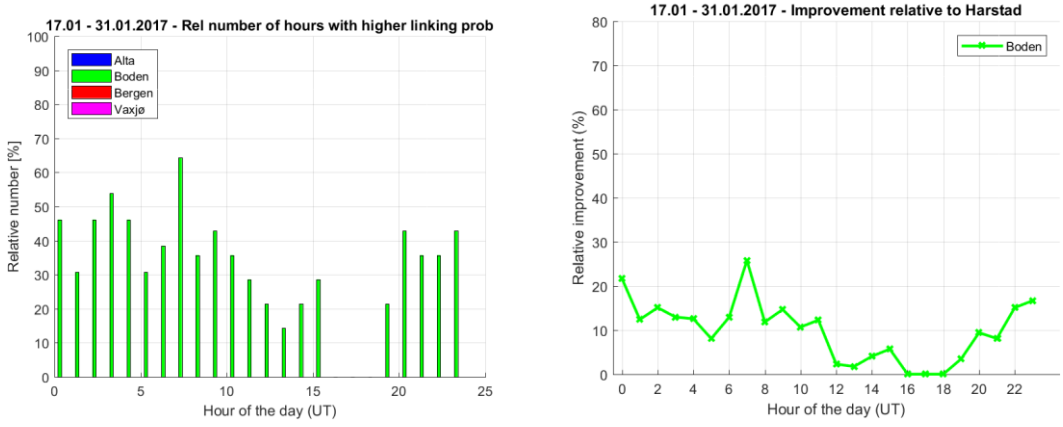

Figure 5.2 January 2017. Space diversity for same period as in Figure 5.1.

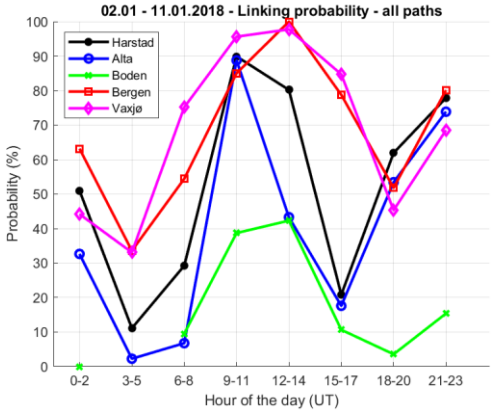

Figure 5.3 January 2018. 9 days analysed in an undisturbed period. (Only 5 days in Boden. Only 4 days with data at night hours on short-haul paths.) No data collected during disturbed conditions.

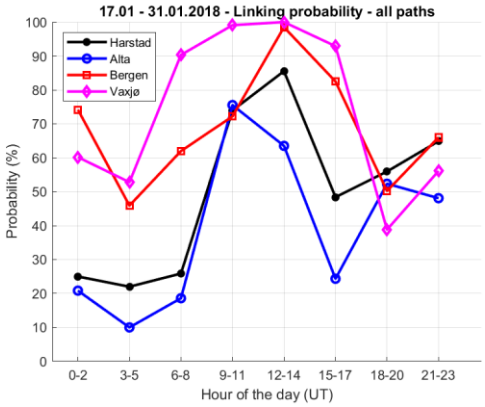

Figure 5.4 January 2018. 13 days analysed in an undisturbed period. (Only 3 days with data at night hours on short-haul paths.) No data collected during disturbed conditions.

Local midday is at 11 UT and we see that for all the periods analyzed in January, the conditions for communications are best around the local midday from hours 9 to 14 UT. For these hours, the diurnal variation of the sun gives a steady ionized F-layer reflecting the HF-signals. For the long-haul paths, the reflection point is farther south than for the short-haul paths and the number of sun-lit hours in the F-layer is higher, giving a longer period of high linking probabilities around noon.

A second, but lower, maximum of linking probability occurs in the hours around geomagnetic midnight, which is at 22 UT. During these hours, particle precipitation is creating auroral E-layers and sporadic ionization at various heights and of various density as observed on ionograms measured in Tromsø. For the long-haul paths, the ionograms measured in Lycksele show that auroral E- layers are also present around geomagnetic midnight at this site. This explains the higher linking probability also for the long-haul paths.

Minima of linking probability occur when there is no ionization present, or during extraordinary absorption events. This is further addressed in Section 5.2.

The linking probabilites are fairly similar on the different short-haul paths (except Boden in the 2nd–11th of January 2018 period, which is probably due to few days of successful measurements). The linking probabilities are also similar on the two long-haul paths, and in general higher than for the short-haul paths.

Figure 5.2 (left) shows the percentage of hours where the linking probability was higher on the path to Boden compared to the path to Harstad. In the night from 19 UT until 10 UT, generally 30–50 % of the hours compared had a better linking probability. (50 % means that the two paths are equally successful in linking over the hours compared.) For the rest of the hours the percentage was less, meaning that the Harstad path was more successful. The average improvement (always positive) is shown in the Figure 5.2 (right). 10–20 % increase in linking probability is experienced if the secondary path to Boden is an option. Our interpretation of the two measures of space diversity is that from 22 UT until 11 UT the two paths are approximately equally successful in linking, but they are complementing each other in such a way that approximately 10–20 % higher linking probability is gained for these hours. For the rest of the day, the gain is less than 10 %.

We have not calculated space diversity for the measurements in 2018 when data on the long-haul paths were available because there was little data collected at night time on the Harstad path. However, if we assume that the night time Harstad curve in 2018 is similar to the corresponding curve in 2017, we could reason that the long-haul paths would provide significant space diversity gain for the periods shown in Figure 5.3 and 5.4.

The distributions of frequencies automatically selected by the radios during the 17th–31st January 2017 period for the paths to Harstad and Boden, are shown in Figure 5.5 and Figure 5.6 respectively. We see that higher frequencies are selected during day time than during night time, which is in agreement with standard frequency predictions. Due to the auroral ionization at night, there are nevertheless times when very high frequencies are selected. The frequencies selected to Boden are generally higher than to Harstad since the path is longer.

During the measurements taken in January 2018 for the longer paths, the frequencies selected were between 4 and 9 MHz during the day and between 4 and 6 MHz during the night. This is also in agreement with predictions. Occasionally the higher frequencies 11 and 13 MHz were selected on the longer paths.

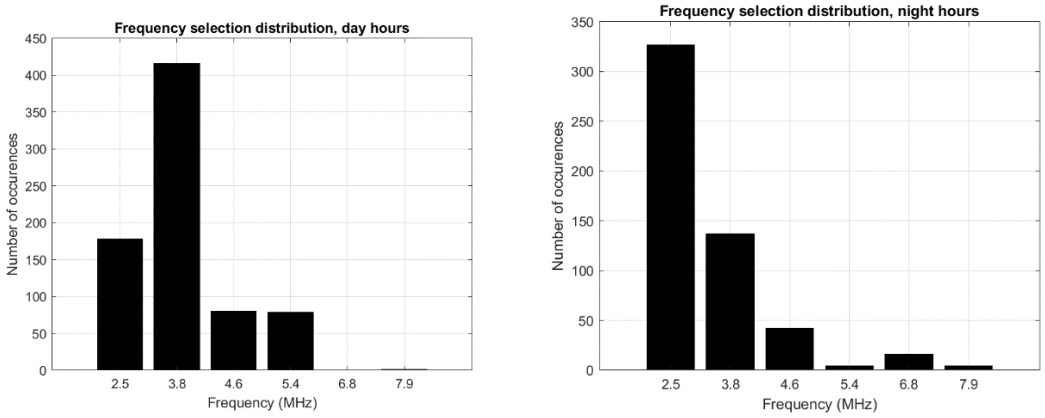

Figure 5.5 Frequency selection on the path to Harstad, 17.01.2017–31.01.2017. Day hours (left), night hours (right).

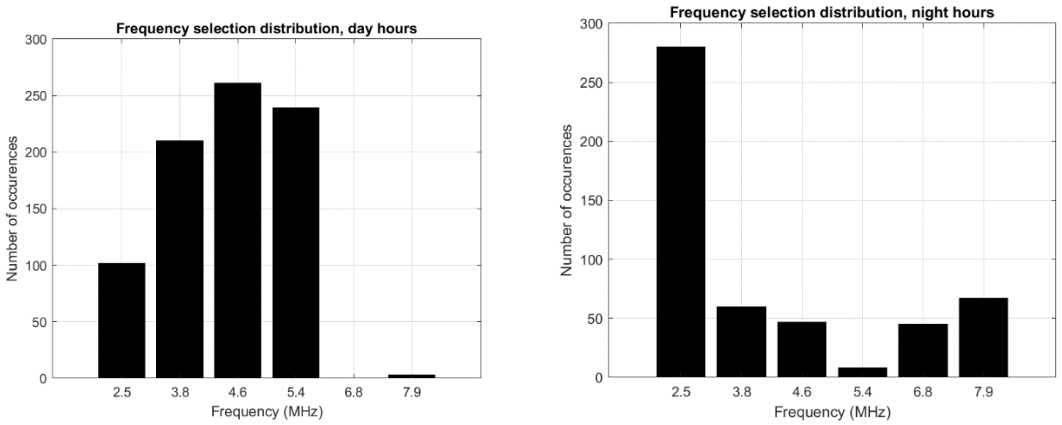

Figure 5.6 Frequency selection on the path to Boden, 17.01.2017–31.01.2017. Day hours (left), night hours (right).

5.1.2 February

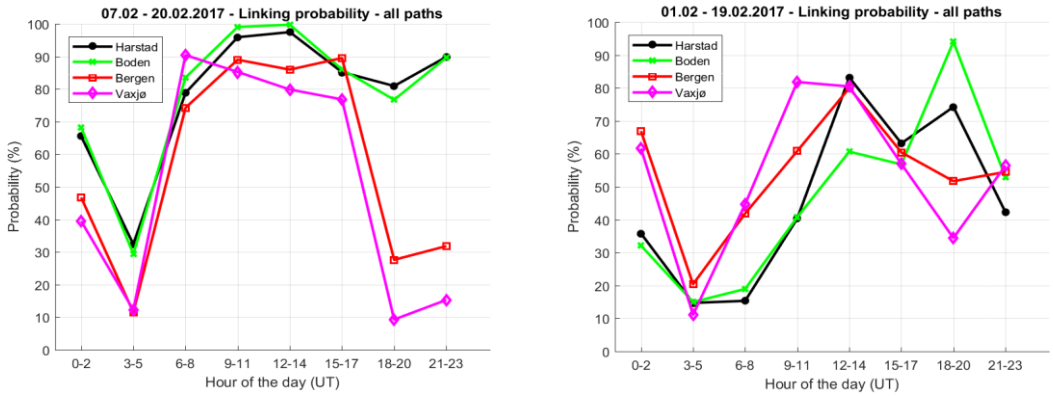

Figure 5.7 February 2017. 11 days analysed in undisturbed period (left). (Only 6 days in Växjö.) 9 days analysed in disturbed period (right). (Only 6 days in Boden.)

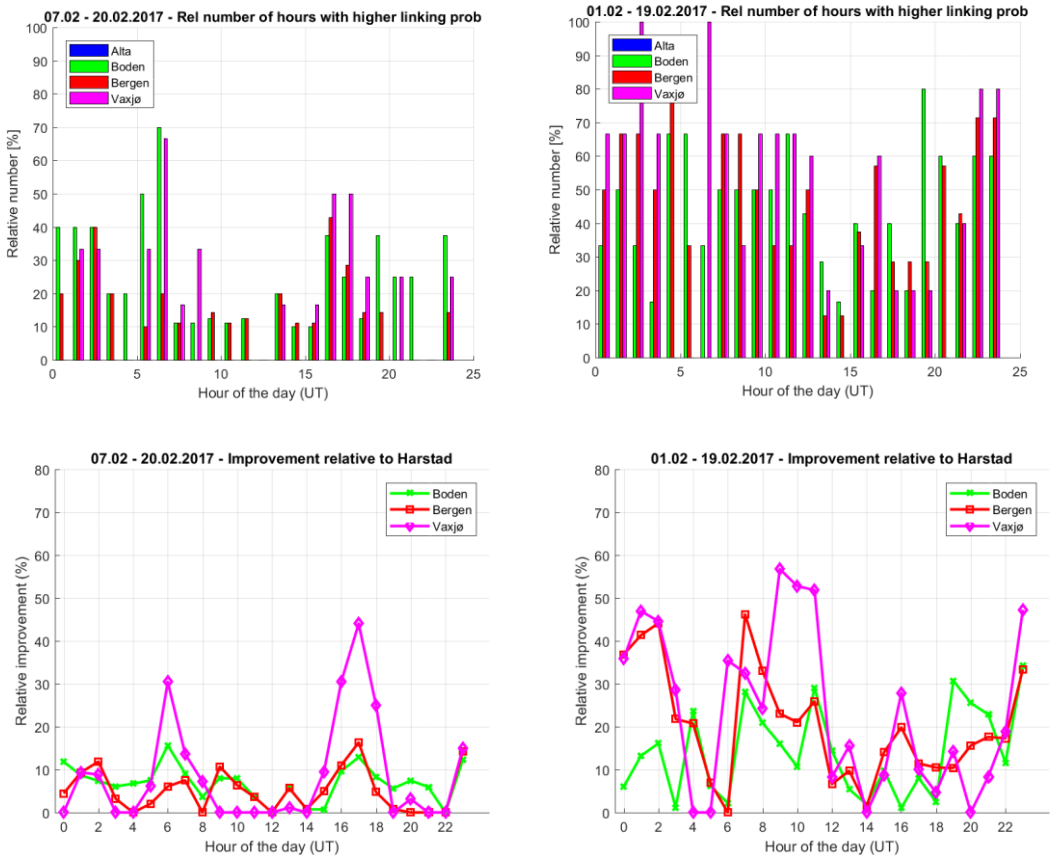

Figure 5.8 February 2017. Space diversity for same periods as in Figure 5.7. (No data collection on the Alta path.)

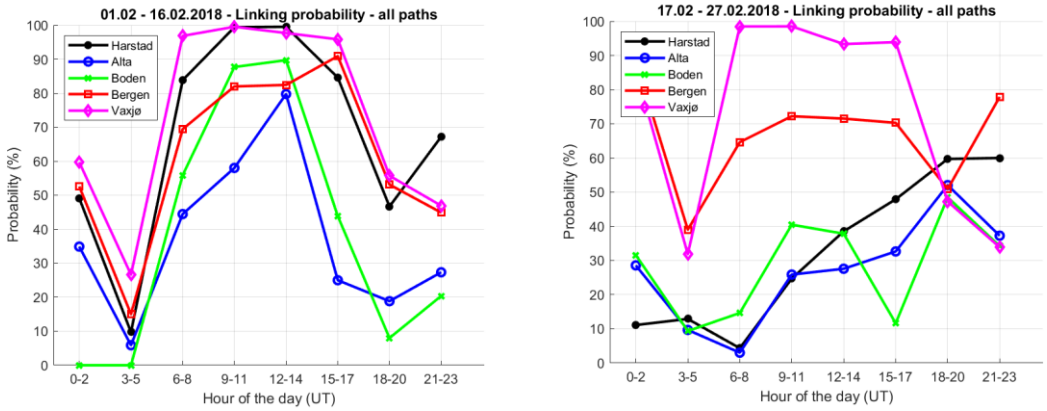

Figure 5.9 February 2018. 15 days analysed in undisturbed period (left). (Only 5 days in Boden. Only 4 days at night hours on short-haul paths.) 7 days analysed in disturbed period (right). (Only 3 days in Boden. Only 4 days in Växjö. Only 2 days at night hours on short-haul path.)

Measurements from February have been divided into undisturbed and disturbed periods, shown left and right in the figures, respectively. The measurements conducted in February 2017 gives the best statistical picture (Figure 5.7 and Figure 5.8) since some of the data sets from February 2018 are rather small (Figure 5.9). The following analysis applies in particular to the February 2017 data set.

Undisturbed conditions – 2017 (left figures)
For the undisturbed periods, linking probabilites on the short-haul network are similar to the linking probabilities on the long-haul network, see Figure 5.7 (this applies partly also to the 2018 data in Figure 5.9). The space diversity plotted in Figure 5.8 shows that 30 % and 45 % higher linking probability could be achieved by using the Växjö path during a few hours around dawn and dusk, respectively. At other hours, there is generally 10 % or less to be gained by linking via another path.

Comparing undisturbed conditions in January and February, on the short-haul paths, the number of hours around noon with high linking probabilities has increased from January to February. This is explained by a longer time period of a sun-lit, high latitude ionosphere in February. This difference cannot be seen on the long-haul paths, where the linking probabilites are fairly similar to the January data. Also for February, auroral ionization around geomagnetic midnight gives high linking probabilites on the short-haul network.

Disturbed conditions – 2017 (right figures)
The disturbed conditions are considerably different from the undisturbed conditions. The linking probability is generally lower, and particularly so in the morning hours. According to the riometer absorption measurements in Abisko, all the disturbed days experienced heavy absorption in the night and morning hours. The duration of absorption varied between a long period 0–14 UT and shorter periods such as 5–7 UT. For most days the absorption continued until 12 UT. According to the ionospheric data from Lycksele for the disturbed days, absorption

is present also at this location and is therefore also affecting the longer paths. However, ionospheric reflections are present on the ionograms from 6 UT onwards, in agreement with the higher linking availabilities measured on the Växjö path for these hours.

The space diversity plotted in Figure 5.8 shows that the absorption is affecting both the short-haul and long-haul paths for the hours 4–5 UT, and there is little advantage in linking via Växjö or Bergen. However, for the hours 23 UT until 11 UT, except for the hours 4–5 UT, there is 30–55 % space diversity gain, which is a considerable increase in linking probability.

Data from 2018

Data from 2018 are displayed in Figure 5.9. The rightmost graph shows measurements from a number of disturbed days. The Växjö and Bergen measurements show the same diurnal variability as from the undisturbed period (leftmost figure), and do not seem to be affected by the increased absorption levels measured in Abisko. Inspection of ionograms measured in Lycksele shows an undisturbed ionosphere for the corresponding days, which supports the observations of high linking probabilites. The ionograms measured in Tromsø, however, show a disturbed ionosphere with D-layer absorption "hiding" the F-layer ionization for several hours. We therefore conclude the following: The linking probabilities towards Växjö are very high compared to the other paths, because the path is outside the disturbed region. We have indications from the ionograms in Lycksele that the picture would have been the same if more days of data in Växjö had been available within the period (only four days of data were available). We do not show the space diversity gains for the 2018-data because of the low number of measurements during night hours on the short-haul network.

Frequencies selected on the Växjö path during the undisturbed and disturbed periods can be studied in Figures 5.10 and 5.11, respectively. We see that during the undisturbed period the frequencies selected are higher at day than at night, in agreement with predictions. During the disturbed period however, higher frequencies are to a larger extent selected at night. This is due to the strong auroral ionization at night that is able to reflect higher frequencies.

The frequencies selected on the Bergen path were similar to those selected to Växjö, except for the most selected frequency being one frequency lower at night time.

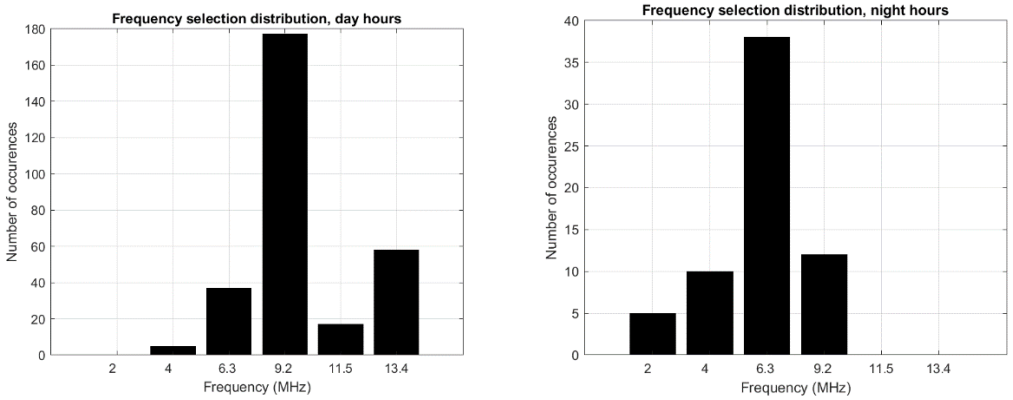

Figure 5.10 Frequency selection on the path to Växjö, undisturbed period 07.02.2017–20.02.2017. Day hours (left) and night hours (right).

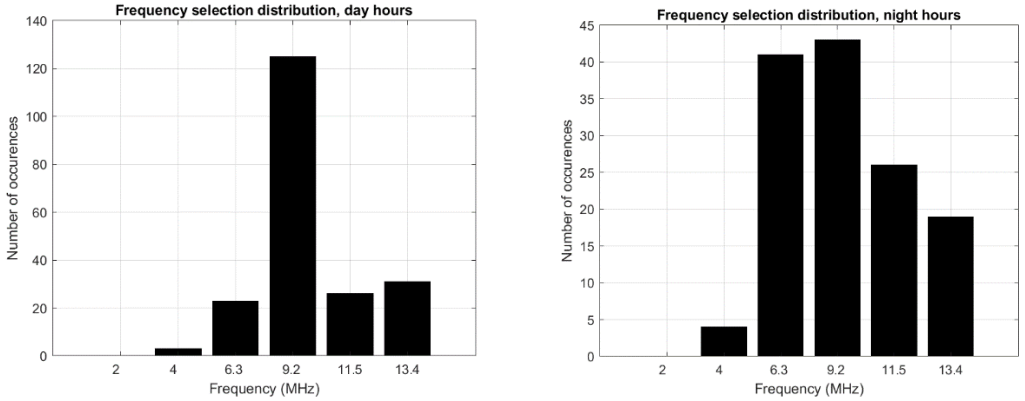

Figure 5.11 Frequency selection on the path to Växjö, disturbed period 01.02.2017–19.02.2017. Day hours (left) and night hours (right).

5.1.3 March

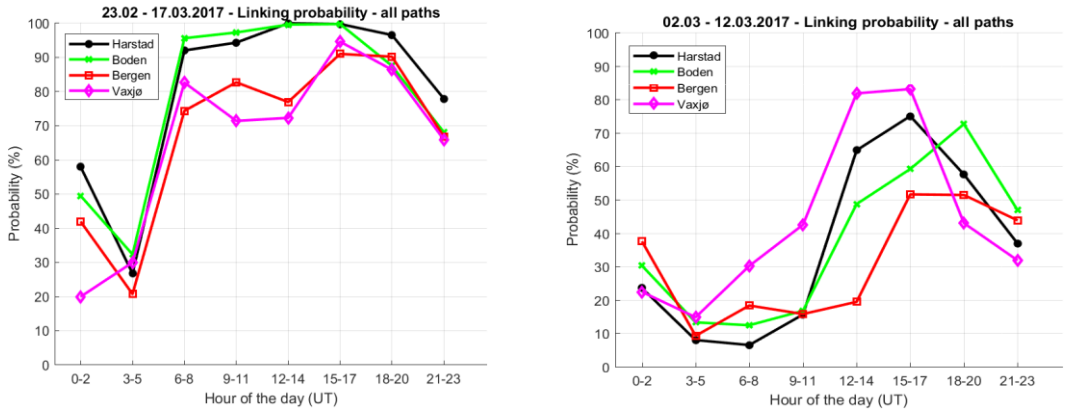

Figure 5.12 March 2017. 11 days analysed in undisturbed period (left). (Only 7 days in Växjö.) 10 days analysed in disturbed period (right).

Figure 5.13 March 2017. Space diversity for the same period as in Figure 5.12.

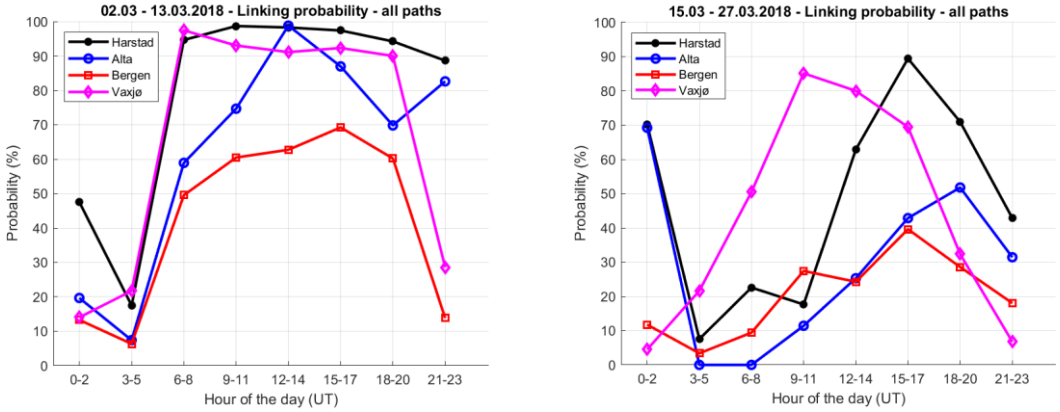

Figure 5.14 March 2018. 11 days analysed in undisturbed period (left). (Only 5 days in Växjö. Only 4 days at night hours on short-haul paths.) 11 days analysed in disturbed period (right). (Only 5 days in Alta. Only 2 days at night hours on short-haul paths.) WBHF on long-haul paths.

Two periods respectively from March 2017 and March 2018 have been analysed. Again, the data sets from 2018 do not contain as much data as the data sets from 2017, so the analysis below applies in particular to the data sets from 2017.

Undisturbed conditions – 2017 (left figures)
When considering the linking probabilites for the undisturbed period in Figure 5.12, the diurnal variation is very much the same on all paths. The linking probability is for most hours high, and it has increased in the afternoon hours compared to the February data, the same trend as we observed when comparing February- with January data. The lowest linking probability occurs for hours 03-05 UT also for March.

The space diversity during the undisturbed period is generally low, with a maximum of 25 % only for a few particular hours. For the day-hours there is no gain at all.

Disturbed conditions – 2017 (right figures)
For the disturbed period in Figure 5.12, the linking probabilites are much the same as for the February data. Absorption events in the morning hours from 03 UT to 11 UT have the largest impact on propagation on the short-haul paths, but influences also the long-haul paths, particularly the path to Bergen. In this dataset the path to Växjö has clearly the highest linking probabilities. A space diversity gain of 10–45 % is obtained by the path to Växjö for all hours except for the morning hours 02–04 UT when the gain is below 10 %.

Data from 2018
For the measurements in 2018 (Figure 5.14), the linking probabilities show approximately the same diurnal variability as for the previous year for both undisturbed and disturbed conditions. The Växjö path is in these measurements considerably better than the Bergen path for both the undisturbed and disturbed periods. This will be discussed in Section 6.1.

We do not show the space diversity gains for the 2018-data because of the low number of measurements during night hours on the short-haul network.

When comparing the frequencies selected for the undisturbed and disturbed periods respectively, the frequencies selected during day-time is approximately the same. For the night hours, however, there is a shift towards higher frequencies for the disturbed period as shown for both the Harstad path and the Bergen path in Figures 5.15 and 5.16 respectively.

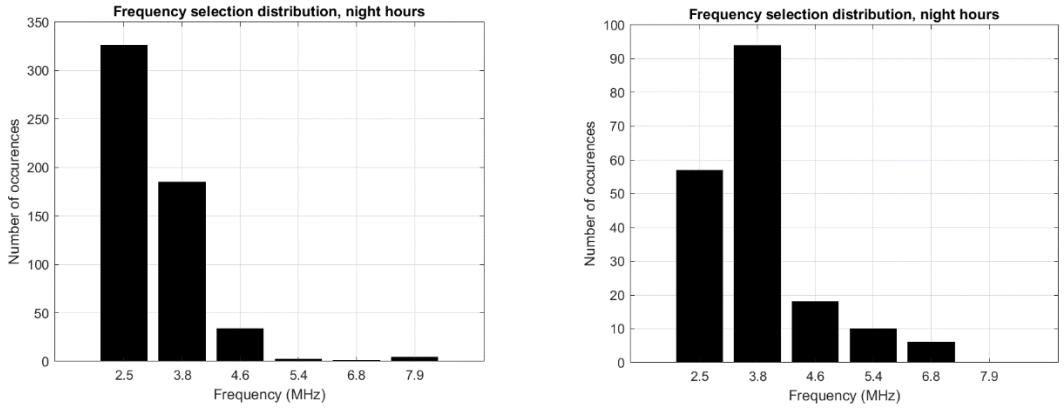

Figure 5.15 Frequency selection at night on path to Harstad for undisturbed period 23.02–17.03.2017 (left) and disturbed period 02.03–12.03.2017 (right).

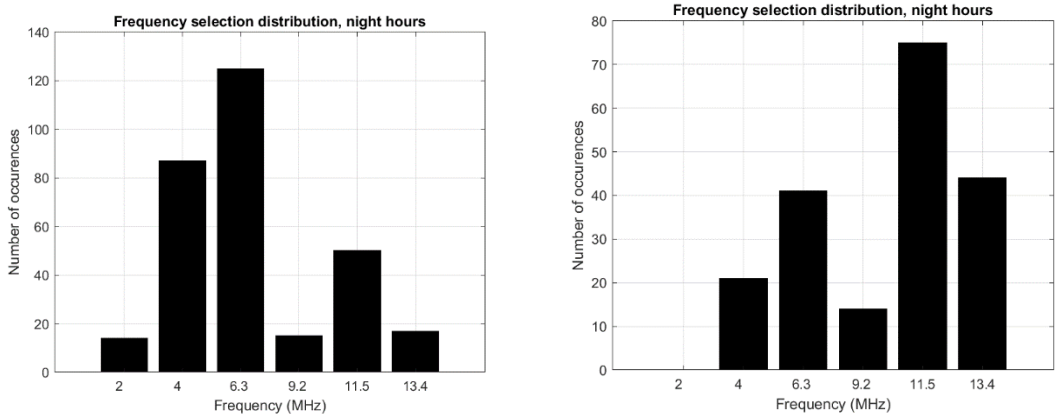

Figure 5.16 Frequency selection at night on path to Bergen for undisturbed period 23.02–17.03.2017 (left) and disturbed period 02.03–12.03.2017 (right).

For the measurements in 2018, wideband HF (WBHF) was run on the long-haul network. Linking procedures are not affected by the use of wideband HF, but the number of link attempts per hour was lower due to a larger file being transmitted when first linked, thereby increasing the interval between each link attempt. The statistical database is therefore smaller for the WBHF measurements than for the 3 kHz measurements. For WBHF, the bandwidth of the data transmission is selected in steps of 3 kHz up to 24 kHz by the radio implementation, depending on the available bandwidth. The selected bandwidths for the undisturbed and disturbed periods

in March 2018 on the path to Bergen are displayed in Figures 5.17 and 5.18, respectively. Higher bandwidths seem to be preferred during the undisturbed day period, but for night times and the disturbed day, 3 kHz is the most frequently selected bandwidth. This is reasonable due to lower signal-to-noise ratios at night and during disturbed periods with excess absorption. The bandwidth selection on the Växjö path showed a similar trend to the Bergen path for the month of March but with a tendency of some larger bandwidths available.

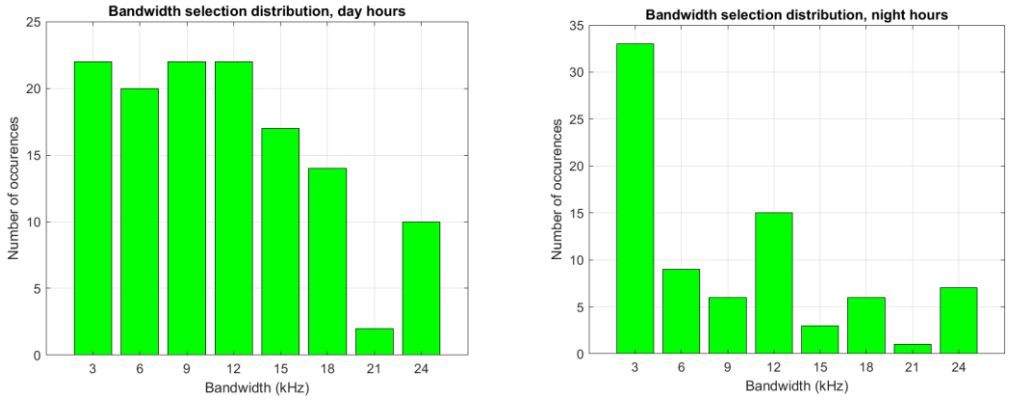

Figure 5.17 Bandwidth selection on path to Bergen during undisturbed period, 02.03–13.03.2018, for day hours (left) and night hours (right).

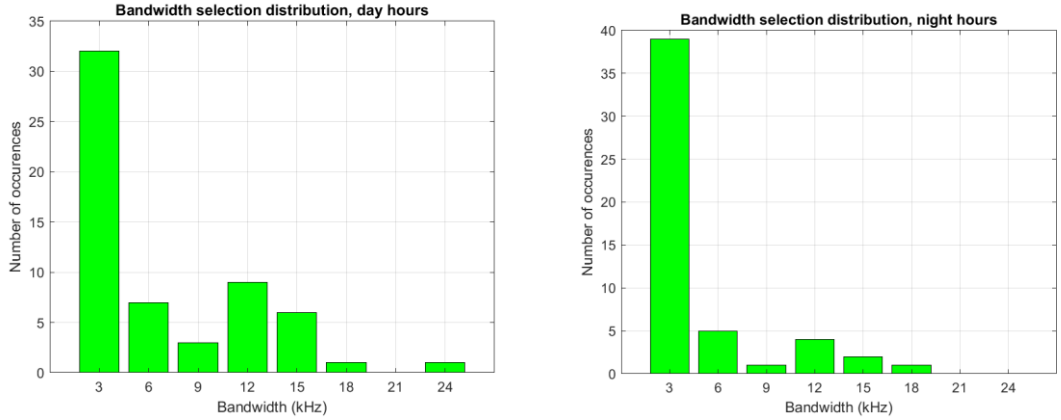

Figure 5.18 Bandwidth selection on path to Bergen during disturbed period, 15.03–27.03.2018, for day hours (left) and night hours (right).

5.1.4 April

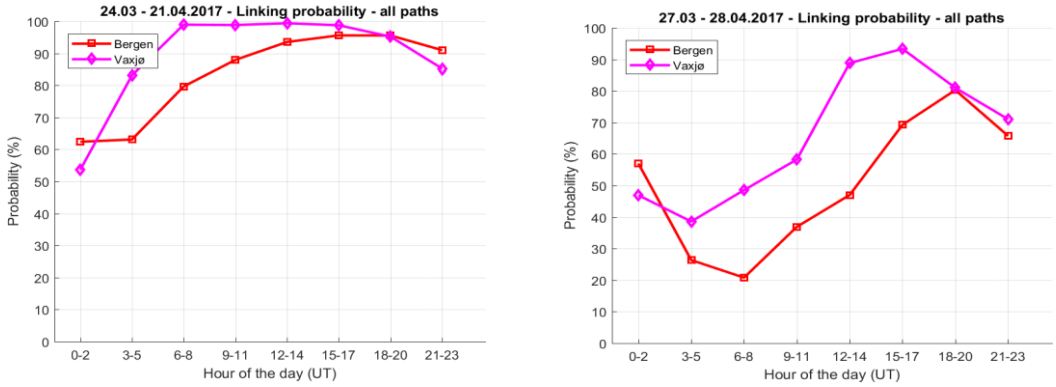

Figure 5.19 March–April 2017. 14 days analysed in undisturbed period (left). 21 days analysed in disturbed period (right). Only long-haul data.

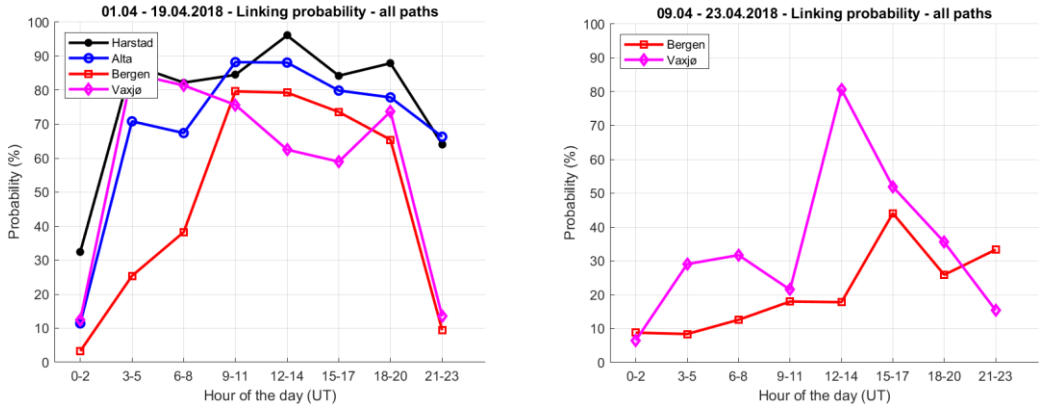

Figure 5.20 April 2018. 14 days analysed in undisturbed period (left). (Only 6 days on Växjö path. Only 2 days at night-hours on short-haul paths.) 8 days analysed in disturbed period (right). (Only long-haul data.) WBHF on long-haul paths.

Data sets from April 2017 and April 2018 are displayed in Figures 6.19 and 6.20. There were not sufficient short-haul data to be analysed for April 2017 and for the disturbed period in 2018. Again, there was very little data collected during night on the short-haul network in 2018. Since WBHF was run on the long-haul network in 2018, also for these data sets (as for the March 2018 data) there were fewer link attempts per hour, and the statistical database is smaller compared to the corresponding database on the short-haul network.

For the undisturbed period the linking success is generally high for most hours. The largest difference to the previous months is that there is no minimum linking probability at hours 03–05 UT, as observed in all previous plots. There is instead a reduced linking probability for the hours right after midnight. This is also indicated in the short-haul dataset from 2018, although data from only two days are analysed and displayed for the night hours.

For the disturbed period, the linking probabilities on the paths to Bergen and Växjö are very similar to the linking probabilities shown for March and therefore not further commented here.

For the wideband HF-measurements in April 2018, the bandwidth most frequently selected was 3 kHz on the path to Bergen for both the undisturbed and disturbed periods, and for day- and night times. The selected bandwidth to Växjö was larger; 24 kHz was available to a large extent during day, and bandwidths up to 18 kHz were available at night. The difference between the bandwidths selected to Bergen and Växjö for the disturbed period can be viewed in Figures 5.21 and 5.22, respectively. The difference in the bandwidth available on the two paths is believed to be due to the generally lower signal-to-noise ratio measured in Bergen (this is further discussed in Section 6.1).

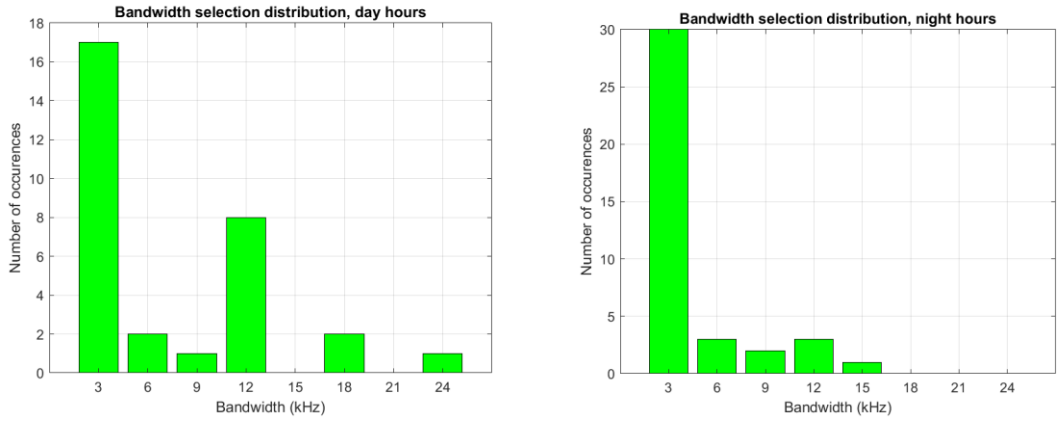

Figure 5.21 Bandwidth selection on path to Bergen during disturbed period, 09.04–23.04.2018, for day hours (left) and night hours (right).

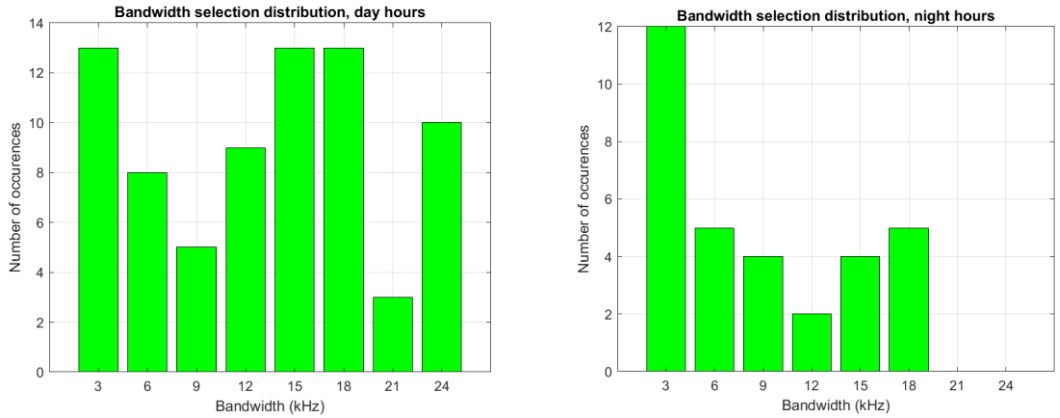

Figure 5.22 Bandwidth selection on path to Växjö during disturbed period, 09.4–23.04.2018, for day hours (left) and night hours (right).

5.1.5 May/June/July

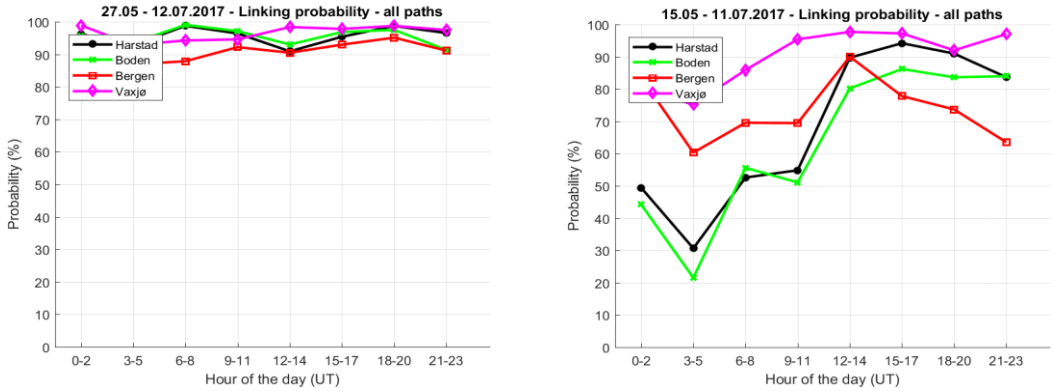

Figure 5.23 May/June/July 2017. 31 days analysed in undisturbed period (left). 13 days analysed in disturbed period (right).

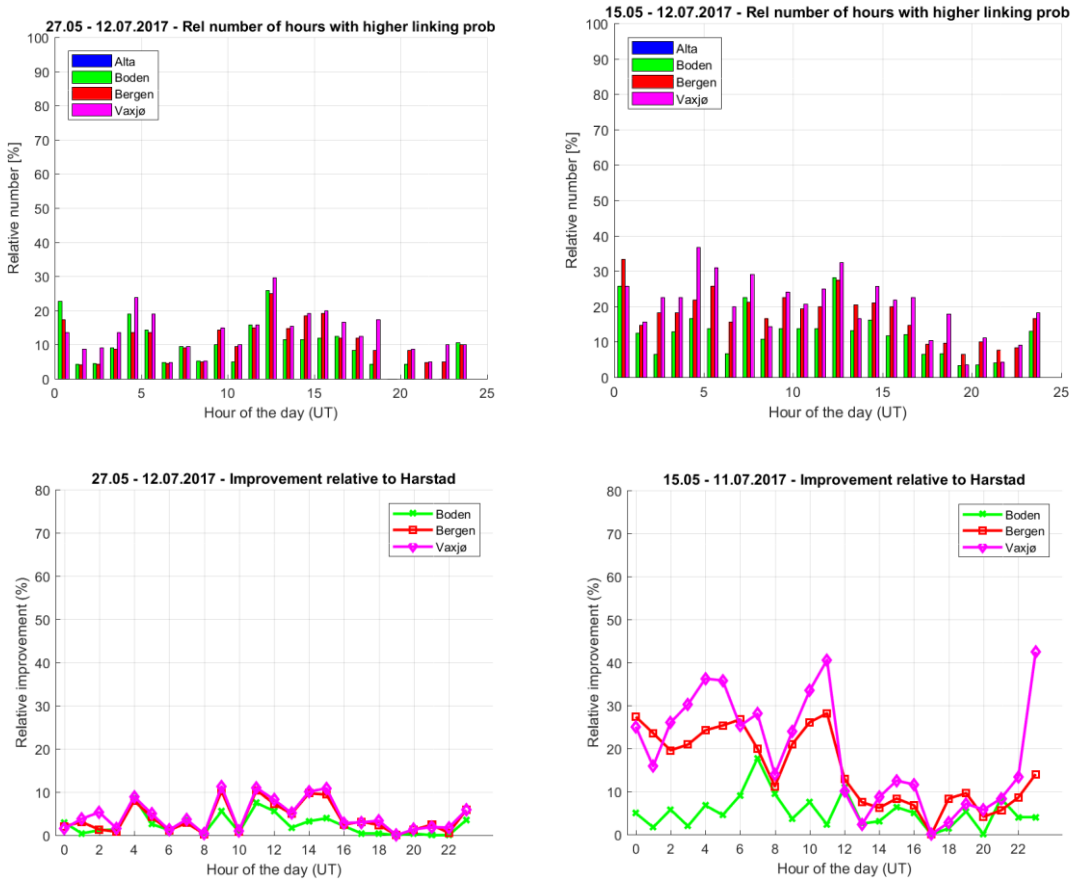

Figure 5.24 May/June/July 2017. Space diversity for the same period as in Figure 5.23.

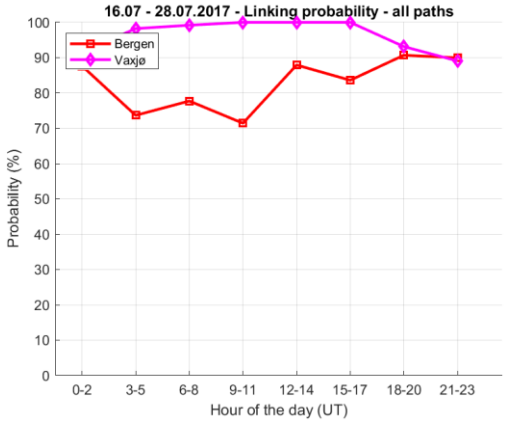

Figure 5.25 July 2017. 10 days analysed in disturbed period with a PCA occuring in the period 14-07–15.07.2017 (Only 7 days on path to Växjö.)

Three months of measurements around the summer solstice 2017 have been combined into one undisturbed and one disturbed period (Figures 5.23 and 5.24). Many data points are therefore used in the analysis, and the statistical confidence should be higher than for some of the previous data plots. We analyze the three months together because we expect the solar conditions to be symmetric around the summer solstice.

The sorting of days into the undisturbed or disturbed period was slightly modified for this data set, compared to the previous data sets. For some of the days, even though absorption events larger than 2 dB was registered at the riometer in Abisko, the HF linking data showed no sign of less linking probability and the plots where very similar to undisturbed days. These few days were therefore included in the undisturbed period, even though they strictly belonged to the disturbed period according to our previous definition. If we had strictly followed our definition of undisturbed/disturbed, the plot for the disturbed period would have shown higher linking probabilities and would have been more similar to the plot for undisturbed days.

The undisturbed period show in general high linking probabilities, between 85 % and 100 % throughout the day on all the paths (Figure 5.23, left). There is no minimum of linking probability at any hour. The space diversity gain is thus small, below 10 % for all hours (Figure 5.24, left).

For the disturbed period, the same trend as for disturbed periods in previous months can be seen, with a minimum of linking probability around the hours 03–05 UT. And again, the long-haul paths show higher linking probabilities in the night and morning hours than the short-haul paths. The space diversity gain for the long-haul paths is for the night- and morning hours between 20 and 40 %, whereas the space diversity gain is below 10 % for the Boden path.

A second disturbed period in July is analysed in Figure 5.25 when only data on the long-haul paths were available. In this period a PCA event occurred on the 14th of July [15]. Following this, a “black-out” on the path to Bergen could be observed in our data in the morning hours on July 17th, but the PCA did not cause a severe deterioriation of propagation lasting for more than

one day. The linking probability for the path to Bergen is thus relatively high for the period shown in Figure 5.25, despite the PCA. We believe that linking would have been difficult on the short-haul paths, if data had been available. No data were available on the Växjö path at that time.

Because the high latitude ionosphere is sunlit throughout 24 hours in May/June, a F2-layer is present even at night on ionograms in Tromsø and in Lycksele. During day time, F2, F1 and E-layers are observed. The solar ionosphere is therefore a steady reflector of the HF-signals throughout the 24 hours. However, the ionograms also show periods around noon with no reflected signals, despite that propagation and linking are measured on the HF-paths. We explain this in terms of solar D-region absorption around noon, which could be strong enough to absorb the ionosonde signal, but not the HF communication signal.

Overlayed the diurnal variability of the ionosphere, which is small for this time period, are the disturbances and excess absorption which are observed in the data from the disturbed period shown in Figure 5.23 (right). The occurrence rate and intensity of these disturbancies should not be dependent on the time of year, only on the phase of the sunspot cycle. We therefore conclude that the main reason for the much better linking probabilities around the summer solstice than in other months is the presence of a steady F2-layer with the same critical frequency throughout the day.

The frequency selection on the path to Bergen is for these months almost identical for the undisturbed and disturbed period, with 9.2 MHz being most frequently selected during day time and 6.3 MHz during night time. The frequency selection has not been analysed on the Växjö path.

For the frequency selection on the Harstad path, in summer time there is no longer a tendency of higher frequency selection during the disturbed night relative to the undisturbed night, as was the case for the March measurements in Figure 5.15.

For measurements in May and June 2018, we reduced the transmitted power at all sites in the long-haul network to 50 W, in order to evaluate the possibility of using less power on such long paths. The following figures show the results from a few different periods (selected based on the availability of data on the different paths).

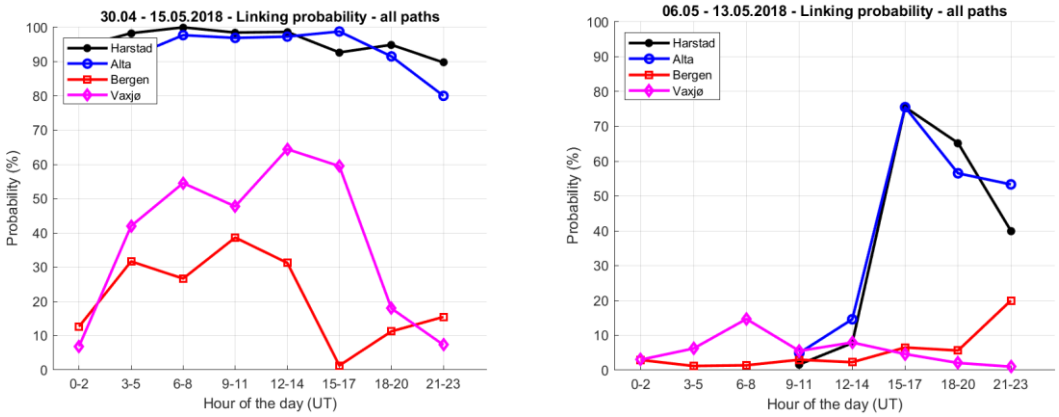

Figure 5.26 May 2018. 7 days analysed in undisturbed period (left). (Only 4 days during night hours at short-haul paths.) 8 days analysed in disturbed period (right). (Only 5 days in Harstad and Alta. No data available at night hours on short-haul path.) For both plots: WBHF on long-haul paths and transmission power is 50 W.

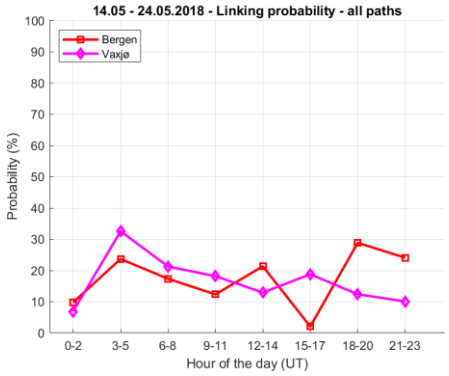

Figure 5.27 May 2018. 10 days analysed in undisturbed period. (Only long-haul data.) WBHF on long-haul paths and transmission power is 50 W.

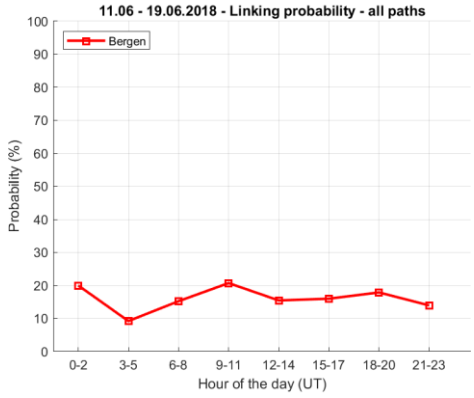

Figure 5.28 June 2018. 9 days analysed in undisturbed period. (Only data on path to Bergen.) WBHF and transmission power is 50 W.

WBHF was run in the long-haul network during the periods shown. This is the most favourable time of the year for HF-propagation as seen for the measurements in 2017, so there is reason to believe that measured linking probabilities with transmitted power only at 50 W will not be higher at other times of the year.

In Figure 5.26 we see that the linking probabilities for the short-haul paths are very similar to those of the previous year (Figure 5.23), with 80–100 % linking probability for all hours of the day for the undisturbed period. The linking probabilities on the long-haul network however, have been reduced drastically due to the lower transmit power. There are nevertheless times when linking is possible with 50 W transmit power, particularly during undisturbed conditions (Figure 5.26, left). The bandwidth selected for WBHF during these measurement periods was most frequently 3 kHz, although all bandwidths, including 24 kHz, were selected in the undisturbed period of measurements from early May 2018.

5.1.6 August

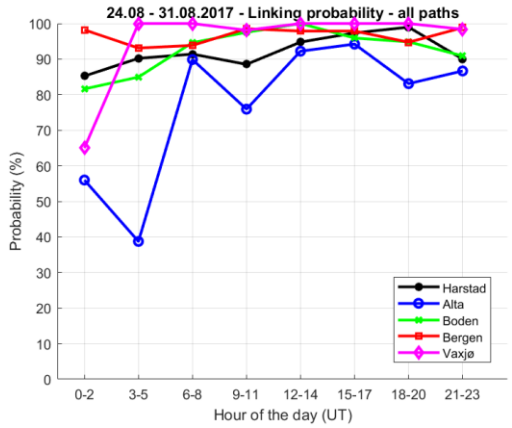

Figure 5.29 August 2017. 8 days analysed, undisturbed period. (Only four days in Växjö and only five days in Bergen.) No data collected during disturbed conditions.

Only one week of data was collected in August 2017. The period of data collection is classified as undisturbed according to the riometer measurements in Abisko. However, there were times at night when there was excess auroral ionization as observed on the ionograms from both Tromsø and Lycksele. Since only four and five days, respectively, exist with data on the Växjö and Bergen paths, we do not show plots of space diversity for this month.

This undisturbed period in August shows the same trend as the May/June/July data with in general, high linking probabilities between 80 % and 100 % throughout the day on all the paths, except for the northernmost path to Alta. The Alta path shows reduced linking probability during night hours with a minimum at hours 03–05.

During the times of auroral ionization as seen on the ionograms (not shown here), the ionosphere is supporting the HF-propagation well on the different paths, but differences in support on the different paths can be seen from hour to hour.

The selection of frequencies is as expected, with a higher frequency selected during day time than at night.

5.1.7 September

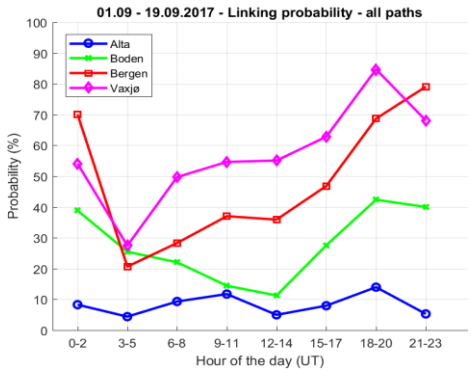

Figure 5.30 September 2017. 19 days analysed in disturbed period with PCA occurring in periods 05.09–08.09.2017 and 10.09–14.09.2017 (Only 14 days on path to Växjö and 5 days on the two short-haul paths.) No data is collected during undisturbed conditions.

Data were collected on four paths during a quite severely disturbed period in September 2017. Two PCA events occurred in this period. Only five days of data were collected on the Alta and Boden paths, but the days covered the first of the two PCA events. Unfortunately, no data were collected on the Harstad path, so space diversity gain compared to this path could not be calculated. Data were collected on the path to Bergen in the whole period of 19 days.

This period clearly shows the much higher linking probabilities on the long paths towards the south than on the short paths within the region highly effected by the PCA events. The improvement in linking probability on the Växjö path compared to the Alta path is between 20–70 %, depending on the time of day. The minimum linking probability occurs at hours 03–05 UT on the long-haul paths, as for other times of the year. The path to Boden shows up to 30 % higher linking probability than the path to Alta at certain hours.

By inspecting the ionograms from Tromsø and Lycksele, it is apparent that the ionosphere above Tromsø is "blacked-out" more often than the ionosphere above Lycksele, even though the latter also shows long periods of no ionospheric reflections at certain days and times. The presence or absence of ionospheric reflections in Tromsø is in good agreement with the observed linking probabilities on the short-haul paths. For the long-haul paths however, the agreement between ionograms from Lycksele and the linking probabilities is slightly less, with the probability of linking being larger than the ionograms would indicate. We believe this is due to the larger possibility of multihop propagation[14] on the longer paths during the disturbed

[14] The signal is reflected several times from the ionosphere between the transmitter and the receiver.

period, and also that the Lycksele site being farther away from the reflection points of the HF-signals.

5.1.8 October

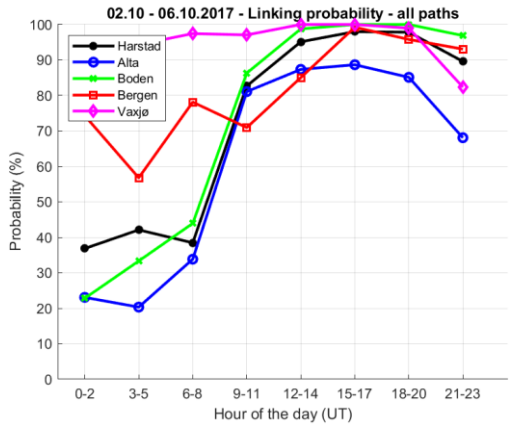

Figure 5.31 October 2017. 5 days analysed in undisturbed period.

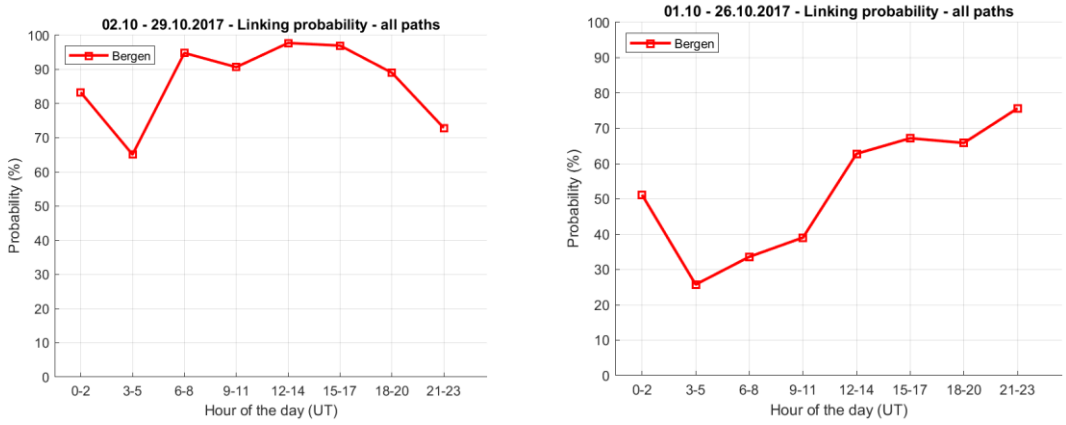

Figure 5.32 October 2017. 19 days analysed in undisturbed period on path to Bergen (left). 10 days analysed in disturbed period on path to Bergen (right).

Only five days in October 2017 had data collection on all paths, and linking probabilities during those five undisturbed days are plotted in Figure 5.31. For the path to Bergen, data were collected through the whole month, and those measurements are therefore sorted and analysed in two periods of undisturbed and disturbed days, respectively (Figure 5.32).

Compared to the summer months, the linking probability is low in the hours after midnight for the short-haul paths. This corresponds well with the riometer measurements in Abisko showing excess absorption during night time, and with the ionosonde in Tromsø showing an auroral ionosphere with large variation in the ionization. Linking probabilities on the Växjö path are similar to the data from the summer months, whereas the linking probabilites on the Bergen path are lower compared to the summer months. Inspecting the ionograms in Lycksele, we observe

that for most of the days there is a steady F2-layer also at night time. These data show that the ionosphere farther south is supporting the HF-propagation better than at the higher latitudes.

The confidence of the Bergen data shown in Figure 5.32 is higher than for the five-day period in Figure 5.31 since relatively many days are analysed together. Figure 5.32 shows that there is a relatively big difference in linking probability between an undisturbed and a disturbed period also on this long southern path.

The frequency selections during these long periods of data collection on the Bergen path are displayed in Figures 5.33 (undisturbed period) and 5.34 (disturbed period). Whereas the frequency selection during the undisturbed and disturbed period is quite similar during day time, there is a preferrence for higher frequencies at night time during the disturbed period. We interpretate this as auroral E-ionization being present also on the Bergen path at night time.

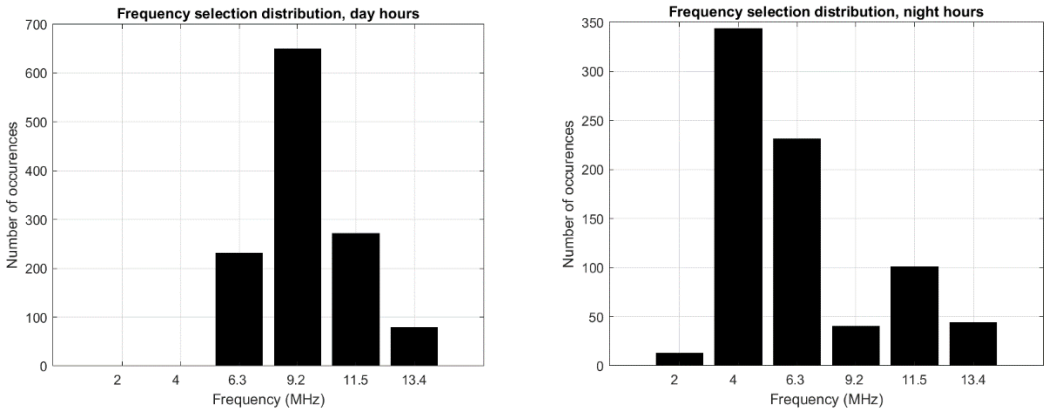

Figure 5.33 Frequency selection on path to Bergen for undisturbed period 02.10–29.10.2017 for day hours (left) and night hours (right).

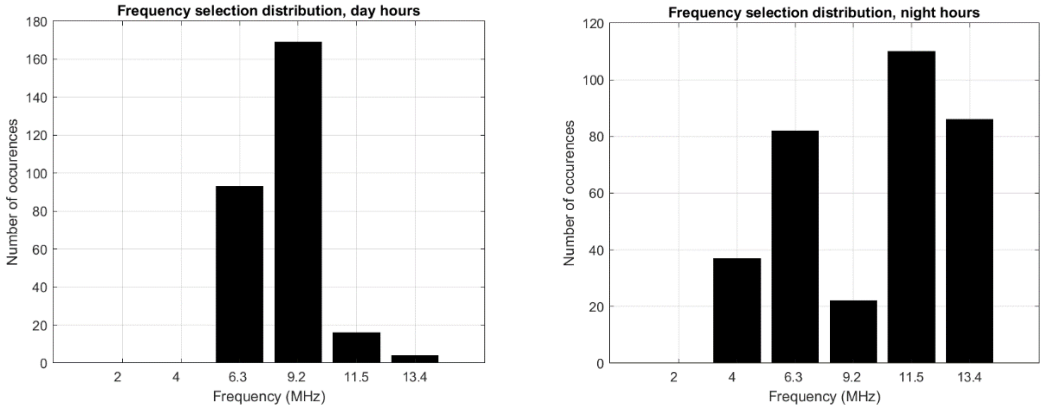

Figure 5.34 Frequency selection on path to Bergen for disturbed period 01.10–26.10.2017 for day hours (left) and night hours (right).

5.1.9 November

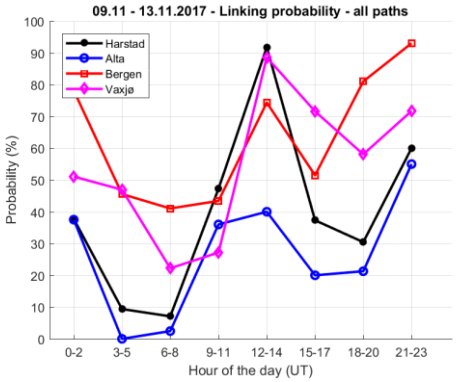

Figure 5.35 November 2017. 5 days analysed including both undisturbed and disturbed days.

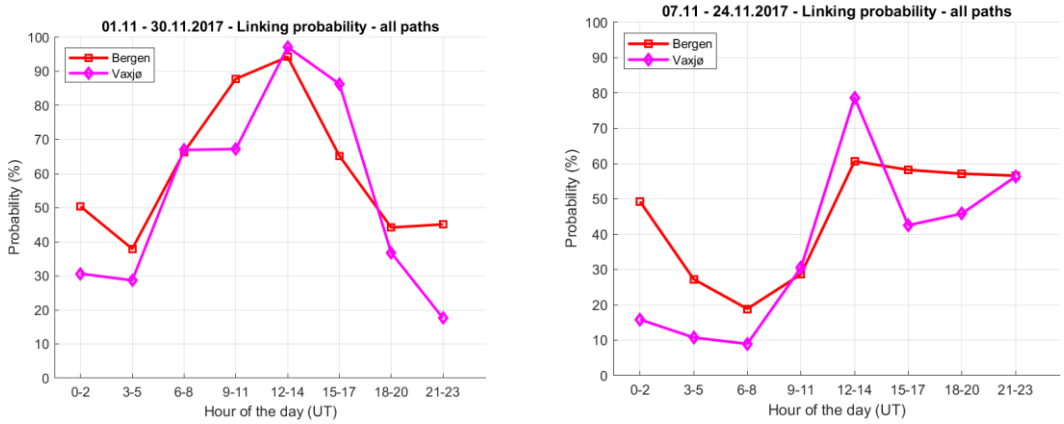

Figure 5.36 November 2017. 20 days analysed in undisturbed period (left). (Only 12 days on path to Växjö.) 10 days analysed in disturbed period (right). (Only 7 days on path to Växjö.)

There were few days of data collection on the short-haul paths in November 2017. Only five days are analysed in Figure 5.35, and since there were so few days, both undisturbed and disturbed days (according to the riometer measurements in Abisko) are combined in the analysed period. When we inspected the linking probabilities on the individual days, the impression was that the ionosphere was rather disturbed for the whole period of five days.

Since data collection took place on all of the days in November on the path to Bergen, and on approximately 20 days on the path to Växjö, another analysis is performed in Figure 5.36, dividing the days into an undisturbed and a disturbed period. Some of the days WBHF was used, which implied fewer measurements on these days (explained in Section 5.1.3).

In Figure 5.35 we see that the number of hours with high linking probabilities in the middle of the day has decreased compared to the previous months, and the curves are becoming more similar shapewise to the January data. The exact shape of the curves should not be compared

because of the low number of days analysed. There is reason to believe, based on ionograms from Tromsø, that if more days of data had been collected in November on the short paths, the linking probability would have been higher during night time. Auroral ionization is observed at night time on many of the ionograms.

In Figure 5.36 we see the "classical" picture of an undisturbed and a disturbed period, respectively. The low linking probability at night in the undisturbed period is mainly caused by low F2-layer support, whereas the low linking probability during morning hours in the disturbed period is caused by auroral absorption. Auroral ionization causes increased linking probability at night for the disturbed period.

Among the days of measurement in November, WBHF was run ten days on the Bergen path and seven days on the Växjö path. We have displayed the bandwidth selection for the undisturbed days on the two paths in Figures 5.37 and 5.38, respectively.

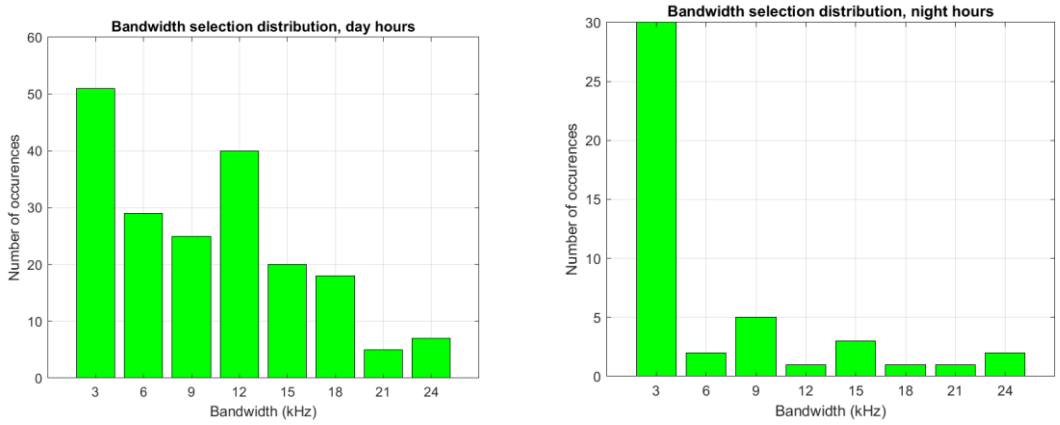

Figure 5.37 Bandwidth selection on path to Bergen during undisturbed period, 01.11–30.11–2017, for day hours (left) and night hours (right).

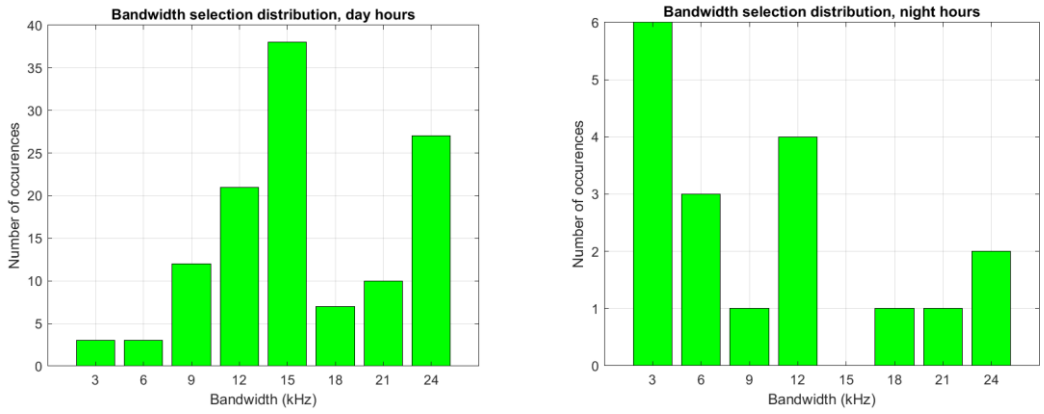

Figure 5.38 Bandwidth selection on path to Växjö during undisturbed period, 01.11–30.11.2017, for day hours (left) and night hours (right).

We observe that higher bandwidths are available during day time than night time, and particularly so on the path to Växjö where 15 kHz seemed to be most frequently available.

For a few days of disturbed conditions (not shown here), 3 kHz was generally most frequently selected on the Bergen path, whereas all frequencies up to 24 kHz were selected during day and basically 3 kHz during night on the path to Växjö.

5.1.10 December

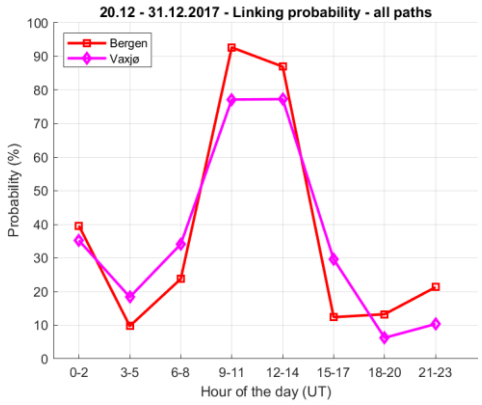

Figure 5.39 December 2017. 12 days analyzed in undisturbed period. WBHF on long-haul paths.

Also in December the number of days with measurements on the short-haul paths was low, and there was also a failure of data collection during night time. Only measurements on the long-haul paths are therefore analysed, and Figure 5.39 shows an undisturbed period where WBHF was run.

December is the month with the lowest elevation angle to the sun, and the number of sunlit hours is smallest. We see that high linking probability is only achieved between the hours 9–14 UT. The low linking probability at night time is caused by the lack of F2-layer support. Comparing this plot with Figure 5.3 (undisturbed period in early January 2018, only one month later), the latter is somewhat more optimistic concerning linking probabilites at night time. One reason may be a larger presence of auroral ionization for the actual days in January giving better support for reflections. We do not believe the difference in the elevation angle of the sun within a 20-day period will have a significant impact on the measurements.

The WBHF bandwidth selections in this period are shown in Figures 5.40 and 5.41. Basically, the same situation as for the November data applies.

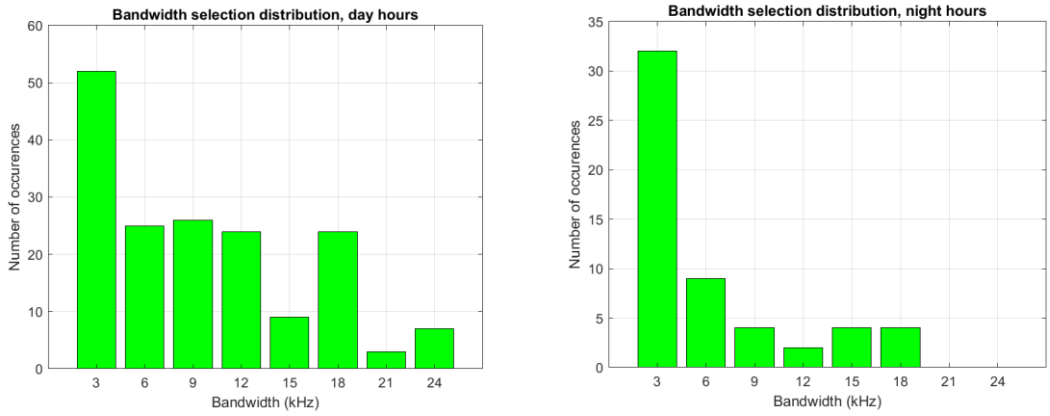

Figure 5.40 Bandwidth selection on path to Bergen during undisturbed period, 20.12–31.12.2017 for day hours (left) and night hours (right).

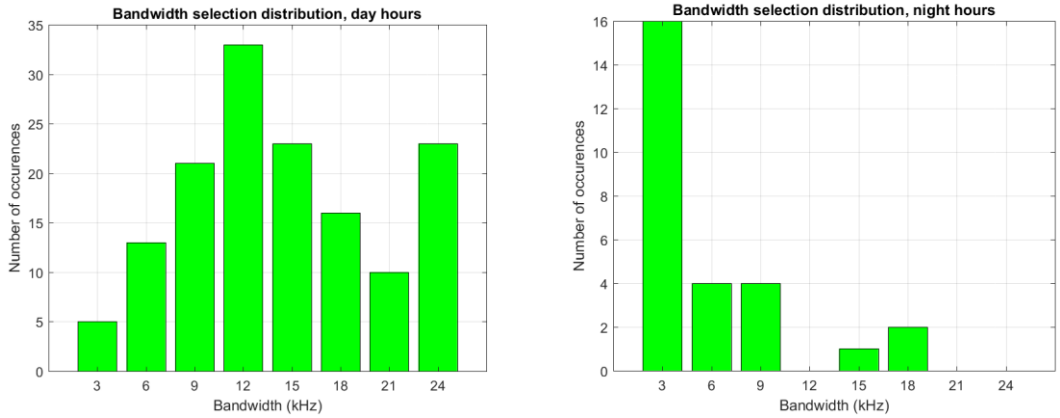

Figure 5.41 Bandwidth selection on path to Växjö during undisturbed period, 20.12–31.12.2017 for day hours (left) and night hours (right).

5.1.11 Summary of results over various months

Linking probability

The probability of linking varies throughout the day, and over the months. In winter time the HF-conditions are most difficult with high linking probabilites only during day time centered around local noon but shifted one hour towards the afternoon. For the short paths in the north the hours with high linking probability were from 9 to 14 UT, and for the long paths towards the south, the hours were from 6 to 17 UT, (thus generally a longer time period on the southern paths). During disturbances the number of hours with high linking probability is reduced and shifted further towards the afternoon. This is in agreement with the observation of absorption occuring in the morning hours (Figures 3.9, 3.10 and 3.11). In general, for the disturbed periods, the linking probabilities are higher on the southern long paths than on the northern short paths. There is also a high possibility of linking in the hours around midnight, particularly on the northern paths. This is due to auroral-E ionization (explained in Section 3.4). An absolute

minimum of linking probability occurs in the hours 03–05 UT (04–06 local time) and this was observed on all paths. D-layer absorption, or the lack of F-layer ionization, is the cause.

Around summer solstice, the HF-conditions are the best with generally high linking probabilites throughout the 24 hours on all paths. The solar conditions create stable and persistent ionization during all 24 hours. However, during disturbances the linking probability is reduced from midnight until morning hours particularly on the northern paths. Again, a minimum of linking probability can be observed for hours 03–05 UT.

For the months between winter and summer, the linking probabilities are transitting from one state as described, to the other.

Space diversity
The numbers calculated for space diversity (with Harstad as the reference path) must be viewed in light of some shortcomings of the measurements as described in Section 7.1.

For the short-haul network, where all stations transmitted at 20 W and similar antennas were used at all sites, the space diversity gain to Boden (path length 370 km) was below 10 % for undisturbed conditions in winter time and generally in summer time. For disturbed conditions in winter time the gain was up to 30 % for the hours 20 to 11 UT.

For the long-haul network where different equipment at different sites could have influenced the results, the results were similar in winter and summer time. For undisturbed conditions the space diversity gain was below 10 %, but for disturbed conditions the gain was 20–50 % for the hours 22–11 UT on the Växjö path. The Bergen path gave less space diversity gain. This may be attributed to the Bergen path being farther north than the Växjö path, experiencing more absorption, but other factors such as antenna gain and noise level may also have contributed to the difference.

Bandwidth available
Wideband HF was tested in a few periods in winter and spring. For undisturbed conditions at day time we found that 18 kHz was available on the path to Bergen and 24 kHz on the path to Växjö. The signal-to-noise ratio in Bergen was generally lower than in Växjö. For the undisturbed night and disturbed conditions (both day and night) the bandwidth available was most frequently 3 kHz, with some occurences of higher bandwidths in Växjö.

In previous measurements on a ~1000 km path in the Arctic [20], the available bandwidth was found to be around 12 kHz, relatively independent of time of day, channel conditions and season, except for the winter night where the lowest frequency around 2 MHz (MF) was selected and 24 kHz bandwidth was available. We did not focus on the throughput achieveable by using larger bandwidths in this study, since for the file size transmitted (100 kByte) the protocol overhead is relatively large, giving a throughput number dominated by this protocol overhead.

Frequencies selected
In the short-haul network frequencies 3–4 MHz was most often selected to Harstad and 4–5 MHz to Boden in day time. During night the frequency 2.5 MHz was most often selected on both paths. No seasonal variation was detected. During disturbances however, the variation in frequency selection increased, with higher frequencies more often selected.

In the long-haul network the higher frequencies 9–13 MHz was selected in day time and 6–9 MHz at night on both the Bergen and Växjö path. There was no detectable seasonal variation in the frequency selection, so the mid-latitude phenomenon of a stronger F2-layer (Figure 3.5) in winter was not observed and verified in our measurements.

5.2 The relationship between linking probability and riometer absorption

In Section 6.1 the periods of disturbed ionospheric conditions were selected based on a rough assessment of the measured riometer absorption in Abisko [8]. In this section we analyse the relationship between the linking probabilities and the measured absorption in Abisko in a more accurate way with the goal of quantifying the absorption levels that will have significant impact on HF communications.

Some examples of linking probabilities and simultaneously measured riometer absorption on single days are shown in the following figures. The resolution of the riometer data is one measurement per minute whereas the linking probability is calculated per hour. In Figure 5.42 we see a strong anti-correlation between the linking probabilities and the absorption on the short-haul paths, whereas the anti-correlation exists, but is somewhat smaller, on the long-haul paths. This is as expected since the absorption measurements in Abisko is much closer to the D-region where absorption takes place on the short-haul paths than on the long-haul paths.

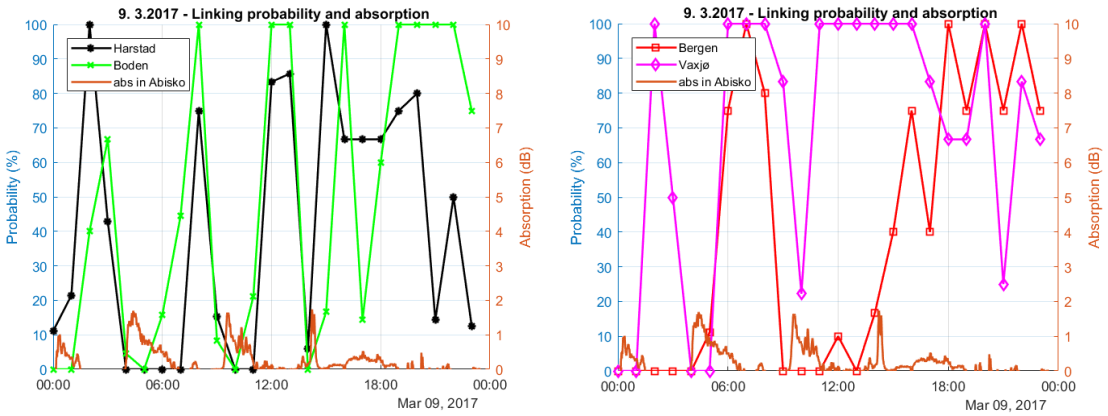

Figure 5.42 Linking probabilities and ionospheric absorption on the 9th of March 2017. Short-haul paths (left) and long-haul paths (right).

Other examples of the generally high anti-correlation between linking probabilities and riometer absorption on the short-haul paths are shown in Figure 5.43. Relatively small ionospheric absorption levels of size less than 0.5 dB seem to have influence on the linking probabilities.

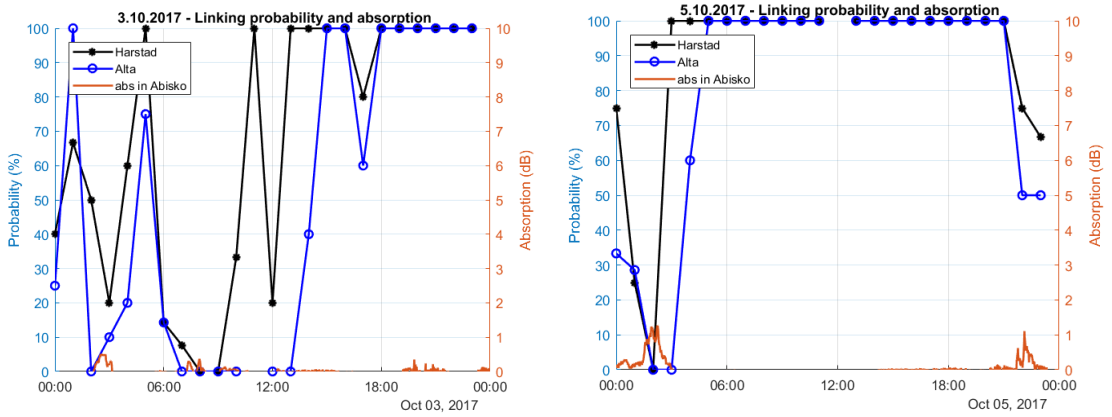

Figure 5.43 Linking probabilities and ionospheric absorption on two selected days in October 2017 on the short-haul paths.

However, there are also times when the linking probability is reduced without an accompanying ionospheric absorption. This effect is clearly shown in Figure 5.44 when communication is difficult during the hours 02-05 UT on both the short-haul and long-haul paths. There is no absorption for these hours. The ionograms in Tromsø (not included here) show no ionospheric reflections at this point in time which we believe cannot be due to absorption because of the proximity to Abisko. We therefore conclude that the reason for zero linking probability at these hours is not absorption but the lack of sufficient F2-layer ionization to reflect the signals.

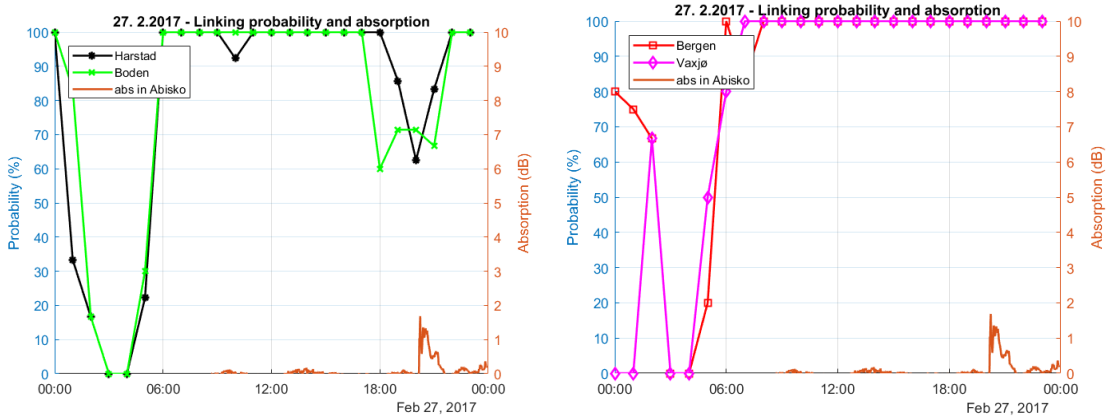

Figure 5.44 Linking probabilities and ionospheric absorption on the 27th of February 2017. Short-haul paths (left) and long-haul paths (right).

Other examples of simultaneous absorption measured in Abisko and linking probabilities on the long-haul paths are shown in Figure 5.45. The 31st of March is a day with high absorption in the first part of the day. There is an "opening" for communications to both Bergen and Växjö around 08 UT, but the ionograms in both Tromsø and Lycksele (not included here) are completely "blacked out" by absorption at this time, and no reflections are seen. Reflections are shown on the ionograms in Lycksele from 16 UT onwards. In Tromsø the reflections are "on and off" throughout the day from 12 UT onwards, showing a very disturbed ionosphere with a

mixture of absorption, auroral ionization and solar ionization. This example illustrates that there may be short periods, “openings”, where communications are possible within a generally disturbed period with high average absorption.

On the 8th of April there are a few absorption events in Abisko above 1 dB. During the longest lasting event, linking to Bergen is impossible whereas linking probability to Växjö is a bit higher. When we inspect the ionograms in Lycksele (not included here), there are no reflections in the period from 07–12 UT, and thus it is likely that absorption is severe also at lower latitudes. There are nevertheless opportunities for communications on this long path. During the smaller absorption event at 03 UT, Bergen has the higher linking probability. The ionogram in Lycksele is for this hour blacked out. Towards the end of the day, absorption in Abisko is again high, and the ionograms in Lycksele show hardly no reflections. The linking probability is for the hour 22 UT low, but for the hour 23 UT high, which supports the experience of a very dynamic ionosphere with no one-to-one explanation for the effects observed on the HF-links. This date also shows the potential value of space diversity since although the Växjö path in general has the highest linking probability, the Bergen path also has the highest linking probability at times.

On the 22nd of April the absorption is severe during the hours 02–11 UT and in the late evening hours. The absorption is causing no linking on neither of the long-haul paths for eight hours, but the Växjö path is recovering the quickest, and before midday. The ionograms in Tromsø (not included here) show no reflections, probably due to absorption, between the hours 03 and 14 UT. The same applies to the ionograms in Lycksele (not included here) between 02 and 16:30 UT. Thus the ionograms show longer black-outs than the HF communication on the paths to Bergen and Växjö.

The 11th of September is in the middle of a PCA event (see Section 5.2.1), and the absorption is not fluctuating, but continuosly large throughout the day. Whereas the Växjö path supports some linking for the hours 00–03 UT and 18–23 UT, the Bergen path is hardly possible to link on. For this case the ionograms in Lycksele (not included here) are in good agreement with the linking probabilities: Reflections are seen for the first hours of the 11th and then again from 18:30 UT onwards.

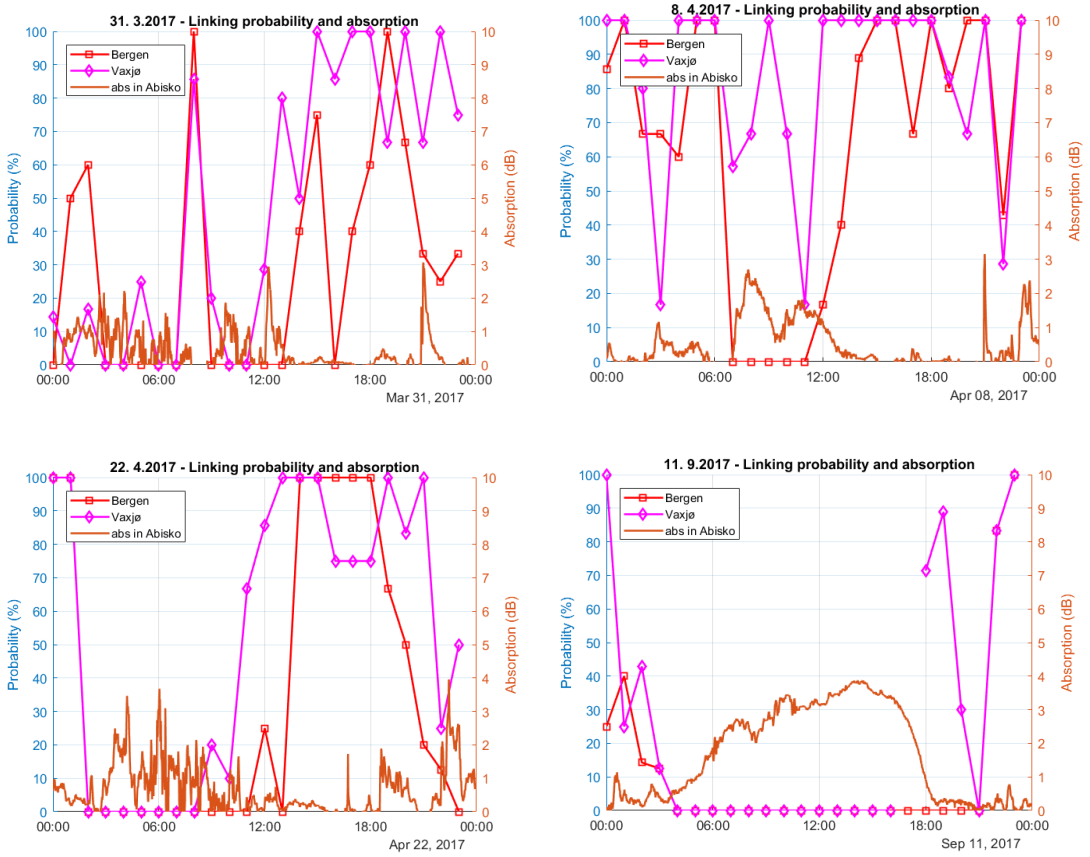

Figure 5.45 Linking probabilities and ionospheric absorption on single days on the long-haul paths.

A correlation analysis was performed on these data to obtain the correlation index of linking probabilites and measured absorption, but as shown by the previous examples, there are factors other than absorption influencing the linking probabilities, so the correlation analysis did not show a clear trend. Instead, we have picked out the hours where the hourly average absorption measured in Abisko exceeds certain values, and we have plotted the complementary cumulative distribution function of the linking probabilities for those hours. This analysis isolates and focuses on measured linking probabilities at times when absorption is high, and thus allows the influence of absorption on HF communications to be studied separately from other factors.

A few seasonal periods of data have been analysed, but the periods are not identical to the periods analysed in Section 5.1. The periods have been selected based on the availability of data on the different paths, since an unequal number of measurements for the different cumulative distribution functions would result in non-comparable curves. Thus the days are a mixture of disturbed and undisturbed days, but most of the measurements come from disturbed days where absorption is the most prevalent.

The following figures show the complementary cumulative distribution function (CCDF) of the linking probabilities. The upper left plot shows *all* measurements in the period. The upper right

plot shows the distribution of linking probabilities for hours where the average absorption measured in Abisko exceeded 0.2 dB. The number of measurements is reduced compared to the left plot since the number of hours with the increased absorption level is lower. The lower two plots show the distributions for hours where the average absorption exceeds 0.5 dB and 1 dB, respectively. If the linking probabilities would be indepedent of the measured absorption, the position of the curves in the vertical direction would be the same in the different plots. The displacement, in the vertical direction, of the curves from the upper left plot shows how sensitive the linking probabilities are to the respective absorption levels of 0.2, 0.5 and 1 dB.

A summary of observations from all the seasonal periods displayed in Figures 5.46 to 5.49 is given after the figures. The Figures 5.46 and 5.47 show measurements from the same month, but the availability of data on the different paths necessitated two different figures.

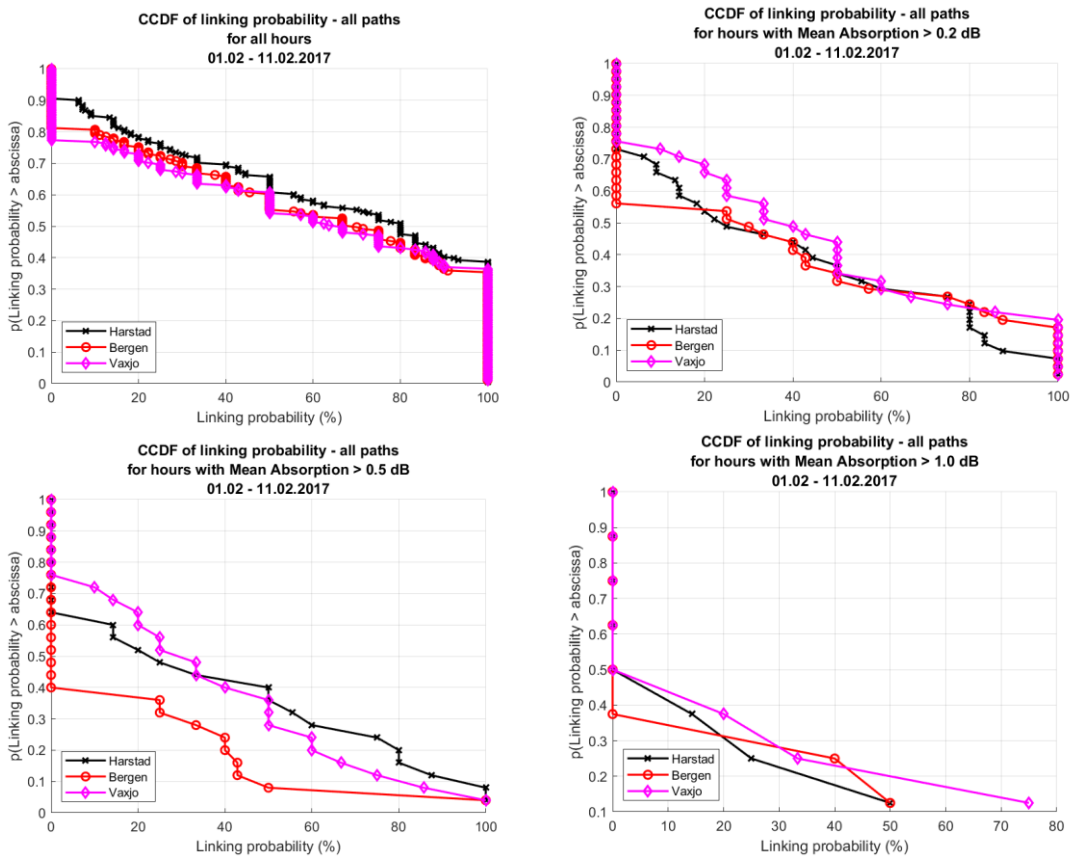

Figure 5.46 *Complementary Cumulative Distribution Function (CCDF) of linking probabilities for 6 days in February 2017. Hours of different absorption levels measured in Abisko are shown in the different plots.*

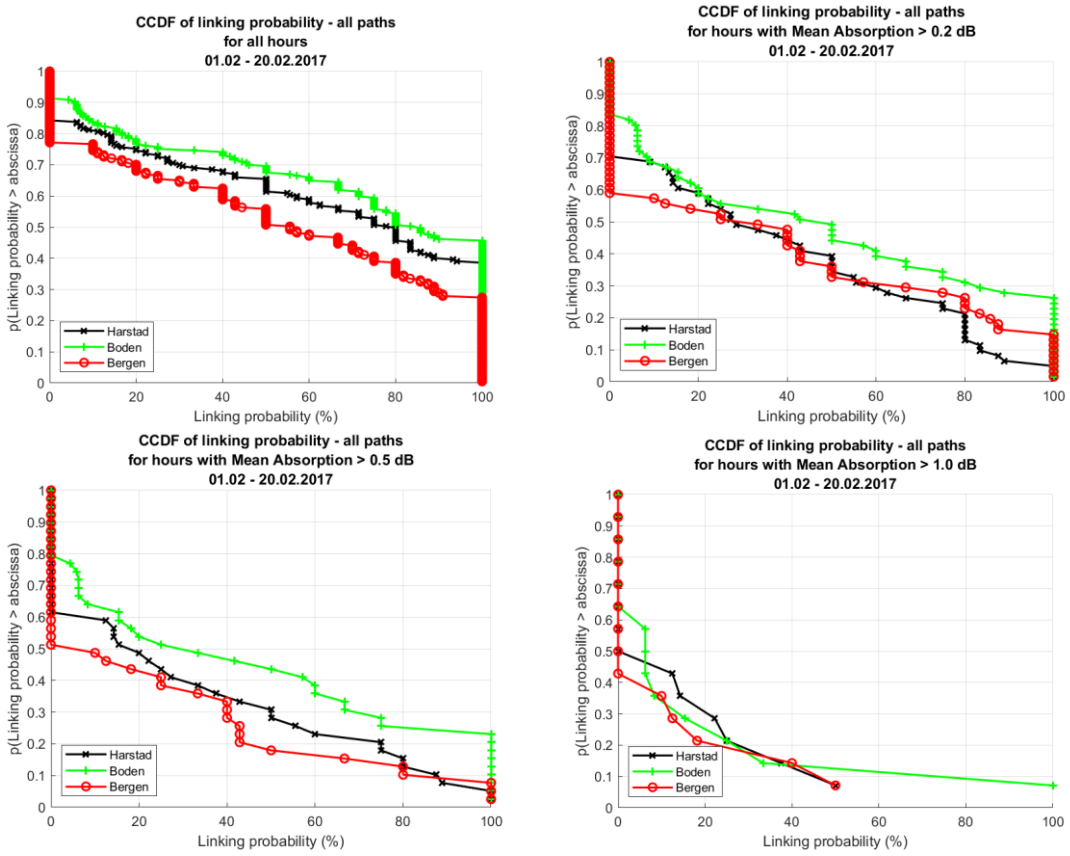

Figure 5.47 Complementary Cumulative Distribution Function (CCDF) of linking probabilities for 7 days in February 2017 (different period from Figure 5.8). Hours of different absorption levels measured in Abisko are shown in the different plots.

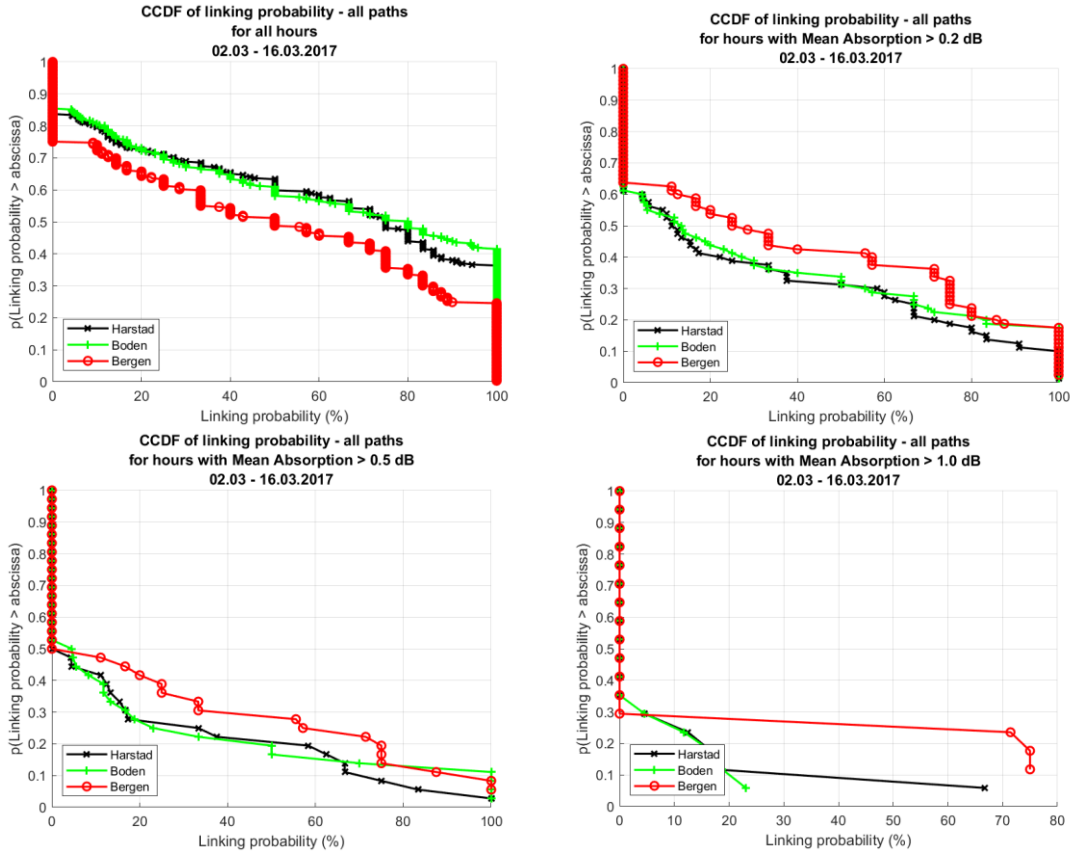

Figure 5.48 Complementary Cumulative Distribution Function (CCDF) of linking probabilities for 6 days in March 2017. Hours of different absorption levels measured in Abisko are shown in the different plots.

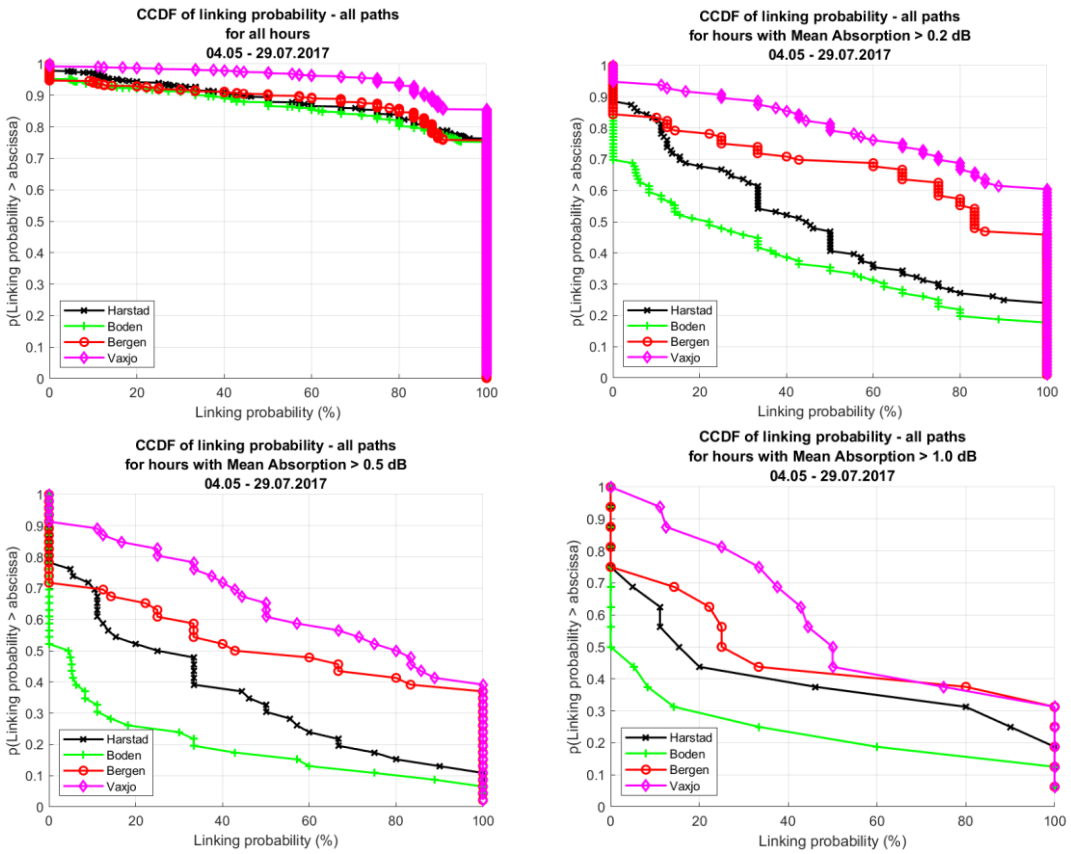

Figure 5.49 Complementary Cumulative Distribution Function (CCDF) of linking probabilities for 40 days in May/June/July 2017. Hours of different absorption levels measured in Abisko are shown in the different plots.

In our analysis of the distribution functions we have compared the probabilities of experiencing linking probabilities of about 50 % and 80 % respectively (on the x-axis). For lower values of linking probability, HF communications will be of little use. We call the conditions at 50 % linking probability for "difficult" and the conditions at 80 % linking probability for “good”.

The influence of riometer absorption measured in Abisko on the linking probabilities on the various HF-paths can be summarized as follows:

- Absorption levels ranging between 0.2 dB and 1 dB have an impact on *all* the HF communication paths, but with varying degree.

- The short-haul paths in the north are sensitive to an increased absorption level of 0.2 dB, and we observe a reduction of the linking probabilities at this level. The probabilities of both “difficult” HF-conditions and “good” HF-conditions are reduced at this level of absorption. The conditions are further reduced when the absorption level increases to 0.5 dB, but the reduction is smaller for this step than for the step between 0 dB and 0.2 dB. At 1 dB absorption the conditions are generally useless for HF

communications, with a slightly more optimistic situation for the summer time. However, the observation at 1 dB is based on very few data points.

- The path to Bergen shows less sensitivity to an absorption level of 0.2 dB than the short-haul paths in the north, although it is affected. The same reduction of conditions apply from 0.0 dB to 0.2 dB as from 0.2 dB to 0.5 dB. The Bergen path is deemed useless for HF communications at an absorption level of 0.5 dB, with an exception for summer conditions.

- The path to Växjö shows, not surprisingly, the least sensitivity to absorption among the paths. At absorption levels of 0.2 dB and 0.5 dB, there is only a minor reduction of the "difficult" conditions whereas the "good" conditions are reduced somewhat more. An absorption level of 1 dB makes the conditions also on this path useless for communications for periods other than the summer period.

- In the summer, the sensitivity to an increased absorption level from 0.0 to 0.2 dB is even larger than in the winter and spring on the short-haul paths. For the long-haul paths, the conditions on the Bergen path are reduced more than on the Växjö path, and for both long-haul paths the reduction of the "good" conditions is the largest. The conditions on all paths are reduced with a similar amount going from 0.2 dB to 0.5 dB of riometer absorption. From 0.5 to 1 dB there is no further reduction of conditions for the short-haul paths and the Bergen path, but some reduction can be seen on the path to Växjö for the "good" conditions. Communications is therefore still possible at an absorption level of 1 dB in summer time.

5.3 Polar Cap Absorption events (PCA) and HF communications

During our measurements, two PCA events occurred as reported by [15]. The largest event occurred in September 2017 with proton fluxes registered by satellites in the period 5th–8th and 10th–14th. We have compiled a time line of different consequences of the PCA in Figure 5.50, measured by different instruments. The figure shows that this PCA had a duration above average and that the influence on HF communications was quite immediate, with very low or no probability of linking. Figure 5.51 gives more details on the HF-conditions, and it shows that the difficult HF-conditions persisted for almost two weeks. The figure displays the number of successful links from the number of attempts. The path to Alta is shown in the first row of plots and the path to Växjö in the last row of plots. Whereas the short-haul paths in the north were almost completely blacked out, the long-haul paths towards the south maintained some connectivity, in particular on the path to Växjö. During such long lasting, severly degraded HF-conditions, it is clearly an advantage to have the opportunity to communicate via a southern node.

The geomagnetic effect of the PCA occurred about three days after the onset of the PCA as shown by the geomagnetic activity index measured at four sites in Norway: Ny Ålesund

(Svalbard), Tromsø (northern Norway), Dombås (mid-Norway) and Karmøy (southern Norway). The excess absorption also had a delay of two days from the onset of the PCA.

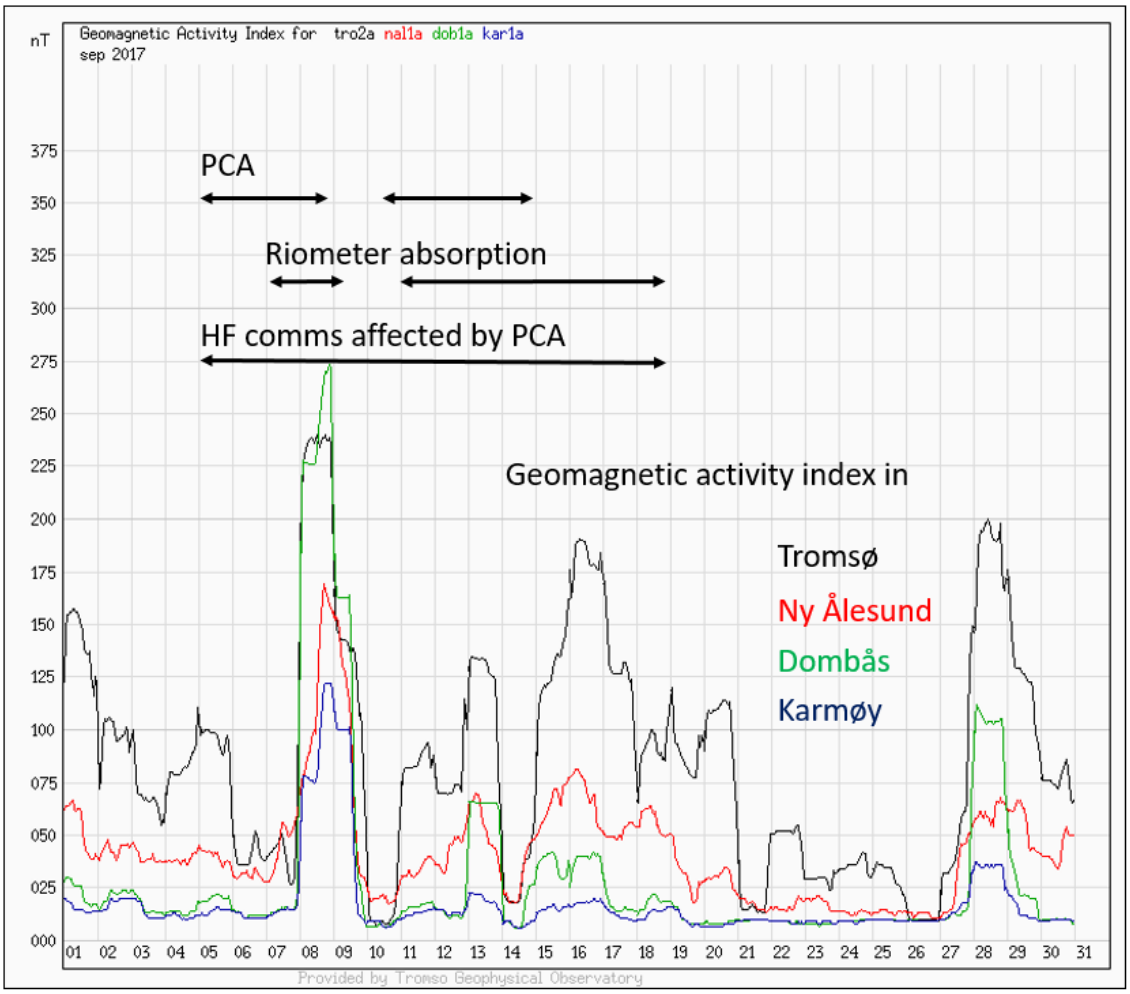

Figure 5.50 Timeline of PCA and other ionospheric observations in September 2017. Proton event (PCA) measured by GOES satellite [15], riometer absorption [8], geomagnetic activity measured by magnetometers [9] and linking probabilities for HF communications. Dates are shown on the x-axis.

7. September 8. September 9. September

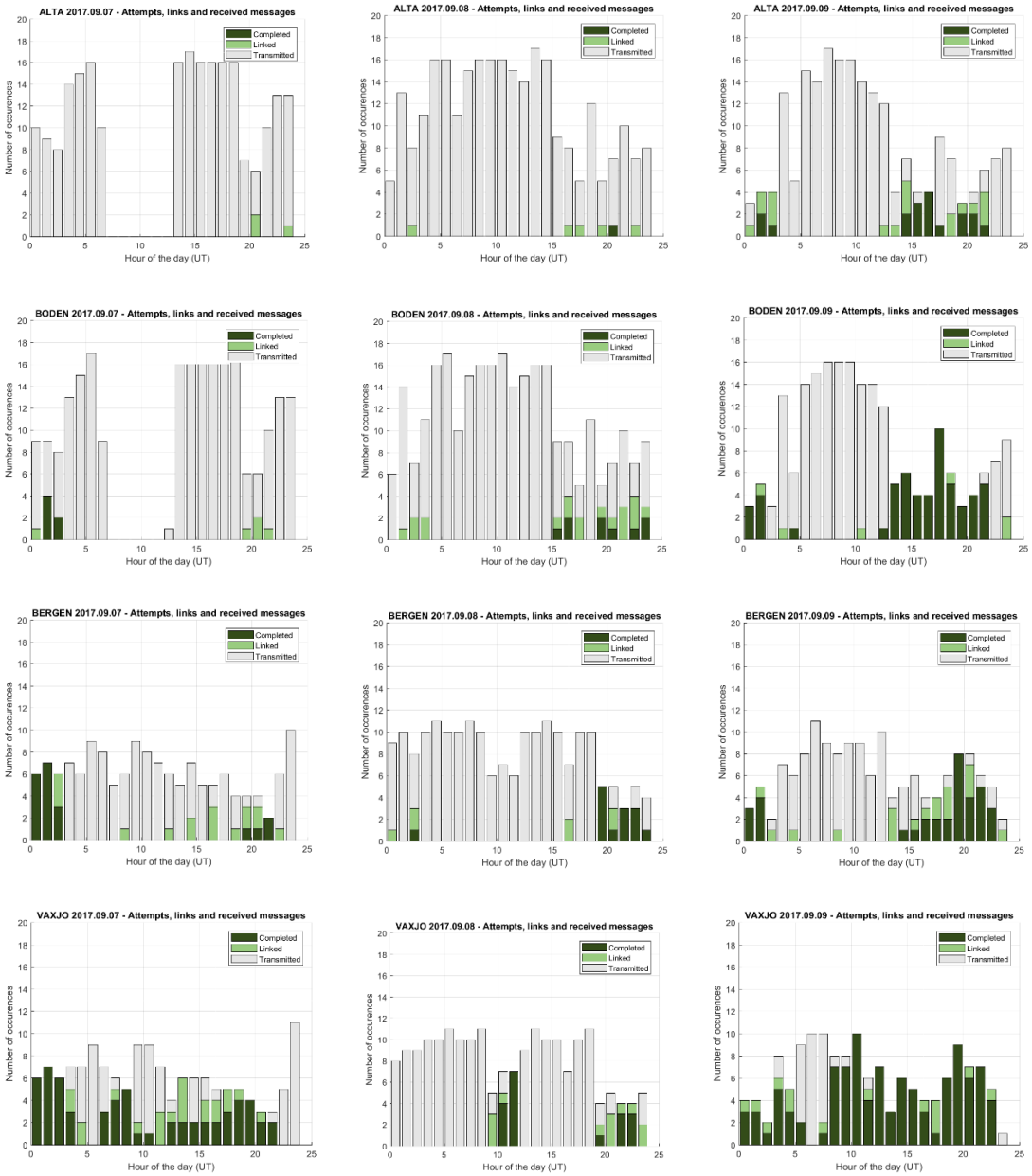

Figure 5.51 Number of link attempts (grey bar), link successes (light green bar) and message successes (dark green bar) for each hour of the three consecutive days 7th, 8th and 9th of September 2017 (columns) and at the different locations Alta, Boden, Bergen and Växjö (rows).

Another PCA occurred on the 14th of July, but this PCA was considerably smaller than the one in September. Unfortunately, data were only collected on the path to Bergen during this period, and communications on this path was only disturbed for one day which occurred two days after the PCA. Also with a delay of two days, increased absorption by the riometers in Finland and

increased geomagnetic activity by the magnetometers in Norway, were registered (see Figure 5.52). A delay of two days of the effects of a PCA is not described in [14], and we have no explanation for that. The consequences of this PCA on the Bergen path were thus minor, and the effect on HF-paths farther north remains unknown.

There were only these two PCA events in 2017, and none registered in 2018, according to [15]. However, about one PCA per month can be expected around solar maximum [14].

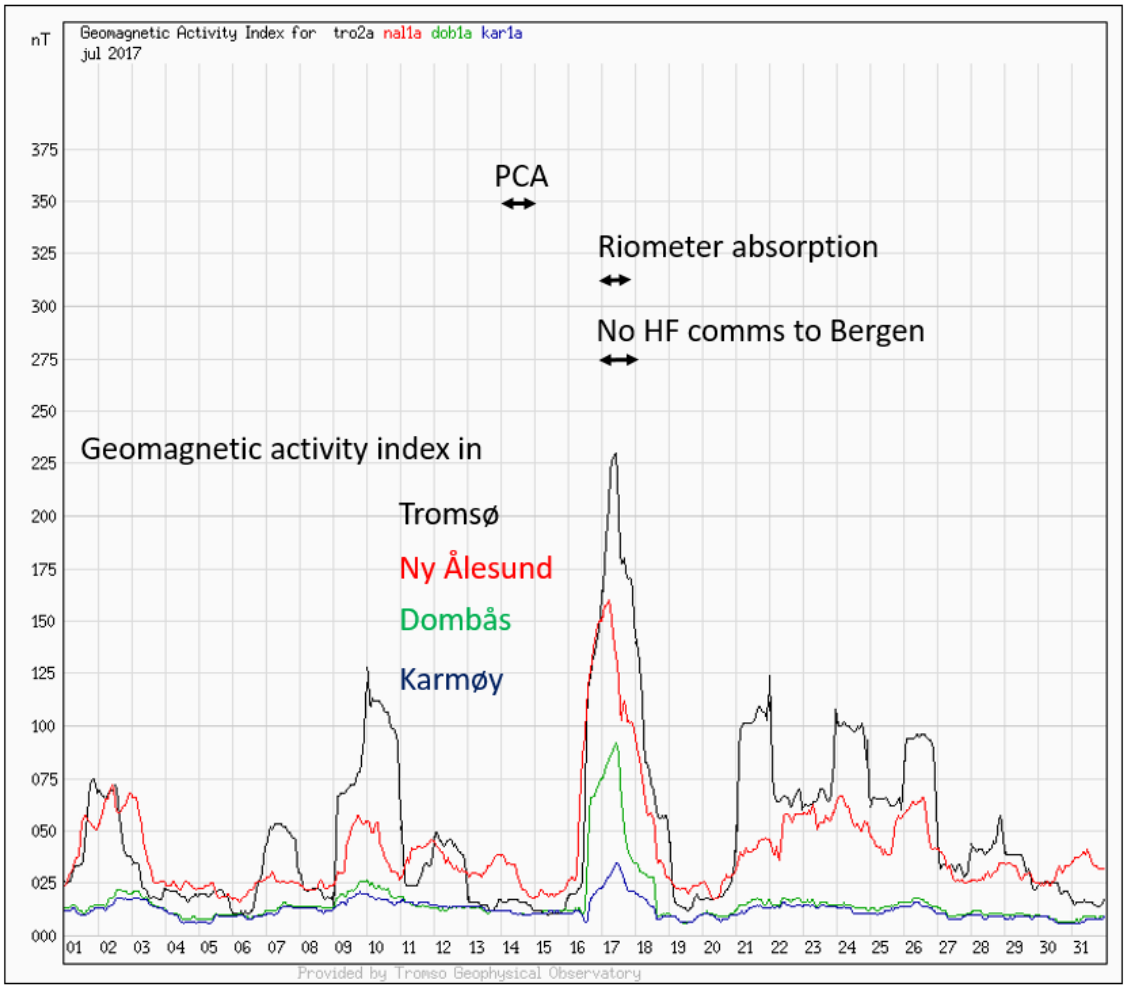

Figure 5.52 Time line of PCA and other ionospheric observations in July 2017. Proton event (PCA) measured by GOES satellite [15], riometer absorption [8], geomagnetic activity measured by magnetometer [9] and linking probabilities for HF communications.

6 Discussion of results and relevance for communications

First we will address some shortcomings of the current measurements and analysis, and then we will discuss the main findings of the study.

6.1 Shortcomings of the measurements and analysis

Since we used actual communication radios for the measurements instead of scientific measuring instruments, we did not have complete control of every parameter of the radio implementation that may have affected the results. An example of such a parameter is the frequency selection. If the automatic frequency selection implementation of the radio was less than optimal, the measured linking probabilities would be affected. By choosing communication radios, however, the results would be closer to a true operational scenario.

For the calculation of space diversity, a major shortcoming of the measurement setup complicated the calculations. The power transmitted was different on the short-haul and long-haul paths, respectively 20 W and 400 W, and the receive antennas on the long-haul paths were different from those of the short-haul paths. The two long-haul receive antennas were also different from one another and had gains of 8 dBi and ~ 0 dBi, respectively. Transmission power and antenna gains are factors contributing to the measured linking probability, so the calculated space diversity gains cannot therefore be attributed to the ionospheric absorption alone. However, measurements showed that 20 W transmit power on the long-haul paths was not sufficient, so this low power would not have been an option on the long-haul paths. Increasing the power to 400 W (+ 13 dB) on the short-haul paths could have been a possibility, but then the measurements would not resemble a true operational scenario with manpacks transmitting at 20 W maximum. If 400 W had been used also on the short-haul paths, it is possible that the measured space diversity gains in this study would have been somewhat lower. However, 13 dB difference in transmit power is a modest number compared to the ionospheric absorption that can occur on oblique incidence paths during disturbances (as shown in Table 3.1). For the short-haul network alone, where the power and antennas were the same on all paths, we believe the space diversity gains calculated can be attributed to the ionospheric absorption alone.

For the two long-haul paths, the path to Växjö generally shows a better performance than the path to Bergen even though the path is about 200 km longer. The antenna in Växjö has an 8 dB higher gain than the antenna in Bergen and the noise conditions may be different. When inspecting hourly averages of the signal-to-noise ratios of the two paths, there is not a steady 8 dB difference between them, but the difference ranges over a 30 dB interval even on a quiet day. So we believe that the better performance on the Växjö path compared to the Bergen path is not entirely due to the antenna advantage (and possibly noise conditions), but also to the lower ionospheric absorption on this path.

For the calculation of space diversity, ideally, linking attempts should be compared for different paths at *exactly* the same instance of time. Since we designed the measurement system so that linking attempts on different paths were done sequentially within the short-haul and long-haul networks respectively, this was not possible, and we have instead compared linking probabilities between the Harstad path and the other paths within the same hour on the same day. To justify this, the channel conditions have to be sufficiently "stationary" within the hour, which may be true on undisturbed days, but probably not during disturbances.

The last shortcoming to be mentioned is that the linking probabilities calculated for each hour is not based on the same number of linking attempts. The number may range from 4–5 to 20, depending on the channel conditions and the speed of the message transfer. Also, the number of days that have been analysed in a certain period varies from path to path, which makes the statistical basis different for each of the paths different.

6.2 Space diversity

To obtain considerable space diversity gain by transmitting via another station presumably south of the disturbed high latitude ionosphere, the secondary path needs to be sufficiently long. However, a long path requires higher transmit power, which may not be available by the operational user, for instance a lower army unit. It has been shown in this study that transmitting 20 W power (3 kHz STANAG 4538 waveform) is not enough to communicate over distances of 1000 km. However, 20 W transmit power is sufficient to obtain some space diversity gain, in the order of 10 %, and occasionally up to 30 % during disturbances in winter time, over distances of 370 km (to Boden). There is thus some robustness to gain by including a network node at a distance of 300–400 km towards the south in a 20 W network.

Transmitting a power of 400 W with the same waveform is sufficient to communicate over distances of more than 1000 km and obtain space diversity gains of up to 50 % during disturbed ionospheric conditions. The largest gains can thus be achieved by units possessing transmitters of 400 W or more, typically higher army units, vessels and stationary HF-infrastructure. Networks comprising several geographically separated infrastructure sites and mobile units could be established to provide robust communications and avoiding the most severely disturbed paths. The set of frequencies to be used has to be chosen carefully based on predictions or the results reported here and in a previous study [20], [21].

The linking probabilites are considerably lower on the path to Bergen than on the path to Växjö. We believe this is due to the less disturbed ionosphere in the south compared to the disturbed ionosphere farther north, as was described for the February 2018 measurements (Section 5.1.2). When studying the ionospheric absorption measured at the various riometer locations of the Finnish riometer chain, we see that the absorption levels decrease steadily with decreasing latitude, and at the position of Oulu (65º N) the absorption is almost negligible compared to Abisko (68.3º N). However, the difference between Bergen and Växjö may also be partly attributed to the different antennas used as discussed in Section 6.1.

One may argue that the concept of a relay node in the south, requiring *two* radio hops to communicate, would reduce the probability of establishing communications. However, the probabilities of linking on the first and second hop are not independent from each other and cannot simply be multiplied, since the presence of an ionospheric layer is likely to support both hops if the geometry of the paths is such that the reflections are likely to occur in the same region of the ionosphere.

6.2.1 Comparison with the previous FFI study

The previous study reported in [4] was very similar to our study, and the results should therefore be compared. The previous study was conducted in 1978/79, near sunspot minimum, and measurements were made three times per day (at dawn, noon and midnight), during three seasons (summer, autumn and winter). There were two paths, one short (460 km) at high latitude and one long (1250 km) towards the south, and relatively high power (~1 kW) was transmitted on both paths (which is different from the present study). A bit error rate count was used, and the reliability of the channel calculated based on the percentage number of measurements with a bit error rate below a threshold. This would compare with our linking probability metric. The focus of the previous study was both on frequency diversity and path diversity, and gains were calculated for different combinations of having single/multiple frequencies and single/multiple paths available. The findings concerning path diversity in [4] and the comparison with our results are as follows:

- When all data (time-of-day, season and degree of disturbance) were analysed together, the gain that can be achieved by relaying the signal via a southern node, is in general 15 %. In our study, we have not combined all of our data, but rather looked at space diversity gain versus time-of-day, season and degree of disturbance. Thus, there are no numbers that can be directly compared. Our study has shown that there is a rather large variation in the space diversity gain over time-of-day and season.

- When the data in the previous study were classified according to the degree of channel disturbance (as measured by a riometer) but with no classification according to time-of-day and season, it was found that the path diversity gain increased with increasing degree of disturbance. The numbers were:
    - Quiet channel conditions (riometer absorption < 0.1 dB): 12 % gain
    - Moderate channel conditions (0.1 < riometer absorption < 2 dB): 17 % gain
    - Disturbed channel conditions (riometer absorption > 2 dB): 25 % gain

  Again, we do not have directly comparable numbers, but the numbers from the previous study are within the same range as our results.

Other interesting observations in the previous study are:

- The reliabilities of the short and long paths are correlated, and they are both affected by excess riometer absorption.

- There is a correlation, but no one-to-one correspondence, between the occurrence of black-outs on the HF-links and the magnitude of the riometer absorption.

- During the PCA event occurring in September 1978, both the short and long paths are affected, but whereas the long path experiences a black-out lasting only one day, the short path is blacked out for several days.

All of these observations comply well with our observations in the present study.

6.3 The use of ionospheric data for improving HF communications

There is no simple one-to-one connection between the observations made on the HF-links and the ionospheric measurements during hours and days following a disturbance on the sun. The ionization caused by the particle precipitation causes irregular reflections and off-great-circle[15] propagation. The ionograms and measured absorption may vary on the timescale of minutes, causing the propagation conditions to vary on the same timescale. However, our comparison of the HF-measurements with the ionospheric data has shown that using such data may give useful insight in the prevailing propagation conditions, and give guidance for making favourable choices for the HF communication networks.

The two types of ionospheric data that have been investigated in this study are ionograms from Tromsø [9] and Lycksele [17], and riometer absorption from Abisko [8]. The ionograms gave the following useful information:

- For the short paths in the north, when the ionogram in Tromsø showed reflections, the probability of linking at HF was high. For the longer paths, the correlation with the Tromsø-ionograms was much lower. Better correlation was obtained with the ionograms in Lycksele, although not as high as for the short paths with the Tromsø-data. (The Lycksele-data available on the Internet were of some lower resolution and quality than the Tromsø-data.)

- The HF-conditions were at times better than the ionograms would indicate, and this applied both to the short and long paths. “Black-outs” on ionograms lasted longer than failure of HF communications. Whereas the ionogram only shows the reflections vertically above the ionosonde, the oblique incidence HF-signal is not reflected exactly in the same vertical position, and it may also be reflected in a larger volume of the ionosphere, thereby increasing the probability of reflection.

- As described in Section 4.2.1, excess D-layer absorption can also be observed on the ionograms, either as a completely blank ionogram, or with an increased minimum observed frequency. A better indicator of absorption is however the riometer measurements.

[15] Propagation that deviates from the direct line between the transitter and receiver.

The ionosonde measurements in Tromsø are automatically analysed, and certain parameters such as the critical frequencies of the ionospheric layers and virtual reflection heights are extracted, if possible. These parameters may be further processed and presented in a relevant way for the HF-operator.

The riometer absorption in Abisko that was analysed in some detail in our study gave the following useful information:

- For the short paths in the north with close proximity to Abisko, absorption levels above 0.2 dB generally corresponded to decreasing linking probability with hardly no linking at an absorption level of 1 dB. There were very few instances of simultaneous high absorption and high linking probabilities. However, low linking probability can not always be explained by high absorption. The explanations may also be lack of ionization (which can be observed on an ionogram) or an increased noise level at the receiver. The long paths towards the south were also affected by the absorption measured in Abisko, but to a lesser extent. The radio operator may counteract absorption by avoiding the area of increased absorption (space diversity), increasing the transmit power (if he has that option), or increasing the frequency (below the limit where the receiver will move into the skip zone).

- Our analysis of a complete year of riometer data showed that for the hours 6–8 UT the percentage of time the absorption exceeded 1 dB was around 8 %. For these hours the linking probability is correspondingly very low. The 0.5 dB absorption level is exceeded approximately 13 % of the time for the hours 2–10 UT, which also give considerably reduced linking probability at HF.

- In the same data set of riometer data, the median duration of absorption events larger than 0.5 dB is 30 minutes, and there is a 90 % chance that the duration of a 0.5 dB event is less than 2.8 hours.

The riometer data from various sites are not necessarily calibrated against the quiet day curve and easily available in a useful format. This must be discussed with the data provider.

Since absorption data only from Abisko was analysed and compared with the HF-measurements, the relevance of other absorption measurements at other geographical positions was not adressed in this study.

We also compared our HF-measurements of linking probability with a high latitude geomagnetic index [23]. Although there is a high correlation between disturbed periods of the geomagnetic data and disturbed periods of the HF-data, the HF-data nevertheless shows better correlation on individual days with the riometer data. This observation is in agreement with [22].

The physical conditions in the lower ionosphere are very important for HF-propagation at high latitudes. A model of the D-region electron densities, called the Ionospheric Model of the

Auroral Zone (IMAZ), has been developed ([22],[19]) and accepted in to the International Reference Ionosphere (IRI) global model [23]. The input values to the IMAZ-model are the solar zenith angle, the solar radio flux $F_{10.7}$, the geomagnetic index, the geomagnetic time and the riometer absorption. The most important input parameter is the riometer absorption [22]. An earlier version of this model was included in a prediction programme for HF communications and predictions were shown in [11] to give very good agreement with measurements at high latitudes.

With the present availability of real-time ionospheric data on the Internet, the robustness of HF communications can be increased by either using prediction tools for HF, driven by real-time ionospheric data as input (forecasts), or by a simpler method; using the real-time data as is, possibly merged into a software application tailor-made for HF communications. Such software applications exist; radio amateurs are using the Voice of America prediction program VOACAP [25] with real-time input data. However, the VOACAP prediction program does not, to our knowledge, contain a high latitude ionospheric model and may therefore not be particularly suited for our latitudes. Other useful tools for the HF-communicator can be found at [15] and [26]. These tools should be further investigated for their applicability to high latitudes, and possibly the most important information should be extracted and presented into an easy-to-use software application for the HF-operator.

The solar flares being the source of ionospheric disturbances are difficult to predict. However, the particle-induced ionospheric phenomena may be predicted, due to their long travel time from the sun (1–4 days). The most intense PCA events and auroral absorption events have been observed when the flare occurred near the central meridian of the sun. The period of solar rotation is about 27 days for the central meridian, and by observing the flares on the sun, it is possible to predict or forecast larger disturbances for the next few days. During the years of minimum sunspot activity the 27 day recurrency is more pronounced than during the years of maximum activity [14].

7 Conclusions and further work

It is clear that HF communications cannot provide ubiquitous real-time communications services to the armed forces at high latitudes. The reason is the dynamic and rapidly changing propagation medium. However, HF communications offers infrastructure independent, long-range communications, at times providing real-time services and throughput at tens of kbit/s, but most of the time non-real time services like messaging, chat and file-transfer at lower data rates. HF communications is thus a complimentary “tool” to other means of communications, and it can be particularly well suited for certain situations. Particularly in the Arctic, the number of communication systems are not that many, but HF communications is one of them. If HF communications is going to be a part of the Norwegian communications infrastructure in the

future, Norwegian Armed Forces should be particulary well trained to use it with new, modern technology and ways to exploit the high latitude ionosphere.

This report has referenced some of the existing knowledge of the high latitude ionosphere and its implications on HF communications, it has suggested how networks can be set up to increase the robustness of communications, and it has pointed out that real-time ionospheric measurements may be used to increase the performance of the networks.

Despite the existence of automated radio technology for use in the HF-frequency band, designed to adapt the signals to the variable channel conditions, we do believe that the HF-operators would benefit from having good knowledge of the high latitude channel. The measurements and analysis of this study may give the following knowledge and advice to the HF-communicator:

- HF has traditionially been point-to-point communications (or broadcast). With new modern technology, networks should be designed so that communications is possible via different paths, exploring the space diversity of the high latitude ionosphere. A southern node could, for instance, be included in a high latitude network. Paths going in the southern direction in Norway or Sweden are affected by ionospheric disturbances, but to a lesser degree than the high latitude paths. Between 10 % and 50 % better linking probability can be gained by utilizing such space diversity. The largest gain is achieved during ionospheric disturbances.

- In summer time the conditions for HF communications are the best (excellent in our measurements), and there is no pronounced diurnal variability. The solar-driven ionosphere seems to dominate over the auroral ionosphere.

- In winter time there is a strong diurnal variation with good conditions only in a few hours around and after noon. The conditions are difficult in the hours of dawn and dusk, particularly for the hours 03–06 UT. Communication attempts should be avoided for these hours if exposure on air is a concern. The conditions are improved at night time because of enhanced ionization due to particle precipitation (auroral E-layers). Normally this ionization is able to reflect higher frequencies, which should therefore be included in the frequency plans.

- Following a solar storm there are many ionospheric disturbances occurring at different time lags and with varying characteristics. The exact shape of the ionization and absorption is impossible to predict in advance, but real-time ionospheric measurements can be used for space situational awareness. Such measurements will tell the HF-operator whether HF communications is expected to be working well or the chance of achieving communications is small. They may also indirectly indicate that technical failure of the equipment may be the problem.

Our comparison of the HF-measurements with other ionospheric data has shown that using such data may give useful insight into the prevailing propagation conditions, and give guidance for

making favourable choices for the communication networks. Real-time ionograms in combination with riometer measurements of absorption were found particularly useful.

We suggest that further work to increase the robustness of HF communications at high latitudes should include:

- Examination of the space weather data sources available on the Internet, including radio amateur tools, with respect to usefulness at high latitudes and for the HF-operator. The criteria for the examination should be the physical phenomena of relevance to HF communications treated in this report, in particular ionospheric absorption and reflection. If traditional prediction programmes using real-time space weather data as input exist, they should be examined.

- Selection of relevant space weather data sources providing real-time data as input to a software application, and development of this software application to a tailor-made, easy-to-use application for the HF-operator. Some of the results from this report can be used in the development. This task possibly includes:

    - Negotiations with ionospheric observatories to make data available online, in appropriate formats. This may include for instance calibration of the measured absorption with regards to the quiet day curve.
    - Further preparations of the data for use in the software application.
    - Establishment of new measurement sites if necessary.

    Already existing space weather sites such as [26] could possibly be expanded to include specific data for HF communications situational awareness.

A Appendix

A.1 Measurement networks

Setermoen in northern Norway was the central site and initiated all the transmissions to five different receivers located in different directions and at different distances from Setermoen. There were two transmitters at Setermoen in separate networks, one of them comprising 20 W radios (RF-5800H) and the other one comprising 400 W radios (RF-7800H). The locations of the receivers are given in Table A.1 along with the antenna type, transmitted power and distance to Setermoen for each site.

	Site	Positions	Antennas	Power	Distance
Short-haul	Setermoen, Tx	68° 51.65’ N, 18° 20.9’E	Broadband wire dipole antenna, HF288D-HP, Comrod	20 W	
	Harstad, Rx	68°47.98’ N, 16°32.66’ E	Broadband wire dipole antenna, HF288D-HP, Comrod	20 W	75 km
	Alta, Rx	69°58.60’ N, 23°17.75’ E	Broadband wire dipole antenna, HF288D-HP, Comrod	20 W	230 km
	Boden, Rx	65°49.45’ N, 21°41.30’ E	Broadband dipole	20 W	370 km
Long-haul	Setermoen, Tx	68° 51.65’ N, 18° 20.9’E	(Dipole antenna first) and Vertical whip antenna, APX80, Comrod. Tuner.	400 W	
	Bergen, Rx	60°23.55’ N, 05°19.40’ E	Vertical marine Tx antenna, AT100D, Comrod	400 W	1130 km
	Växjö, Rx	56°53.35’ N, 14°48.16’ E	Broadband fan dipole antenna, type 3065, Andrews, 8 dBi gain	400 W	1345 km

Table A.1 Characteristics of each measurement site.

A.2 Test procedures

The two 3G HF-networks ran in parallel and independently of each other, governed by a script that initiated transmissions, monitored the network functions, logged data and restarted software and hardware if malfunctions occurred. Using the Harris Wireless Messaging Terminal (WMT), a transmission consisted of a Fast Link Setup (FLSU) and a 10 kbyte message that was sent sequentially to each of the receivers in the network. The FLSU consists of a protocol handshake between the transmitter and receiver using a fixed robust waveform. The following traffic waveforms and 3G protocol make use of adaptive data rate which results in different transmission durations depending on the quality of the channel, but a maximum of 20 minutes was allowed for each transmission. The number of measurements per hour thus varies depending on the channel conditions but is approximately the same for all the paths in the same network.

Radio status information was logged from the Telnet interface connection of the radios and data such as link success/failure, message completion success/failure, frequency, signal-to-noise ratios and throughput were extracted from the logs.

The transmission frequency for each of the stations was selected automatically by the transmitting radio after some channel evaluation. The intervals at which the channel evaluation (frequency sounding) took place was determined by the radio implementation. This process occurred approximately every second hour.

A.3 Analysis

For each hour there was a number of transmission attempts from Setermoen to each of the receivers. From the number of transmission attempts, the number of link successes and the number of completed message transfers per hour were counted. The probability of linking is calculated as the percentage of the transmission linking attempts that succeeded. Likewise, the probability of complete message transfer is calculated as the percentage of transmissions that both succeeded linking and transferring the whole message. In Figure A.1, as an example, the counts of transmission attempts, link successes and message successes are shown per three hours, but similar plots exist per hour. Data shown to the left are days from an ionospherically undisturbed period and the data to the right are days from a disturbed period. Linking probabilities are calculated for different paths for the same periods.

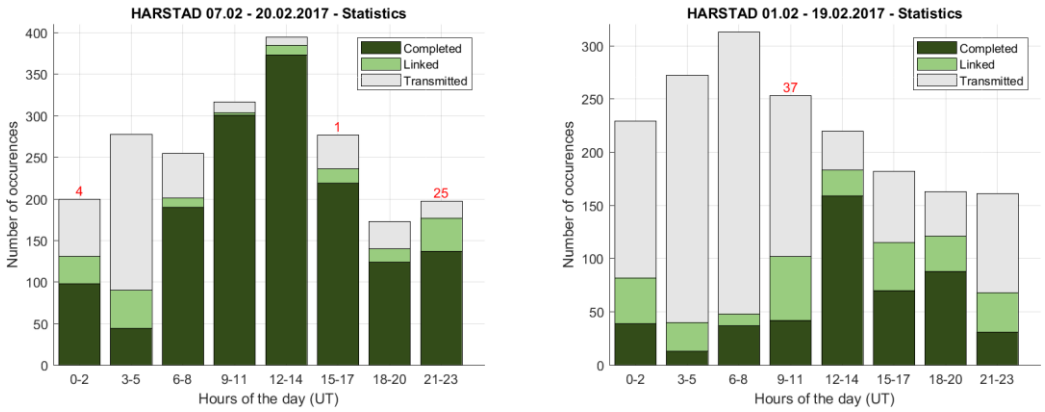

Figure A.1 Total number of transmission attempts, link successes and complete message transfers on the path to Harstad. Left: Undisturbed channel conditions, 11 days analysed. Right: Disturbed conditions, 9 days analysed. (Red numbers represent an error situation with no effect on link successes but on message successes.)

Abbreviations

ALE – Automatic Link Establishment
CCDF – Complementary Cumulative Distribution Function
CD&E – Concept Development and Experimentation
FFI – Forsvarets forskningsinstitutt (Norwegian Defence Research Establishment)
FLSU – Fast Link Set-Up
HF – High Frequency
IMAZ – Ionospheric Model for the Auroral Zone
IRI – International Reference Ionosphere
MF – Medium Frequency
PCA – Polar Cap Absorption event
SID – Sudden Ionospheric Disturbance
STANAG – Standardization Agreement (NATO)
UT – Universal Time
WMT – Wireless Messaging Terminal

References

[1] CD&E Eksperimentrapport 1606 *"HF i nettverk"*, Cyberforsvaret, Konseptutvikling og eksperimentering, 2017.

[2] Mjelde T.M.O., *"HF i nettverk – Oppsett og gjennomføring av tester"*, FFI-Eksternnotat 19/00486, 2019.

[3] Jodalen V., Mjelde T.M.O., *"An investigation of space diversity at HF to obtain better linking probability under the disturbed high latitude ionosphere",* Conference Proceedings, Nordic Shortwave Conference 2019, Fårø, Sweden, 2019.

[4] Thrane E.V., *"Results of transmission tests in Norway using high frequency radio waves reflected from the ionosphere"*, Internal Report, Norwegian Defence Research Establishment, 1979.

[5] Jodalen V., Bergsvik T., Cannon P. S., Arthur P. C, "*The performance of HF modems on high latitude paths using multiple frequencies"*, Radio Science Vol. 36 , No. 6 , p. 1687, 2001.

[6] Serinken N., Jorgenson M., Moreland K., W., Chow S., *"Polarization diversity in high frequency radio data systems"*, Electronic Letters 32 (19), October 1996.

[7] Jorgenson M., *"Building resilient networks at HF"*, Conference Proceedings, Nordic Shortwave Conference 2019, Fårø, Sweden, 2019.

[8] Sodankylä Geophysical Observatory, University of Oulu, http://www.sgo.fi/Data/Riometer/

[9] Tromsø Geophysical Observatory, The Arctic University of Norway (UiT), http://www.tgo.uit.no/

[10] Thrane E.V., *"Propagation II: Problems in HF propagation"*, AGARD Lecture Series No.145, Propagation Impact on Modern HF Communications System Design, NATO, 1986.

[11] Jodalen V., *"A study of observed and predicted HF propagation characteristics at high latitudes"*, FFI/Publication-96/01107, 1996.

[12] Ranta H., *"Riometer measurements of ionospheric absorption at high latitudes"*, Report No 34, Sodankyla Geophysical Observatory, Sodankya, Finland, 1978.

[13] Holt O., Landmark B., Lied F., *"Analysis of riometer observations obtained during polar radio blackouts"*, JATP, 23, p. 229, 1961.

[14] Eriksen K. W., Landmark B., Lied F., Mæhlum B., Thrane E.V., *"High frequency radio communications*, AGARDograph 104, Technivision, Maidenhead, England, 1967.

[15] https://www.sws.bom.gov.au/HF_Systems

[16] https://www.digisonde.com/pdfs/Digisonde-4D_Specs_Nov2009.pdf

[17] http://www2.irf.se/

[18] Kero A., Vierinnen J., McKay-Bukowski D., Enell C. F., Sinor M., Roininen L., Ogawa Y., *"Ionospheric electron density profiles inverted from a spectral riometer measurement"*, AGU Publications, Geophysical Research Letters, 10.1002/2014GL060986, 2014.

[19] McKinnell L-A., Friedrich M., *"A neural network-based ionospheric model for the auroral zone"*, Journal of Atmospheric and Solar-Terrestrial Physics 69 (2007) 1459-1470, www.elsevier.com/locate/jastp, 2007.

[20] Jodalen V., Mjelde T. M., Sander J., Batts W., *"All results from wideband HF measurements in the Arctic 2015-16"*, FFI-notat 16/00569, 2016.

[21] Jodalen V., Mjelde T. M., *"HF-kommunikasjon i Arktis – analyse basert på målinger"*, FFI-rapport 16/00576, 2016.

[22] Friedrich M., *"Handbook of the Lower Ionosphere"*, Verlag der Technischen Universität Graz, 2016, ISBN: 978-3-85125-485-3, e-book ISBN: 978-3-85125-486-0

[23] https://services.swpc.noaa.gov/text/daily-geomagnetic-indices.txt

[24] http://irimodel.org/

[25] https://www.voacap.com/

[26] https://www.swpc.noaa.gov/communities/space-weather-enthusiasts

[27] http://sesolstorm.kartverket.no/

About FFI

The Norwegian Defence Research Establishment (FFI) was founded 11th of April 1946. It is organised as an administrative agency subordinate to the Ministry of Defence.

FFI's MISSION

FFI is the prime institution responsible for defence related research in Norway. Its principal mission is to carry out research and development to meet the requirements of the Armed Forces. FFI has the role of chief adviser to the political and military leadership. In particular, the institute shall focus on aspects of the development in science and technology that can influence our security policy or defence planning.

FFI's VISION

FFI turns knowledge and ideas into an efficient defence.

FFI's CHARACTERISTICS

Creative, daring, broad-minded and responsible.

Om FFI

Forsvarets forskningsinstitutt ble etablert 11. april 1946. Instituttet er organisert som et forvaltningsorgan med særskilte fullmakter underlagt Forsvarsdepartementet.

FFIs FORMÅL

Forsvarets forskningsinstitutt er Forsvarets sentrale forskningsinstitusjon og har som formål å drive forskning og utvikling for Forsvarets behov. Videre er FFI rådgiver overfor Forsvarets strategiske ledelse. Spesielt skal instituttet følge opp trekk ved vitenskapelig og militærteknisk utvikling som kan påvirke forutsetningene for sikkerhetspolitikken eller forsvarsplanleggingen.

FFIs VISJON

FFI gjør kunnskap og ideer til et effektivt forsvar.

FFIs VERDIER

Skapende, drivende, vidsynt og ansvarlig.

FFI's organisation

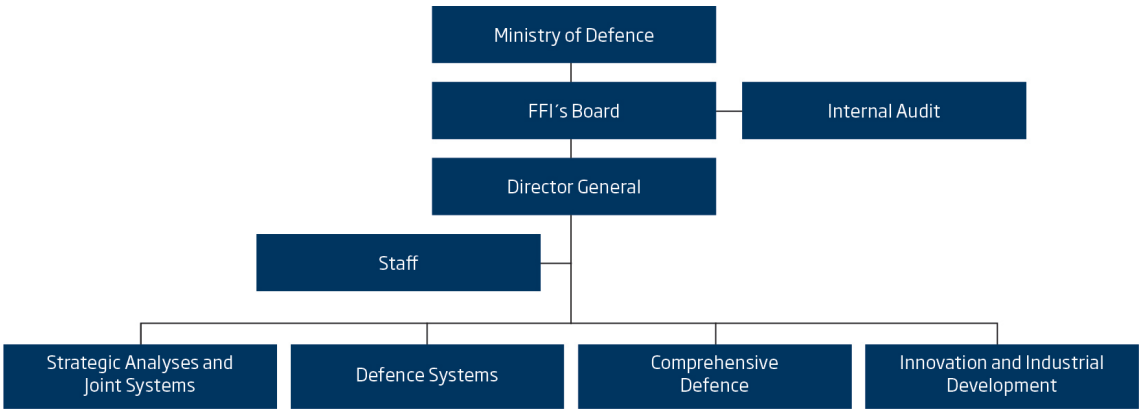

Forsvarets forskningsinstitutt
Postboks 25
2027 Kjeller

Besøksadresse:
Instituttveien 20
2007 Kjeller

Telefon: 63 80 70 00
Telefaks: 63 80 71 15
Epost: ffi@ffi.no

Norwegian Defence Research Establishment (FFI)
P.O. Box 25
NO-2027 Kjeller

Office address:
Instituttveien 20
N-2007 Kjeller

Telephone: +47 63 80 70 00
Telefax: +47 63 80 71 15
Email: ffi@ffi.no

FFI Forsvarets forskningsinstitutt
Norwegian Defence Research Establishment